University of Milan, Milan

European School of Molecular Medicine

PhD Thesis by

Stefano Santaguida, M.Sc.

Understanding the spindle assembly checkpoint and the error correction machinery within the kinetochore framework

Sponsoring Institution: *European Institute of Oncology, Milan, Italy*

Supervisor: *Prof. Andrea Musacchio, European Institute of Oncology, Milan, Italy*

External Supervisor: *Prof. Stephen Taylor, University of Manchester, Manchester, UK*

Submitted on September 2010

TABLE OF CONTENTS

List of Figures

List of Tables

List of Abbreviations

APC/C, anaphase-promoting complex/cyclosome**; NMMII,** nonmuscle Myosin II**; PI3K,** phosphatidyl-inositol 3-kinase**; RZZ,** ROD–ZWILCH–ZW10**; STLC,** S-trityl-l-cysteine**.**

List of Publications

The work described in this thesis has been published in the following articles:

Santaguida and Musacchio, *The life and miracles of kinetochores*, EMBO J. 2009 Sep 2;28(17):2511-31.

Santaguida et al, *Dissecting the role of MPS1 in chromosome biorientation and the spindle checkpoint through the small molecule inhibitor Reversine*, J Cell Biol. 2010 Jul 12;190(1):73-87.

Abstract

Kinetochores are large protein assemblies built on chromosomal loci named centromeres. Four distinct modules accomplish the main functions of kinetochores. The first module, in the inner kinetochore, contributes a sturdy interface with centromeric chromatin. The second module, the outer kinetochore, contributes a microtubule-binding interface. The third module, the spindle assembly checkpoint, is a feedback control mechanism that monitors the state of kinetochore-microtubule attachment to control progression of the cell cycle. The fourth module discerns correct from improper attachments, preventing the stabilization of the latter and allowing the selective stabilization of the former. The catalytic activity of the MPS1 kinase is crucial for the spindle assembly checkpoint and for chromosome bi-orientation on the mitotic spindle. In this thesis, I report work showing that the small-molecule Reversine is a potent mitotic inhibitor of MPS1. Reversine inhibits the spindle assembly checkpoint in a dose-dependent manner. Its addition to mitotic HeLa cells causes the ejection of Mad1 and the RZZ complex, both of which are important for the spindle checkpoint, from unattached kinetochores. By using Reversine, I also demonstrated that MPS1 is required for the correction of tensionless chromosome-microtubule attachments. An important conclusion from this work is that MPS1 acts downstream from the AURORA B kinase, another crucial component of the error correction pathway. My studies describe a very useful tool to interfere with MPS1 activity in human cells. They also shed light on the relationship between the error correction pathway and the spindle assembly checkpoint, and suggest that these processes are co-regulated and are likely to involve the same catalytic machinery.

Introduction

An overview of kinetochore function and organization

At each mitosis, cells face the tremendous challenge of separating the sister chromatids in two identical pools. This process, on which all cells rely to remain viable, is usually executed with great accuracy. Its perturbation results in aberrations in chromosome numbers (aneuplodies), which are a cause of disease and correlate with cellular transformation (Weaver and Cleveland, 2006).

Crucial to accurate cell division are kinetochores, protein scaffolds built on chromosomes to promote the separation of sister chromatids through an interaction with the mitotic spindle. The primary function of kinetochores is to create load-bearing attachments between chromosomes and microtubules in a dividing mother cell. The correct partitioning of sister chromatids to the daughter cells depends on such attachments (Walczak and Heald, 2008; Wittmann et al., 2001). The ability of kinetochores to couple to growing or disassembling microtubules (Rieder and Salmon, 1998) has attracted considerable theoretical interest (e.g. Grishchuk et al., 2008; Hill, 1985). Low- and high-resolution structural snapshots of several candidate kinetochore-microtubule couplers have revealed a variety of modes of binding and shapes, including "rings, bracelets, sleeves and chevrons" and "slender fibrils" (Davis and Wordeman, 2007; McIntosh et al., 2008). The relative contribution from these different structures to force generation and chromosome motility is an active area of investigation.

The simplest currently studied kinetochores, *S. cerevisiae*'s, bind a single microtubule (reviewed in McAinsh et al., 2003; Westermann et al., 2007). They contain approximately 60 proteins, almost 40 of which are clustered in 7 different complexes, the CBF3, Ndc80, Mtw1, Spc105, Ctf19, Dam1, and Ipl1 complexes (Figure 1) (McAinsh et al., 2003; Westermann et al., 2007). With few exceptions (most notably the CBF3 and Dam1 complexes), these complexes are conserved from yeast to humans (Cheeseman and Desai, 2008; Musacchio and Salmon, 2007).

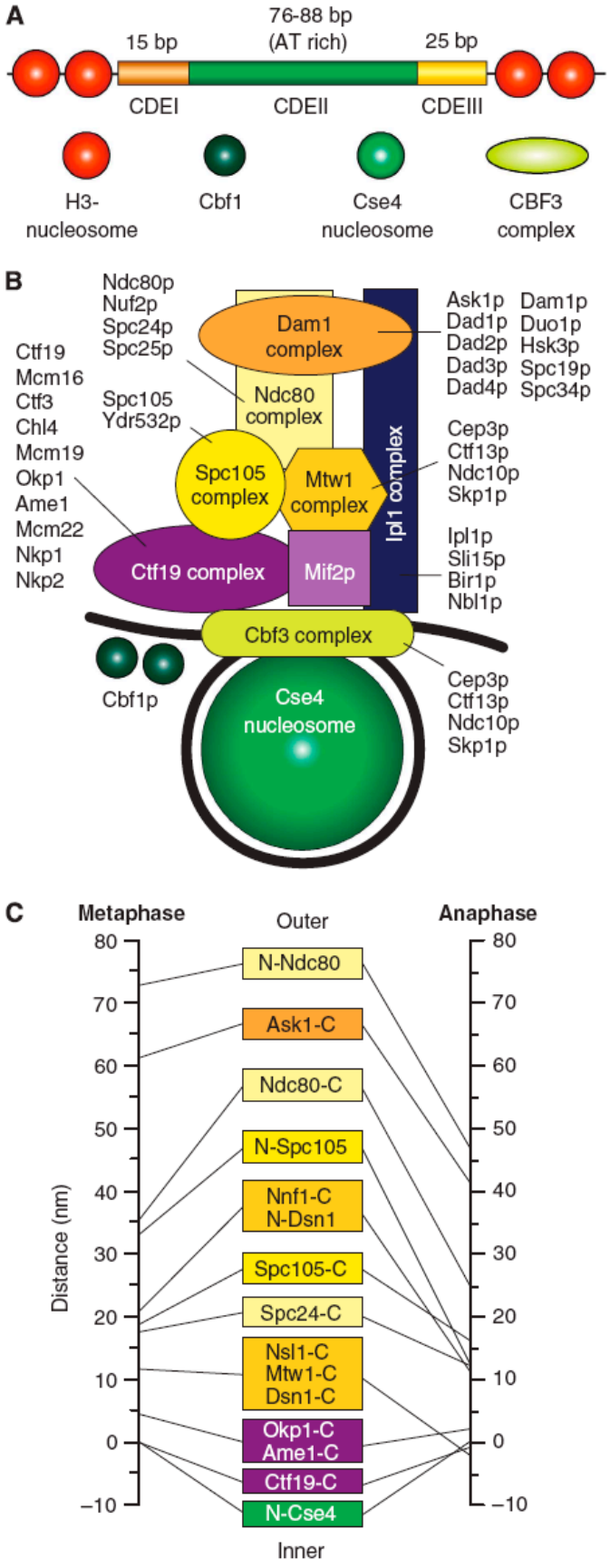

Figure 1 The kinetochore of S. cerevisiae

(**A**) The 125-bp centromere of *S. cerevisiae* is subdivided in the CDEI, CDEII, and CDEIII regions. CDEI recruits a dimer of Cbf1. CDEII folds around a specialized nuclesome containing Cse4. The CBF3 complex binds CDEIII. H3-containing nucleosomes flank the centromere. Neither Cbf1 nor CBF3 have homologues in higher eukaryotes. (**B**) The Cse4-containing nucleosome wraps around the ~125-bp centromeric DNA (black). Mif2p (homologous to CENP-C) is a linker protein creating a connection with the Mtw1, Spc105 and Ndc80 complexes (homologous to Mis12, KNL-1 and Ndc80 complexes of higher eukaryotes). Together with the Dam1 complex, the Ndc80 complex reaches the microtubule-binding region. The Ipl1p complex is equivalent to the chromosome passenger complex (CPC) of higher eukaryotes. It is believed to span from the inner to the outer region of the kinetochore. The kinase activity associated with this complex is directed onto the Ndc80 and Dam1 complexes and regulates the attachment process. Names of constituent subunits are displayed. (**C**) Average location of kinetochore proteins along the axis of the *S. cerevisiae*'s kinetochore-microtubule attachment in metaphase and late anaphase (Joglekar et al., 2009). N- and C- indicated N- and C-termini.

Conservation suggests that the larger kinetochores of higher eukaryotes, which bind multiple microtubules (kinetochore fibres or K-fibres), may be built from the repetition of a basic microtubule-binding module similar to the one existing in budding yeast (Blower et al., 2002; Joglekar et al., 2008; Zinkowski et al., 1991). But evidence in favour of this idea, known as the "repeat subunit" model, is modest. Kinetochores in vertebrates appear as trilaminar plates, with electron dense inner and outer kinetochore plates and an electron lucent middle layer (Figure 2). The inner plate contains kinetochore proteins implicated in the creation of an interface with centromeric chromatin. The outer plate contains kinetochore proteins that interact with the plus ends of microtubules bound "end-on". A fibrous corona, extending outward from the outer plate, is visible in the absence of microtubules and contains microtubule motors, such as CENP-E, and components of the spindle checkpoint, such as the Rod-ZW10-Zwilch (RZZ) complex, both of which only exist in metazoans (reviewed in Cleveland et al., 2003). A recent electron tomography reconstruction of the outer plate revealed a fibrous, flexible network apparently lacking a well-defined organization (Dong et al., 2007) (Figure 2). While no orderly structure was observed, it is possible that structural work on the microtubule-binding unit will eventually reveal hidden regularities.

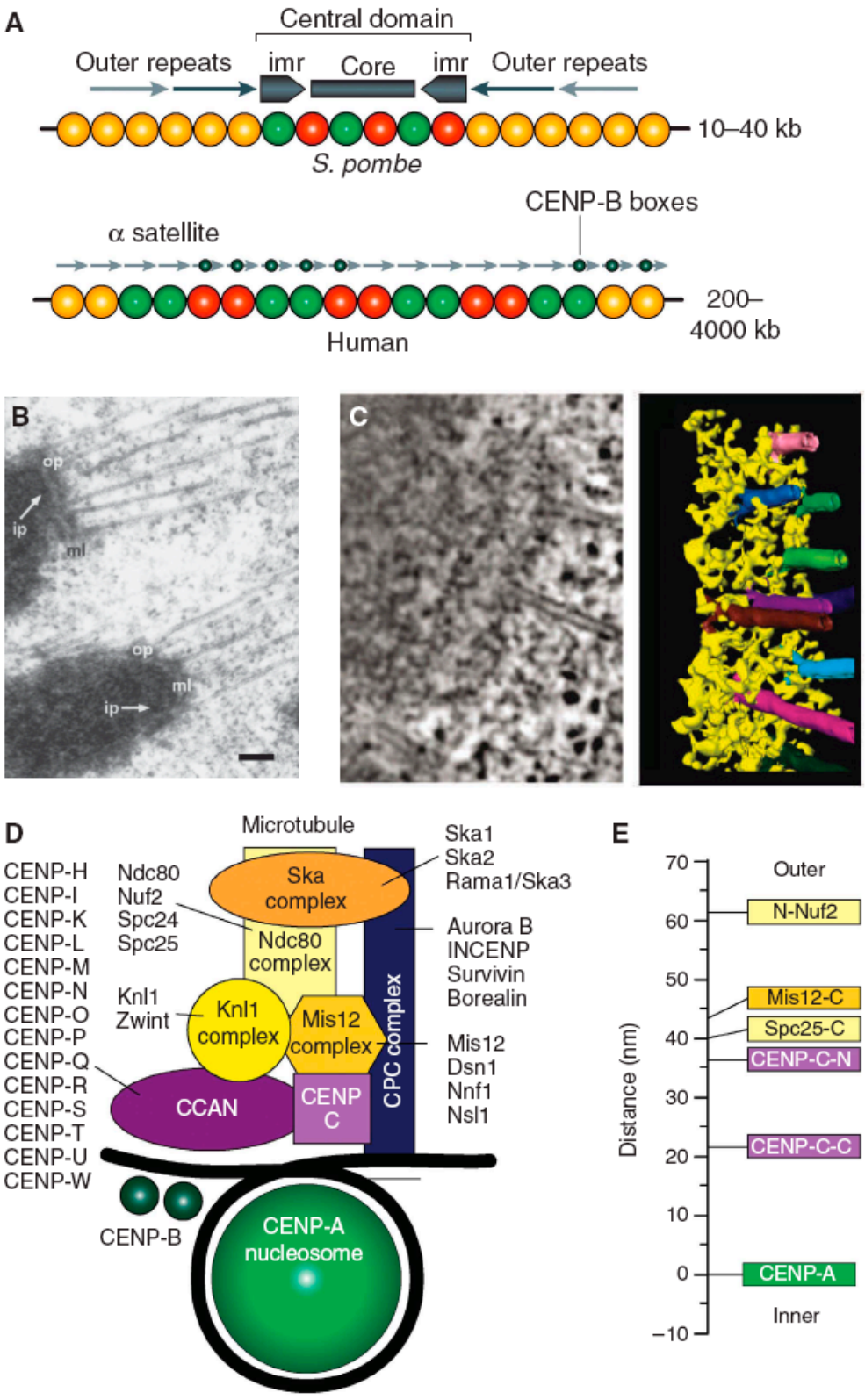

Figure 2 Trilaminar plates with repeat subunit model

(**A**) The central domain of the centromere of *S. pombe* possesses a pair of inverted repeat sequence arrays (marked as *imr*, for innermost repeat). They flank an unconserved central core sequence. Both CENP-A and H3-

containing nucleosomes map to the central domain. The central domain is flanked by the cohesin-rich outer domains, consisting of peri-centromeric heterochromatin. In humans, α-satellite DNA is composed of a core of highly ordered 171-bp repeats termed α-I satellite DNA, which is framed on either side by divergent repetitive sequences and retrotransposons, referred to as α-II satellite DNA. At the outskirts, the centromeric chromatin becomes rich in long interspersed element 1 (LINE-1 elements). On normal human chromosomes, the centromere forms on a small subdomain of the α-I satellite DNA, but there are cases in which the centromere forms on DNA devoid of α-satellite repeats. The α-I satellite DNA contains a sequence known as the CENP-B box, which binds in a sequence specific manner to the CENP-B protein and facilitates, but is not strictly required for, kinetochore formation. Panel was adapted from (Allshire and Karpen, 2008) (**B**) Adjacent kinetochores from a metaphase cell obtained by rapid freezing and freeze substitution. The prominent outer plate (op) structure stains as heavily as chromatin, and is separated from the underlying inner plate (ip) by a well-defined, translucent, middle layer (ml). Bar represents 200 nm. (**C**) Electron tomography of the outer plate shows a network of cross-linked fibres, 10 nm in diameter and up to 80–90 nm long, of unknown molecular identity. The long fibres aligned in the plane of the outer plate in the absence of microtubules (not shown), but re-oriented as they bound to the side of microtubules (Dong et al., 2007). (**D**) A scheme for the outer kinetochore of metazoans analogous to that presented in Fig. 1B. (**E**) Average location of kinetochore proteins along the axis of the kinetochore-microtubule attachment in metaphase in *D. melanogaster*. N- and C- indicated N- and C-termini.

The study of reciprocal requirements of kinetochore proteins for kinetochore recruitment and assembly has defined a possible plan for the assembly of inner and outer kinetochore plates (e.g. Hori et al., 2008; Liu et al., 2006). In a remarkable recent feat, the position of kinetochore proteins along the inter-kinetochore axis of *S. cerevisiae*'s and *D. melanogaster*'s kinetochores was mapped with nanometer accuracy (Joglekar et al., 2009; Schittenhelm et al., 2007). The picture emerging from these analyses is consistent with a model in which kinetochore proteins are piled-up according to an inside-out scheme from the centromere towards the microtubule-binding site (Figures 1 and 2). At least two alternative variants of assembly are conceivable, as discussed below.

Kinetochores are also involved in at least two fundamental and possibly related feedback mechanisms. The first mechanism allows the discrimination between correct and incorrect kinetochore-microtubule attachments (Kelly and Funabiki, 2009; Pinsky and Biggins, 2005).

Correct attachments become stabilized, whereas incorrect attachments are labile and eventually become corrected (Li and Nicklas, 1995; Nicklas and Koch, 1969). The correct configuration of attachment of the sister kinetochores is to opposite spindle poles (bi-orientation or amphitelic orientation). This configuration allows the equational division of sisters to the daughter cells at anaphase (Figure 3).

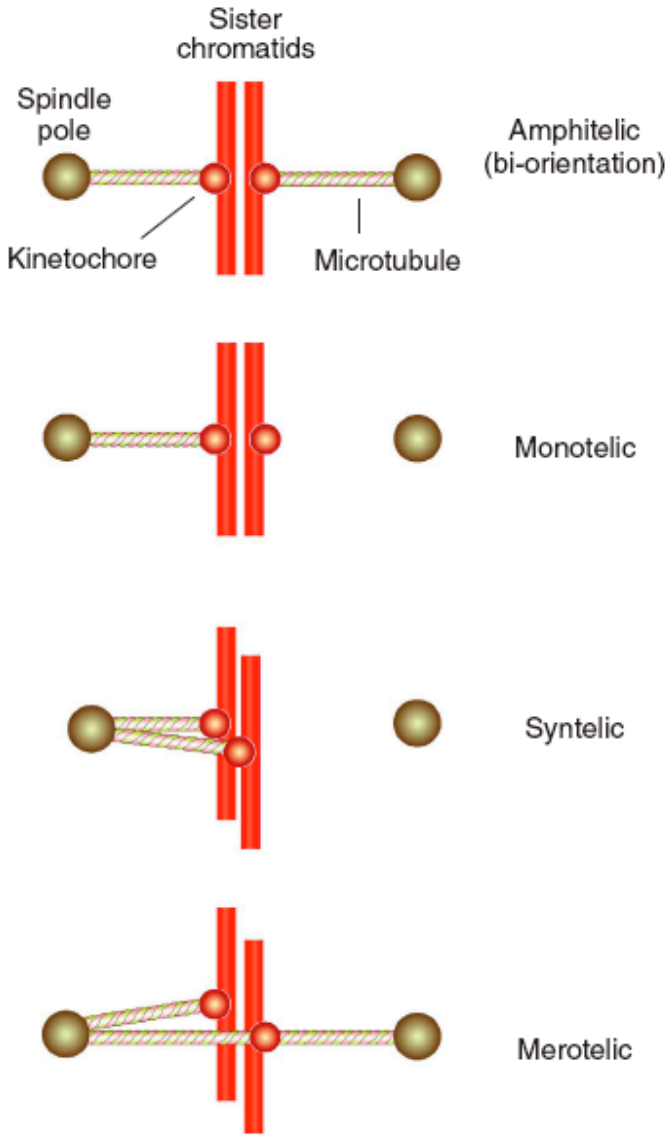

Figure 3 Bi-orientation, erroneous attachments

A single sister chromatid pair is shown for simplicity. In amphitelic orientation (bi-orientation) each of the two opposing sister kinetochores is bound to microtubules originating from the proximal pole. This is the correct form of attachment. Monotelic attachment is a normal condition during prometaphase before bi-orientation.

Premature loss of sister chromatid cohesion at this early stage, for instance as a consequence of a cohesion defect or a mitotic checkpoint defect, can yield aberrant segregation with both sister chromatids distributed to the same daughter cell. Persistent cohesion between chromosomes in anaphase will result in similar errors. In syntelic attachment, both sisters in a pair connect to the same pole. In merotelic attachment, a sister is attached to both poles. This condition occurs quite frequently during mitosis.

Errors during the phase of attachment, such as syntelic and merotelic attachment, fail to become stabilized and become corrected (e.g. Cimini et al., 2003; Lampson et al., 2004; Nicklas and Koch, 1969).

The second mechanism works by synchronizing the process of microtubule attachment with the progression of the cell cycle oscillator. Specifically, loss of cohesion between sister chromatids and mitotic exit through degradation of Securin and Cyclin B, two events that are controlled by the cell cycle machinery, must be coordinated with the completion of kinetochore-microtubule attachment (Peters, 2006). The feedback mechanism responsible for this coordination is the spindle assembly checkpoint (Musacchio and Salmon, 2007).

Kinetochore-microtubule attachment: an overview

A quarter of a century ago, the "search and capture" model laid the foundations for understanding the process of kinetochore-microtubule attachment (Kirschner and Mitchison, 1986). The model incorporated the recently described process of microtubule dynamic instability to propose that mitotic microtubules explore space dynamically and become selectively stabilized once they hit their targets. In mitosis, kinetochores act as targets, and indeed the stabilization of kinetochore-bound microtubules, i.e. the increase of their half-lives, is a crucial function of kinetochores (Mitchison et al., 1986; Rieder and Salmon, 1998; Zhai et al., 1995).

There is also evidence that kinetochores can nucleate microtubules, or at least, that they can capture and promote the growth of small microtubule stubs generated in their vicinity

(Khodjakov et al., 2003; Tulu et al., 2006; Witt et al., 1980). The Ran pathway contributes to nucleating microtubules proximally to chromatin and may act as a source of short microtubules for kinetochore capture and elongation. Microtubules are polymers of αβ-tubulin dimers. They are polar structures, with plus ends exposing β-tubulin and minus ends exposing α-tubulin. Kinetochores bind to the +end of microtubules. Microtubules growing from kinetochores have the expected orientation, i.e. their plus end is at the kinetochore (Euteneuer and McIntosh, 1981).

A remarkable feature of kinetochores is that they maintain attachment to growing or disassembling microtubules (Rieder and Salmon, 1998). For instance, kinetochores remain attached during anaphase or during the oscillations about the metaphase plate known as "tug-of-war". Furthermore, kinetochores slide towards the plus end to maintain their position on treadmilling microtubules (also known as microtubule flux), i.e. microtubules that incorporate tubulin subunits at the plus ends and release them at the minus end without net growth (Mitchison and Salmon, 1992). How do kinetochores maintain coupling to a disassembling microtubule? Hill's thermal ratchet model, or biased-diffusion model (Hill, 1985) proposes that a surface providing an array of microtubule binding sites might translocate along successive equivalent binding sites on a disassembling microtubule if the translocation from site to site implies relatively small activation energies (i.e. it is fast) and if the total binding energy is sufficiently large (Figure 4A-D). Under these conditions, when binding sites are removed from the edge of the binding surface upon microtubule disassembly, "biased diffusion" of the coupler towards the minus end restores the number of binding sites on the microtubule.

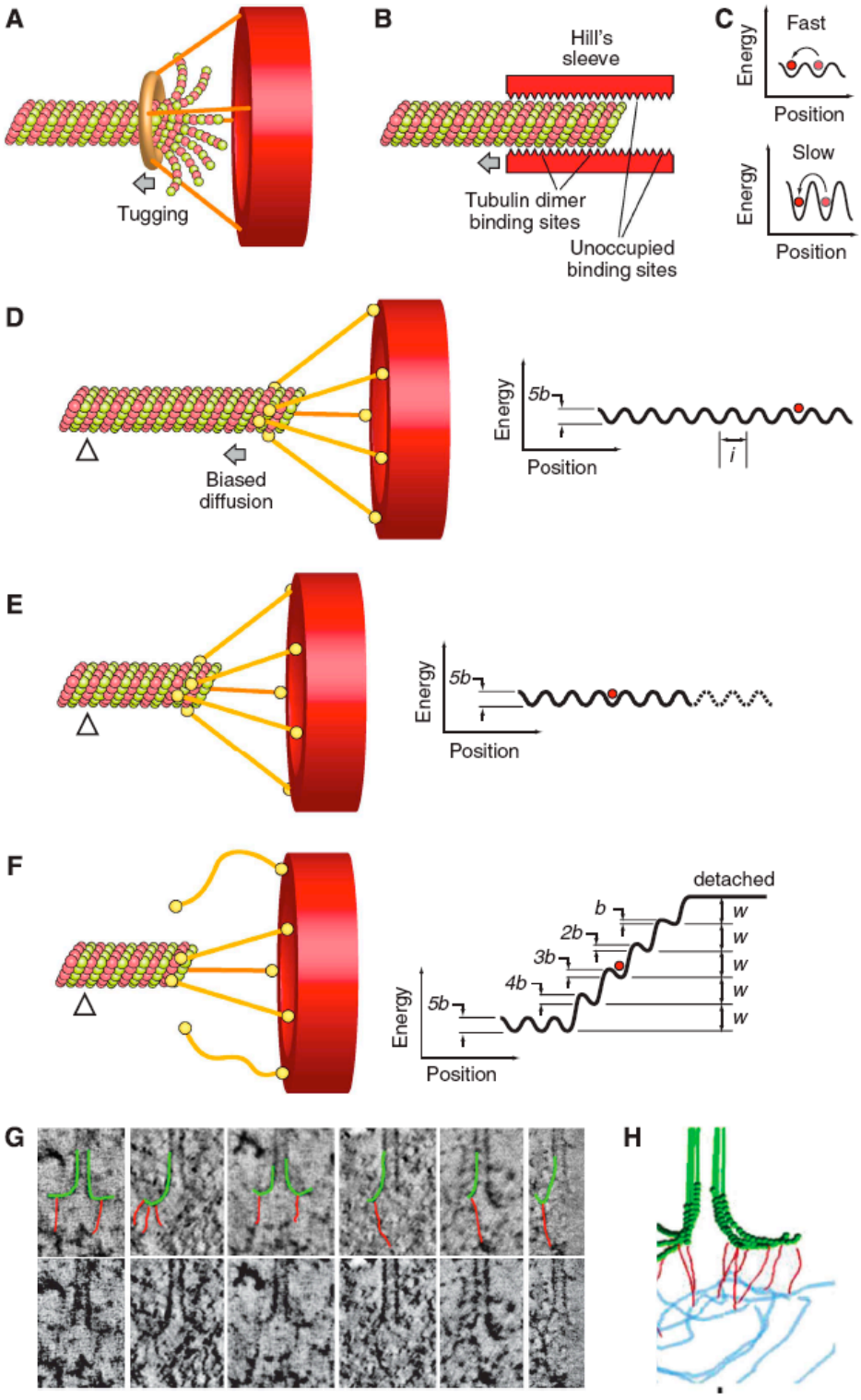

Figure 4 Biased diffusion

This schematic view of the Hill model is an adaptation from (ref. Powers et al., 2009). While the original formulation of the model depicted the microtubule-binding site of the kinetochore as a "sleeve" surrounding the microtubule (Hill, 1985), this is not an obligatory condition and the description holds for the fibrous coupler shown here. (**A**) Kinetochores are shown as red hollow discs. The coupler is an elongated molecule with two

globular domains at either end, one for kinetochore binding and one for microtubule binding, and it is inspired by the Ndc80 complex (see Figure 5). Coupling is along the lattice and is mediated by five microtubule-binding elements. The free-energy landscape for this coupler is shown on the right. *l* denotes spacing of sites. The red circle represents the current position of the coupler on the surface. The energy landscape is corrugated because movement along the filament requires breaking and reforming some bonds (see panel **D**). *b* is the activation energy, *w* is the binding energy. The triangle represents a fiduciary mark along the microtubule. (**B**) The microtubule has depolymerised and the coupler has diffused on the surface towards the plus end. (**C**) The release of the coupler (two out of five binding sites have been lost here) implies an increase in free energy because the bond energies, *w*, must be overcome to move the couple past the filament tip. The heights of the activation energies *5b*, *4b*,…., *b*, decrease as the coupler begins to move past the tip. (**D**) The overall activation energy required for sliding along the lattice may cause diffusion to be slow or fast. To be effective, diffusion has to occur with kinetics that must be compatible with the kinetics of microtubule depolymerization. (**E**) With a ring coupler encircling a microtubule (inspired by the Dam1 ring, discussed in Figure 5), force is provided by flared depolymerising protofilaments, which exercise a pressure against the base of the sleeve. (**F**) The bottom row shows tomographic slices of kinetochore microtubule ends. The same gallery is also shown in the top row with protofilaments and their associated kinetochore fibrils, indicated by graphic overlays. (**G**) A tomographic reconstruction of a kinetochore-microtubule interface with associated fibrils. **F** and **G** panels are from (ref. McIntosh et al., 2008).

In reconstituted *in vitro* systems, several kinetochore components behave as expected for a Hill's coupler. For instance, microbeads coated with Ndc80 complex (a fibrous component of the KMN network whose function at the kinetochore is described below) track the ends of a depolymerising microtubule (McIntosh et al., 2008; Powers et al., 2009). However, analogous results can be obtained by immobilizing proteins with different structural features, including microtubule motors, MAPs, or even simply streptavidin for binding to biotinylated microtubules (Grishchuk et al., 2005; Lombillo et al., 1995). Thus, at least *in vitro* biased diffusion along a depolymerising microtubule can be achieved with diverse structural designs and does not require a continuous encircling structure around microtubules.

Besides biased diffusion, there is another way in which microtubule-disassembly can be harnessed to perform work. The protofilaments (PFs) at the plus end of a shrinking

microtubule are flared as a result of lattice distortion when the GTP cap is liberated (Mandelkow et al., 1991). The release of mechanical strain from a bending microtubule PF can be harnessed to do mechanical work (Grishchuk et al., 2005; Koshland et al., 1988). Almost three decades ago it was proposed that kinetochores might maintain attachment to microtubules by encircling the microtubule with a processive sliding collar (Margolis and Wilson, 1981). A ring could in principle be utilized to propel kinetochores if peeling protofilaments at a disassembling tip "tugged" the side of the ring causing it to slide processively along the microtubule (Figure 4E) (Grishchuk et al., 2008).

A recent EM tomographic reconstruction of kinetochores in PtK1 cells demonstrated the existence of fibrils linking the inner face of flared PFs to the inner plate of the kinetochore (Figure 4F,G) (McIntosh et al., 2008). It was proposed that the fibrils, whose molecular identity is unknown, might restrict the bending of PFs to promote PF stabilization, and could translocate towards the microtubule lattice when coupled to a depolymerising microtubule. Thus, slender fibrils might provide a synthesis between Hill's thermal ratchet model and the harnessing of force by microtubule depolymerization.

The molecular machinery of kinetochore-microtubule attachment

Several microtubule-associated proteins (MAPs), including EB1, CLASP, Ch-TOG/XMAP215, APC (adenomatous polyposis coli), Clip170, Nde1/Ndel1 and Lis1, and the kinesin-13 kinesins Kif2a and MCAK, which are devoid of microtubule motor activity but rather act as microtubule de-stabilizers, have been implicated in the control of kinetochore microtubule dynamics (reviewed in Maiato et al., 2004). On the other hand, none of the MAPs identified at mitotic kinetochores appears to be essential for forming load-bearing kinetochore-microtubule attachments (Cheeseman and Desai, 2008).

While ATP-powered molecular motors could in principle couple kinetochores to disassembly microtubule tips (Lombillo et al., 1995), most if not all chromosome motion after metaphase

alignment, and in particular poleward movement at anaphase, is due to the ability of kinetochores to remain attached to assembling or disassembling microtubules (Coue et al., 1991; Koshland et al., 1988). Consistently, minus-end directed motors are dispensable for poleward chromosome translocation in yeast (Grishchuk and McIntosh, 2006; Tanaka et al., 2007).

The dispensability of MAPs and motors for generating load-bearing attachment indicates that kinetochores contain specialized machinery to deal with microtubule binding (Davis and Wordeman, 2007; Maiato et al., 2004). The KMN network complex (an acronym for Knl-1, Mis12, Ndc80) has emerged as a crucial components of such machinery (reviewed in Cheeseman and Desai, 2008). The KMN is a conserved 10-subunit assembly gathering 3 distinct sub-complexes, known as Knl1, Mis12 and Ndc80 (Figures 1B and 2D) (Cheeseman et al., 2004; De Wulf et al., 2003; Desai et al., 2003; Liu et al., 2005; Nekrasov et al., 2003; Obuse et al., 2004; Pinsky et al., 2003; Przewloka et al., 2007; Westermann et al., 2003). Preventing kinetochore recruitment of the microtubule-binding component of the KMN network by RNAi or other methods results in a kinetochore-null phenotype, i.e. load-bearing kinetochore-microtubule attachments cannot be formed and kinetochores exhibit only residual, motor-driven motility (Cheeseman et al., 2006; Cheeseman et al., 2004; DeLuca et al., 2005; DeLuca et al., 2006; Desai et al., 2003; Emanuele et al., 2005; Kerres et al., 2004; Kline et al., 2006; McCleland et al., 2003; Vorozhko et al., 2008; Wigge and Kilmartin, 2001).

The ~170 kDa Ndc80 complex contains 4 subunits: Ndc80 (also known as Hec1), Nuf2, Spc24 and Spc25 (Figure 5A). It is a stable sub-complex of the KMN network (Ciferri et al., 2005; Wei et al., 2005) and it adopts a ~60-nm dumbbell shape that crosses the kinetochore vertically from the inner to the outer plate (Ciferri et al., 2005; Ciferri et al., 2008; DeLuca et al., 2006; Joglekar et al., 2009; Schittenhelm et al., 2007; Wei et al., 2005). Two sub-complexes, containing the Spc24:Spc25 and Nuf2:Ndc80 subunits, respectively, occupy opposite ends of the dumbbell (Ciferri et al., 2005; Wei et al., 2005). Globular domains in each of these sub-

complexes flank extended coiled-coil regions that meet in a tetramerization domain within the central shaft (Figures 5A-B).

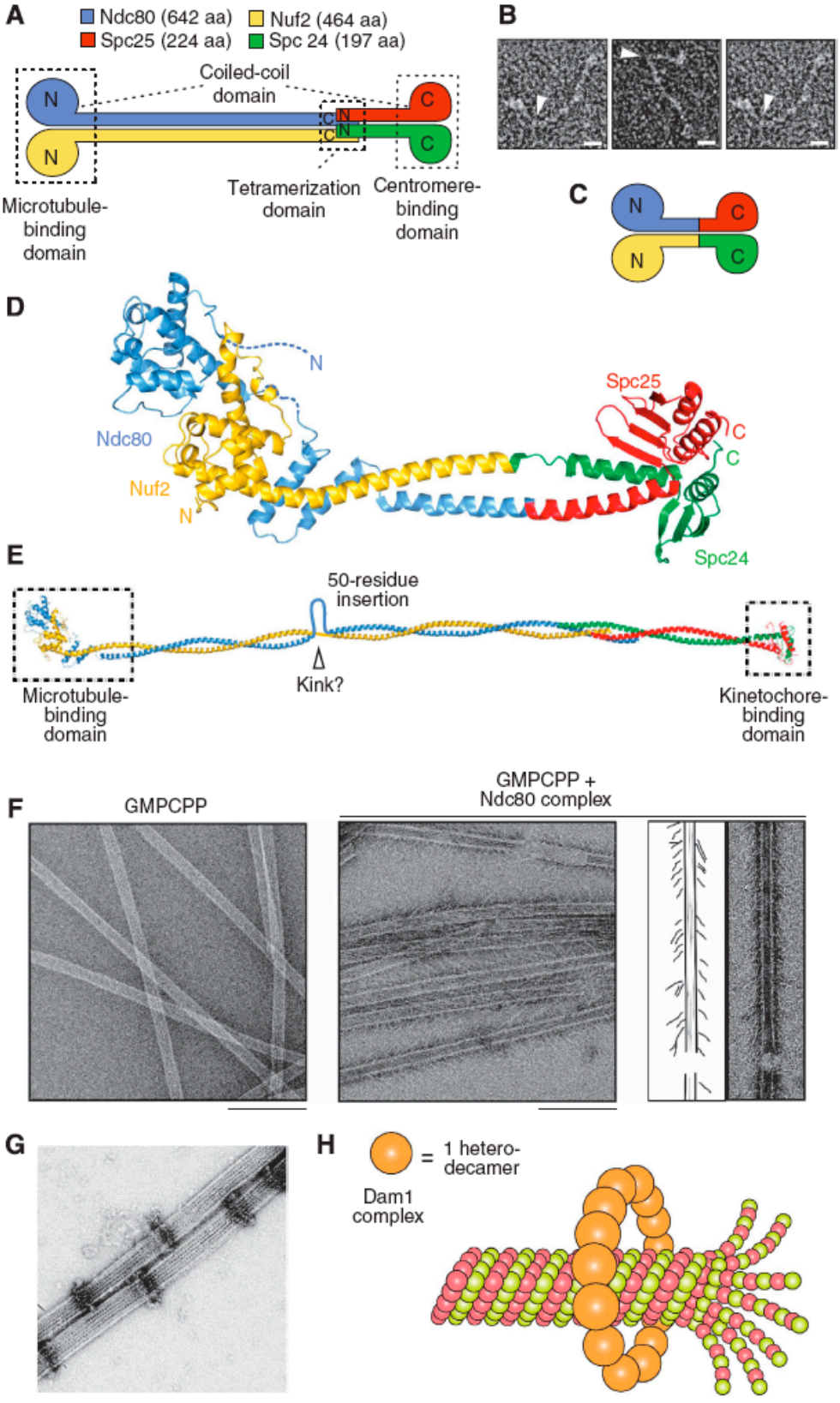

Figure 5 The molecular machinery of kinetochore-microtubule attachment

(**A**) Topology of the Ndc80 complex. Ndc80 and Nuf2 engage in a dimer. They contain N-terminal CH domains followed by a coiled-coil region that mediates inter-subunit interactions. Spc24 and Spc25 have N-terminal coiled-coils that mediate inter-subunit interactions, followed by globular domains that are responsible for binding to the Mis12 complex. Tetramerization engages the C-terminal region of the Ndc80:Nuf2 dimer and the N-terminal region of the Spc24:Spc25 dimer. aa =amino acids. N and C indicate the N- and C-termini, respectively. Panels A and D were reproduced from (ref. Ciferri et al., 2008). (**B**) Gallery of three individual Ndc80 complexes. Arrowheads mark a prominent kink along the shaft. The scale bar corresponds to 10 nm. The images are reproduced from (ref. Wang et al., 2008). (**C**) By fusing the C-termini of the Ndc80 and Nuf2 subunits to the N-termini of the Spc25 and Spc24 subunits, respectively, a "bonsai" version of the Ndc80 complex was created. Most of the coiled-coil in the central shaft was deleted. The resulting complex retains the ability to bind microtubules *in vitro* and to localize to kinetochores when injected into living cells (Ciferri et al., 2008). (**D**) Overall view of the 2.9 Å crystal structure of the bonsai-Ndc80 complex (PDB ID 2VE7). The two CH domains pack in a tight dimeric assembly. An 80-residue N-terminal disordered segment in the Ndc80 subunit escaped structure determination (dashed line). Together with the globular region of Ndc80:Nuf2, this segment contributes to microtubule binding. (**E**) A model of the full length Ndc80 complex. The model is based on previous electron microscopy work on the Ndc80 complex (Wang et al., 2008; Wei et al., 2005) and on a cross-linking and mass spectrometry analysis that identified the register of coiled-coil interaction within the central shaft (Maiolica et al., 2007). The regions contained in the crystal structure of bonsai-Ndc80 are boxed. The coiled-coil is interrupted by a 50-residue insertion in the Ndc80 sequence that increases the overall flexibility of the Ndc80 rod. (**F**) *Left*: Negatively stained control microtubules stabilized with GMPCPP, a non-hydrolysable GTP analogue that stabilizes the microtubule lattice. *Middle*: Negatively stained GMPCPP microtubules in the presence of 5 μM Ndc80 complex (*C. elegans*). The Ndc80 complex forms angled rod-like projections on the microtubule lattice. *Right*: Traces of the EM images depicting the angled rod-like complexes bound to the lattice. Scale bars represent 200 nm. Panel was reproduced from (ref. Cheeseman et al., 2006) (**G**) Negative stain electron microscopy of Dam1 rings assembled around microtubules *in vitro*. Bar = 50 nm. Panel reproduced from (ref. Westermann et al., 2005). (**H**) The Dam1 complexes are heterodecamers. They contain one copy each of 10 essential budding yeast proteins. Dam1 rings form by oligomerization of individual complexes around microtubules.

The Spc24:Spc25 dimer binds to the Mis12 and Knl1 complexes near the inner plate (Joglekar et al., 2009; Kiyomitsu et al., 2007; Schittenhelm et al., 2007). The Nuf2:Ndc80 dimer, on the

other hand, points outward and binds microtubules directly (Cheeseman et al., 2006; Ciferri et al., 2008; Wei et al., 2007). Structural work, including a structure of a "bonsai" Ndc80 complex (Figure 5C-6D) revealed that the microtubule-binding domain of Ndc80:Nuf2 combines an 80-residue unstructured basic region of Ndc80 (pI ~10.8) and two tightly packed calponin-homology (CH) domains, one in each chain (Figure 5C-6D) (Ciferri et al., 2008; Wei et al., 2007). Lysine residues in the two CH domains contribute to high-affinity microtubule binding (Cheeseman et al., 2006; Ciferri et al., 2008; Wei et al., 2007). On microtubules, the acidic C-terminal tails of tubulin subunits (so called E-hooks) are important for high-affinity binding to the Ndc80 complex (Ciferri et al., 2008; Powers et al., 2009; Wei et al., 2007).

Despite these advances, the exact mode of binding of microtubules by the KMN network remains unclear. A comparison of the crystal structure of the Ndc80:Nuf2 globular regions and three-dimensional EM maps obtained by helical reconstruction of Ndc80:Nuf2 bound to microtubules suggested that a binding mechanism involving both the CH domains of Ndc80 and Nuf2 is unlikely (Wilson-Kubalek et al., 2008). Other studies suggested that the basic N-terminal tail of Ndc80 might be sufficient for high-affinity microtubule binding, even in the absence of CH domains (Guimaraes et al., 2008; Miller et al., 2008). Finally, Knl1 may also contain a microtubule-binding region, but the boundaries of the region responsible are unknown (Cheeseman et al., 2006).

At high concentrations, the Ndc80 complex binds along the microtubule lattice of microtubules stabilized with taxol or non-hydrolysable GTP analogues (Figure 5F)(Cheeseman and Desai, 2008; Ciferri et al., 2008; Wei et al., 2007; Wilson-Kubalek et al., 2008). At low concentration, the Ndc80 complex shows a modest preference for depolymerizing plus ends of dynamic microtubules, a preference that is greatly enhanced when the Ndc80 complexes are cross-linked with antibodies (Powers et al., 2009). Beads coated with the Ndc80 complex undergo biased diffusion towards the minus-end of a depolymerising microtubule and can resist 0.5-2.5 pN of tensile force (McIntosh et al., 2008; Powers et al., 2009). As explained above, these observations suggest that Ndc80 acts as a Hill's

coupler. By quantitative fluorescence microscopy of GFP-tagged kinetochore proteins in *S. cerevisiae* and *S. pombe*, it was found that there are 6-8 copies of the KMN network per microtubule-attachment site, while approximately 30 KMN complexes per microtubule-attachment site are found at kinetochores in X. *laevis* extracts (Emanuele et al., 2005; Joglekar et al., 2008; Joglekar et al., 2006).

Besides the KMN network, other kinetochore-bound complexes have attracted considerable attention as microtubule-coupling devices at the kinetochore. Most notably, the Dam1 complex, an essential hetero-decameric complex of *S. cerevisiae*, has been extensively studied for its ability to form rings around microtubules (Figure 5) (Miranda et al., 2005; Westermann et al., 2005) and more generally for its support to the process of chromosome segregation (e.g. Asbury et al., 2006; Cheeseman et al., 2001; Franck et al., 2007; Grishchuk et al., 2008; Tanaka et al., 2007; Westermann et al., 2006). Approximately 16 hetero-decameric complexes have been predicted to account for a full ring around the microtubule, and this is also approximately the number of Dam1 complexes present at one microtubule-binding site in this organism (Joglekar et al., 2006; Westermann et al., 2006). Rings, however, have not been observed in electron tomograms of the *S. cerevisiae*'s kinetochore-microtubule interface and are not required for processive attachment of the Dam complex to microtubules (Gestaut et al., 2008; McIntosh, 2005; O'Toole et al., 1999). A bead coated with the Dam1 complex undergoes assembly- and disassembly-driven motility and remains coupled to a disassembling microtubule against a force of 0.5-3 pN (Asbury et al., 2006). Furthermore, high tension applied to the Dam1 complex stabilizes the microtubule plus end, an essential function of kinetochores as explained above (Franck et al., 2007). However, the generality of these findings is questioned by the observation that the Dam1 complex is conserved but is not essential in fission yeast (Gachet et al., 2008; Sanchez-Perez et al., 2005), and that homologues of the Dam1 complex have not been identified in higher eukaryotes.

The 3-subunit Ska complex (Figure 2D) was recently identified as a new microtubule-binding activity at metazoan kinetochores (Gaitanos et al., 2009; Hanisch et al., 2006; Theis et al.,

2009; Welburn et al., 2009). Ablation of the Ska complex by RNAi leads to a very severe attachment phenotype that is reminiscent of the kinetochore-null phenotype observed with Ndc80 complex depletions (Gaitanos et al., 2009; Theis et al., 2009; Welburn et al., 2009). Because the Ska complex is recruited to kinetochores via the Ndc80 complex, the implication is that the effects from inhibiting Ndc80 by RNA interference are the convolution of two phenotypes caused by loss of the Ndc80 complex as well as of the Ska complex. The Ska complex does not associate tightly with the Ndc80 complex and its association with kinetochores might be stabilized by microtubules (Gaitanos et al., 2009; Hanisch et al., 2006; Theis et al., 2009). It has been proposed that the Ska complex is a functional homologue of the Dam1 that can form rings around microtubules (Welburn et al., 2009), but this notion requires further evaluation.

Sli15p and Bir1p of *S. cerevisiae*, respectively homologous to INCENP and Survivin in higher eukaryotes, are part of a chromosome passenger complex (CPC), which also includes the Ipl1/Aurora B kinase, and in metazoans, an additional protein known as Borealin/DasraB/CSC-1 (Ruchaud et al., 2007; Vader et al., 2006). Sli15p and Bir1p possibly provide for an additional kinetochore-microtubule coupling mechanism (Sandall et al., 2006). Budding yeast centromeric (CEN) DNA binds to microtubules in a CBF3-dependent manner following incubation in a cell extract (Hyman et al., 1992; Kingsbury and Koshland, 1991; Severin et al., 1997; Sorger et al., 1994).

However, CBF3 is not sufficient, indicating that other factors are necessary to link CBF3-CEN DNA to microtubules (Sorger et al., 1994). The Bir1p:Sli15p complex was identified as a potential additional factor in linking the CBF3-CEN DNA complex to microtubules *in vitro* (Sandall et al., 2006). Indeed, Sli15p/INCENP contains a microtubule-binding site in its C-terminal region (Sandall et al., 2006).

While molecular motors are dispensable for anaphase chromosome movement, they play an important auxiliary role in the initial side-on capture of microtubules and in the congression of chromosomes to the metaphase plate. These functions require cytoplasmic Dynein, a minus-

end directed motor, and CENP-E, a plus-end directed motor, respectively (for examples, see Alexander and Rieder, 1991; Kapoor et al., 2006). The RZZ complex interacts with the KMN network to recruit Spindly, Dynein and the SAC proteins Mad1 and Mad2 to kinetochores. The coiled-coil protein Spindly is important for the coordination of the conversion of side-on to end-on attachments, but the molecular details of this process require further investigation (Civril and Musacchio, 2008; Gassmann et al., 2008; Griffis et al., 2007; Yamamoto et al., 2008).

Vertical and horizontal kinetochores

The architecture of the kinetochore, and most notably the relationship between the inner and outer plates, remains elusive. Our understanding of kinetochore assembly derives from proteomic analyses describing the composition of the more tightly interacting complexes and sub-complexes (see above). Furthermore, the effects from depleting certain kinetochore proteins on the (mis)localization of other kinetochore proteins have been extensively studied (e.g. Hori et al., 2008; Liu et al., 2006; McClelland et al., 2007; McIntosh et al., 2008). Although the results cannot always be univocally interpreted, they support a map of "epistatic" relationships in which the inner kinetochore components are indeed required for the localization of the outer kinetochore components (Figure 6A). For instance, CENP-A, CENP-T/W, CENP-C and the CCAN CENP-H/I/K proteins all contribute, to different extents, to the recruitment of the KMN network and associated proteins (e.g. Hayashi et al., 2004; Hori et al., 2008; Liu et al., 2003; Liu et al., 2006; McClelland et al., 2007; McIntosh et al., 2008; Mikami et al., 2005; Okada et al., 2006; Saitoh et al., 2005). In the absence of accurate physical maps of kinetochores, it is unknown whether the relationships described in Figure 6A correspond to actual physical contacts between complexes. Alternatively, the inner kinetochore proteins may contribute to an organization of the centromere-kinetochore interface that promotes the recruitment of the outer kinetochore proteins, for instance by mechanisms based on post-translational modification.

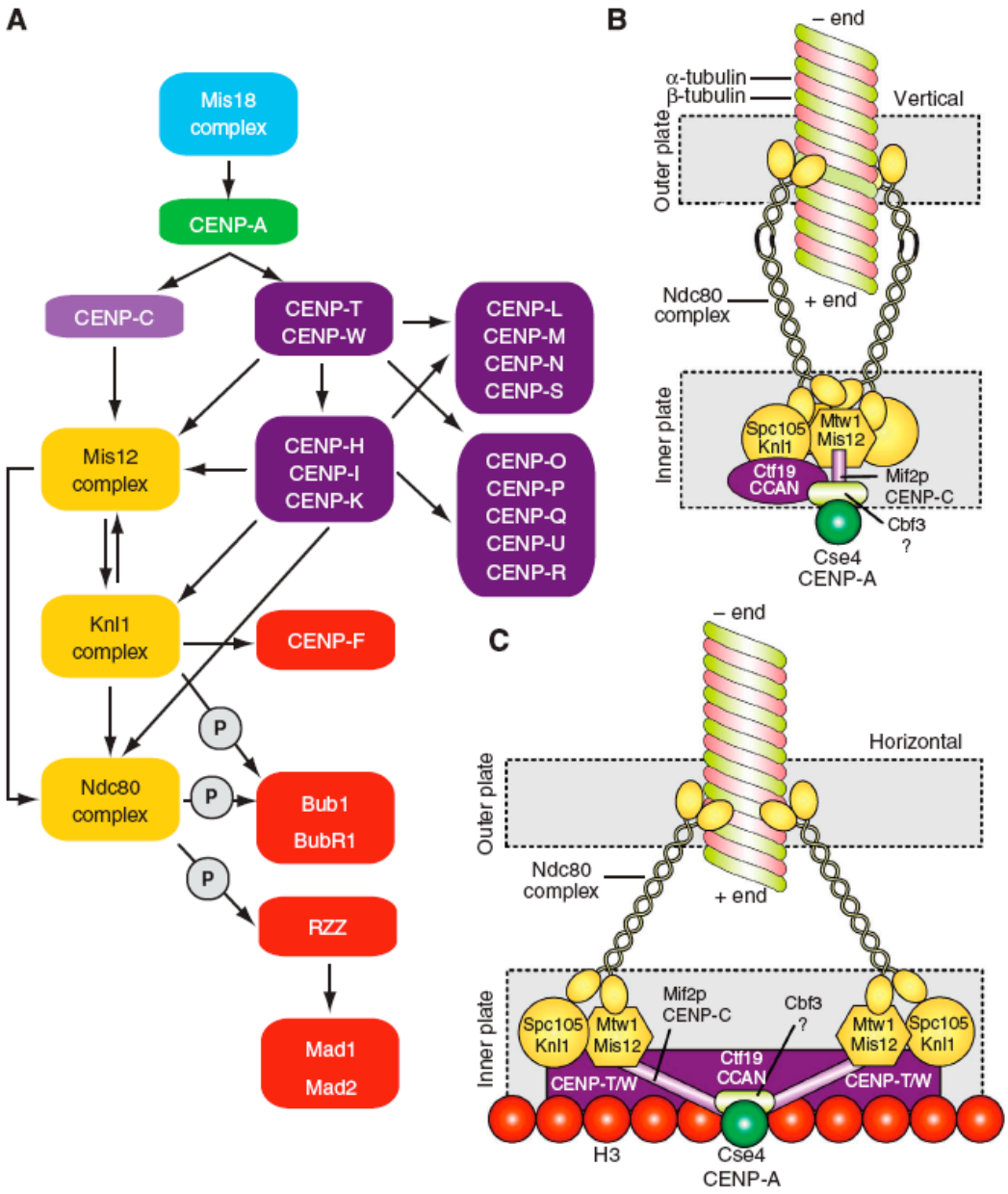

Figure 6 Models of kinetochore assembly

(**A**) "Epistatic" relationships between kinetochore proteins. Arrows indicate a dependency for localization, where the pointed end indicates a protein(s) that require proteins at the barbed end for kinetochore localiation. The list of proteins shown here is not comprehensive. The circles enclosing a "P" indicate post-translational modifications. (**B**) The vertical layout. Kinetochore proteins ultimately converge on a single Cse4p/CENP-A nucleosome (e.g. Joglekar et al., 2009). Given that there are 6-8 KMN network complexes per Cse4/CENP-A nucleosome, it is sensible to assume that this special nucleosome is placed directly below the microtubule, approximately on the same axis, with the different KMN network surrounding the microtubule roughly equidistantly (only two KMN complexes are shown here). **(C**) The horizontal model. Rather than being placed

along an idealized vertical line from the inner to the outer kinetochore, the kinetochore components are distributed horizontally. Specifically, the KMN network components are linked to the kinetochore core by Mif2p/CENP-C, but are also establishing specific contacts with H3 nucleosomes through CENP-T/W.

At least two alternative designs for kinetochores, both of which are compatible with the super-resolution microscopic analyses of the distribution of kinetochore proteins along the inter-kinetochore axis described in Figure 1C and 2E are conceivable (Joglekar et al., 2009; Schittenhelm et al., 2007). In discussing these kinetochore designs, which can be named "vertical" and "horizontal", one refers to an archetypical single-microtubule binding unit. The kinetochore of *S. cerevisiae* provides a useful framework for such a unit, but I implicitly adopt the idea that kinetochores binding multiple microtubules are at least in part modular and that they contain an array of equivalent units (see below).

In the "vertical" kinetochore (Figure 6B), the components of the inner and outer kinetochore are recruited sequentially onto the CENP-A platform along a vertical plan of assembly. In this model, CENP-A provides the physical basis for the recruitment of all additional kinetochore proteins, starting from the inner kinetochore (CCAN and CENP-C) and continuing with the KMN network. In this model, strong physical contacts between the inner and outer kinetochore layers are likely, because the forces exercised by bound microtubules converge directly, through the outer kinetochore, on the single specialized CENP-A nucleosome and associated CENP-C and CCAN. Indeed, CENP-C (Mif2p in *S. cerevisiae*) has been identified as a low-abundance component of KMN precipitates, as well as a binding partner of Cse4/CENP-A (Ando et al., 2002; Cheeseman et al., 2004; Westermann et al., 2003), and may therefore act as a linker between inner and outer kinetochores. A puzzling aspect is that with only 1-2 molecules per Cse4 nucleosome, CENP-C is significantly sub-stoichiometric with respect to KMN network complexes (Joglekar et al., 2006).

Another possible linkage between the inner and outer kinetochore is provided by the reported interaction between Nuf2 and CENP-H (Mikami et al., 2005). However, linkages involving

CCAN subunits are unlikely, because the ablation of the CCAN subunits affects but does not abolish the recruitment of outer kinetochore components, including KMN network subunits, and the resulting phenotypes are clearly distinct (Hayashi et al., 2004; Liu et al., 2003; Liu et al., 2006; McClelland et al., 2007; McIntosh et al., 2008; Mikami et al., 2005; Okada et al., 2006; Saitoh et al., 2005). For instance, while Ndc80-depleted cells are unable to form a metaphase plate, cells depleted of CCAN subunits have milder chromosome congression and segregation phenotypes and can form stable attachments (Foltz et al., 2006; Fukagawa et al., 2001; Liu et al., 2003; McClelland et al., 2007; Minoshima et al., 2005; Nishihashi et al., 2002; Okada et al., 2006).

An objection to the vertical model is that force exercised by a bound microtubule through the KMN network components converges onto a single Cse4p/CENP-A nucleosome, rather than being distributed over a larger attachment site. A related prediction is that the microtubule (25-nm diameter) connects to the Cse4p/CENP-A nucleosome, a much smaller structure (10 nm or less) (Bloom et al., 2006). If the single Cse4p nucleosome broadly lies along the microtubule's long axis, the KMN complexes would have to radiate from this central point outward to be able to bind to the external wall of the microtubule (Figure 6B). This geometry is inconsistent with that observed upon reconstitution of the interaction of recombinant Ndc80 complexes with microtubules *in vitro*, and showing that individual Ndc80 complexes bind microtubules with a 20-60° angle (Figure 5F) (Cheeseman et al., 2006; Wilson-Kubalek et al., 2008). If this binding mode also existed in cells, the Spc24:Spc25 globular regions would project onto the kinetochore at a distance of 20-40 nm from the microtubule axis and therefore from the Cse4p/CENP-A nucleosome.

In the "horizontal" model, this geometric limitation is resolved by placing the KMN complexes away from the "central" CENP-A nucleosome, anchoring them to H3 nucleosomes surrounding the CENP-A nucleosome (Figure 6C). A desirable feature of this design is that microtubule-generated pulling forces are distributed over several distinct contact points rather than on a single point as in the vertical model. The CENP-T:CENP-W dimer

has been recently shown to contribute to the stability of the outer plate, as previously observed for the Ndc80 complex (DeLuca et al., 2005; Hori et al., 2008). CENP-T and CENP-W are homologous proteins showing sequence similarity to the Negative Cofactor 2 (NC2) complex, which contains a histone-fold domain. Budding yeast homologues of these proteins have not been identified.

CENP-T was originally purified using CENP-A as bait (Foltz et al., 2006), possibly due to co-purification with CENP-A upon partial micrococcal nuclease cleavage. On more stringent analyses, however, the CENP-T:CENP-W dimer revealed an association with H3 nucleosomes (Hori et al., 2008). CENP-C was also found in contact with H3 nucleosomes, in agreement with its role in recruiting the KMN network. Direct association between CENP-C and the CENP-T:CENP-W complex have not been identified (Hori et al., 2008). In summary, the CENP-T:CENP-W complex may contribute to creating a binding site for KMN network and associated proteins on H3 nucleosomes surrounding CENP-A. An indirect confirmation of this model derives from the observation that the KMN network interacts with HP1 (heterochromatin protein 1), a protein that binds to the methylated form of Lys9 of histone H3 (Obuse et al., 2004; Przewloka et al., 2007).

The organization of kinetochores that bind multiple microtubules

The question whether regional centromere/kinetochores containing multiple microtubule-binding sites (Figures 7A-B) are built from the repetition of a simpler functional unit remains open. The existence of a regularly repeated microtubule-binding unit has not emerged from tomographic reconstructions of the outer plate, which instead depicted the microtubule-binding interface of the outer kinetochore as a disorganized "velcro" or "spider's web" for microtubule attachment (Figure 2C) (Dong et al., 2007).

On the other hand, similarity in composition, abundance ratios, and epistatic relationships of kinetochore complexes with relatively minor differences from yeast to humans, suggests that

at least the hierarchical relationship between different kinetochore layers is maintained from point to regional centromere/kinetochores. For instance, the ratio between KMN components and the core subunits of the kinetochore (e.g. CENP-A) is conserved in yeasts with point and regional centromeres, and has lead to suggest that the kinetochore of *S. pombe* contains 3 to 5 units modelled on the single microtubule-binding site of *S. cerevisiae* (Joglekar et al., 2008). Furthermore, kinetochore proteins occupy relative analogous positions within the kinetochore layouts of the point centromere/kinetochore of *S. cerevisiae* and the regional centromere/kinetochore of *D. melanogaster* (Figures 1C and 2E) (Joglekar et al., 2009; Schittenhelm et al., 2007).

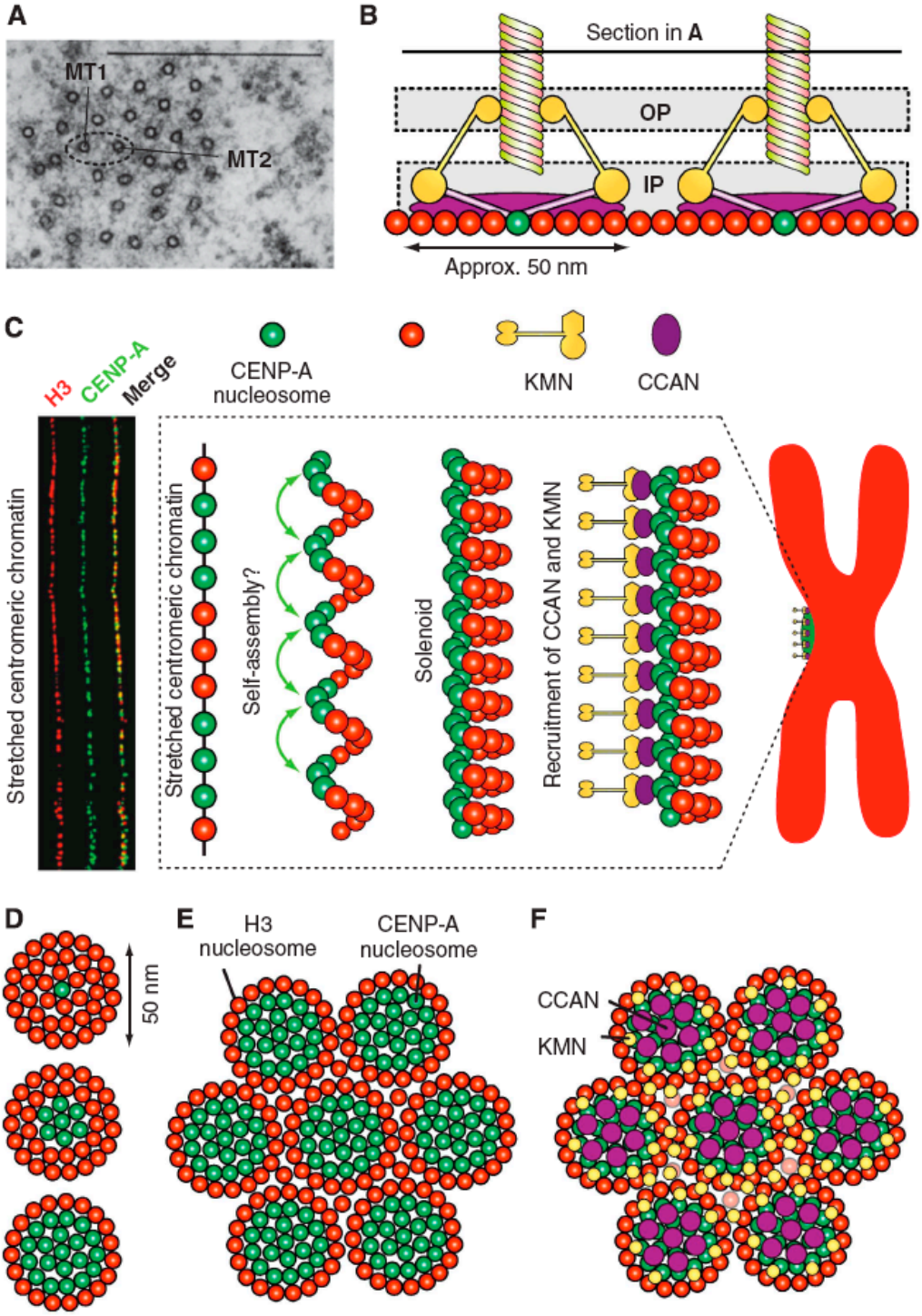

Figure 7 Speculative "repeat subunit" models

(**A**) A transverse section through the K-fibre of a metaphase PtK1 cell, showing multiple microtubules. Bar = 0.5 μM, magnification 60000x. Source of figure is (ref. Rieder, 1981). (**B**) Horizontal clustering of modules (only two are shown) may explain the distribution of microtubules in the K-fibre shown in **A**. (**C**) The solenoid model. *Left*: Centromere stretching experiment indicating that the array of CENP-A nucleosomes, coalesced in three-dimensional space, are not contiguous along the DNA but are interrupted by spacers containing blocks of H3-containing nucleosomes. The image was reproduced from (ref. Blower et al., 2002). *Rigth*: CENP-A nucleosome coalescence could be entirely self-directed, or alternatively, it might necessitate the action of bridging factors - perhaps components of the CCAN - to organize into the array that forms the foundation of the mitotic

kinetochore. The panel is an adaptation from (ref. Black and Bassett, 2008). (**D**) Three distinct hypothetical patterns of CENP-A and H3 nucleosomes with different ratios of H3 to CENP-A. CENP-A is always shown at the centre, and is surrounded by H3. (**E**) The pattern at the bottom of panel **D** is now shown to "coalesce" in a larger assembly. (**F**) Speculative pattern of deposition of CCAN and KMN modules on the pattern shown in **E**. CCAN is on CENP-A nucleosomes, whereas KMN goes to H3 nucleosomes.

Regional centromere/kinetochores can disassemble into smaller "units" if their connection with centromeric chromatin is artificially loosened (O'Connell et al., 2008; Zinkowski et al., 1991). The actual structural organization of the "units" has not been elucidated. However, chromatin fibre analyses of centromeric chromatin in humans and flies suggest that CENP-A comes in discrete blocks that alternate with H3-containing blocks (Figure 7C) (Blower et al., 2002). It has been proposed that CENP-A and H3 might be sorted on different faces of an "amphipathic" super-helical arrangement of centromeric chromatin, a solenoid in which the CENP-A containing face will be facing outward towards the kinetochore, and the H3 containing face will be embedded in the centromere (Figure 7C) (Blower et al., 2002; Marshall et al., 2008; Zinkowski et al., 1991).

The solenoid model neglects the emerging role of H3 in the assembly of the outer kinetochore (see above). An alternative speculative model is that CENP-A nucleosomes are surrounded by H3 nucleosomes to create the centromeric-inner kinetochore moiety of a microtubule-binding unit. Three possible examples of this organization, with progressively larger numbers of CENP-A nucleosomes, are illustrated in Figure 7D. The functional units, in turn, might coalesce into a larger array (Figure 7E). If the KMN network is recruited to H3 nucleosomes, this type of construction in the inner kinetochore might be directing the KMN network complexes to the edges of each microtubule-binding unit (Figure 7F). There are 6-8 KMN complexes per microtubule binding site (Joglekar et al., 2008; Joglekar et al., 2006). The speculative configuration of the centromere/inner kinetochore in Figure 7E would position the KMN complexes at the appropriate distance from a microtubule-binding site identified by a "hole" in the distribution of the KMN network complexes in correspondence of the CENP-A/CCAN complexes in the underlying chromatin (Figure 7F). The "holes" would allow

microtubules to penetrate deeply within the outer kinetochore surface, allowing the KMN complexes to surround the microtubule to stabilize the end-on configuration. Because the KMN network complexes are elongated, flexible fibrous structures, the "holes" may be difficut to visualize in tomographic reconstructions of the outer plate in the absence of microtubules (Dong et al., 2007).

Feedback controls in mitosis

Fidelity of cell division is due to feedback controls. The first control mechanism halts the process of cell division and instates a mitotic arrest when chromosome-microtubule attachment is perturbed in different ways (reviewed in Rieder and Palazzo, 1992). This ability of eukaryotic cells configures a checkpoint (Hartwell and Weinert, 1989; McIntosh, 1991; Rieder and Palazzo, 1992), generally known as the spindle assembly checkpoint (reviewed in Musacchio and Salmon, 2007), and herewith often abbreviated as "spindle checkpoint" or simply "checkpoint". The checkpoint cannot be satisfied under conditions that perturb chromosome-microtubule attachment, most typically the depolymerization of microtubules (lack of attachment). In humans, spindle checkpoint components include enzymes, such as the BUB1, BUBR1, MPS1, and PRP4 kinases, and protein-protein interaction devices such as BUB3, MAD1, MAD2, and the 3-subunit ROD-ZWILCH-ZW10 (RZZ) complex (Musacchio and Salmon, 2007).

During prometaphase, the checkpoint proteins are recruited to unattached kinetochores, large protein assemblies built on chromosomal *loci* known as centromeres (Cleveland et al., 2003). An approximately 550-kDa, 10-subunit assembly, the KMN network (from the initials of its sub-complexes, the Knl1, Mis12, and Ndc80 complexes), provides the microtubule-binding core of the outer kinetochore (Santaguida and Musacchio, 2009). Kinetochore recruitment of the checkpoint proteins is an obligatory condition for sustained checkpoint signalling. Its

impairment invariably leads to a failure in the checkpoint response (for examples and discussions, see Meraldi et al., 2004).

Spindle checkpoint activity converges on the generation of an APC/C inhibitor known as the mitotic checkpoint complex (Musacchio and Salmon, 2007). Mad2, BubR1 and Bub3 contribute, in different ways, to the formation of the mitotic checkpoint complex. Cdc20, the target of the checkpoint proteins in the mitotic checkpoint complex, is a positive regulator of the APC/C (anaphase-promoting complex/cyclosome), an ubiquitin-ligase whose activity is required for progression into anaphase. By inhibiting Cdc20, the spindle checkpoint prevents APC/C activation towards crucial substrates for anaphase such as Cyclin B and Securin, and, consequently, mitotic exit (Musacchio and Salmon, 2007).

The second control mechanism, generally referred to as "error correction", prevents the stabilization of kinetochore-microtubule attachments unless they are under full tension (Li and Nicklas, 1995; Nicklas and Koch, 1969). Improper kinetochore-microtubule attachments, such as merotelic or syntelic attachments, are probably distinguished from proper attachments (amphitelic attachment, or biorientation) because they are not under full tension. The molecular basis of (de)stabilization of improper attachments is being actively investigated. The first protein to become clearly implicated in this process was the AURORA B kinase (reviewed in Ruchaud et al., 2007). AURORA B is a member of the AURORA-family of S/T kinases, which also includes the ubiquitously expressed AURORA A, involved in spindle bipolarization, and AURORA C, whose role is poorly understood but likely limited to meiosis (Ruchaud et al., 2007). AURORA B is part of the chromosome passenger complex, whose subunits also include INCENP, SURVIVIN and BOREALIN (Ruchaud et al., 2007). Inactivation of Ipl1, the only AURORA kinase in *S. cerevisiae*, leads to the stabilization of syntelic attachments, implicating Ipl1 in their correction (Tanaka et al., 2002). In vertebrates, inhibition of AURORA B by small molecules or RNAi leads to the accumulation of merotelic and syntelic attachments (Cimini et al., 2006; Ditchfield et al., 2003; Hauf et al., 2003; Knowlton et al., 2006; Lampson et al., 2004). The regulation of microtubule-destabilizing

enzymes known as MCAK and KIF2B by AURORA B may be important for correction (reviewed in Kelly and Funabiki, 2009; Pinsky and Biggins, 2005; Vader and Lens, 2008). Furthermore, AURORA B phosphorylates NDC80, a subunit of the KMN network, on at least 6-8 sites near the microtubule-binding interface, causing a strong decreases of microtubule-binding affinity (Cheeseman et al., 2006; Ciferri et al., 2008; DeLuca et al., 2006; Guimaraes et al., 2008; Miller et al., 2008). Thus, stabilization of kinetochore-microtubule attachment might be concomitant with NDC80 dephosphorylation.

Besides being implicated in the spindle assembly checkpoint, BUB1, BUBR1, and MPS1 have also been shown to take part in bi-orientation and possibly in error correction (reviewed in Kang and Yu, 2009). The detailed mechanisms through which these proteins may contribute to these functions are being actively investigated. For instance, it was recently proposed that MPS1 acts upstream of AURORA B to control AURORA B function in bi-orientation (Jelluma et al., 2008).

The molecular bases of feedback control of kinetochores: error correction

The ability to discriminate between correct and incorrect microtubule attachments, selectively stabilizing the former and preventing the stabilization of the latter, is crucial for chromosome stability during cell division (Li and Nicklas, 1995; Nicklas and Koch, 1969). Attachment errors, such as syntelic and merotelic attachments, can be artificially stabilized in high numbers if the activity of the Aurora B kinase is inhibited with a small molecule inhibitor (e.g. Cimini et al., 2006; Ditchfield et al., 2003; Hauf et al., 2003; Lampson et al., 2004). In a revealing assay, re-activation of Aurora B results in the correction of improper attachments after inhibitor washout (Lampson et al., 2004). A similar accumulation of attachment errors is generated when temperature-sensitive mutants of Ipl1, the only Aurora kinase of *S. cerevisiae*, are exposed to the non-permissive temperature (Tanaka et al., 2002). These studies implicate Ipl1/Aurora

B as an essential component of the error correction mechanism required to prevent the stabilization of improper attachments.

The exact molecular details of the correction mechanism are elusive, but the regulation of microtubule binding factors at the kinetochore is probably crucial (Kelly and Funabiki, 2009). For instance, Aurora B phosphorylates the basic N-terminal tail of Ndc80, neutralizing the positive charge and lowering the affinity of Ndc80 for microtubules (Cheeseman et al., 2006; Ciferri et al., 2008; DeLuca et al., 2006). Aurora B also controls the activity of MCAK and Kif2a, two kinesin-13 family members that are implicated in the regulation of the stability of kinetochore microtubule (Andrews et al., 2004; Bakhoum et al., 2009; Huang et al., 2007; Knowlton et al., 2006; Knowlton et al., 2009; Lan et al., 2004; Ohi et al., 2003; Zhang et al., 2007). Overall, these interactions may modulate the binding affinity of kinetochores for microtubules, as well as the dynamics of the microtubule plus end.

The molecular bases of feedback control of kinetochores: the spindle checkpoint

The challenge of studies on feedback control at kinetochores is to explain their dynamic relationship with the molecular machinery controlling microtubule attachment, a task now made easier by the identification of the likely key players of kinetochore-microtubule attachment (reviewed in Cheeseman and Desai, 2008; Tanaka and Desai, 2008). Emphasizing the tight relationship between feedback control mechanisms and microtubule attachment, the majority of SAC proteins are recruited to the Knl1/Mis12/Ndc80 (KMN) complex (as discussed in Burke and Stukenberg, 2008).

Since the early days, the relationship of the error correction machinery with the SAC has proved a great intellectual challenge and a topic of speculation (McIntosh, 1991; Rieder and Palazzo, 1992). It is widely believed that Aurora B has an indirect role in SAC control. Specifically, Aurora B may elicits SAC signalling when, by destabilizing improper tensionless

kinetochore-microtubule attachments, it creates unattached kinetochores that in turn recruit *bona fide* checkpoint proteins such as the products of the *MAD* and *BUB* genes, which then combine to halt cell cycle progression (Pinsky and Biggins, 2005; Pinsky et al., 2006). As observed above, however, unattached kinetochores are also tensionless, and Aurora B is active at kinetochores of nocodazole-treated cells, which lack any attachment (Liu et al., 2009a).

This raises the question whether Aurora B activity is directly implicated in SAC control. In agreement with this hypothesis, Aurora B is required for kinetochore recruitment of SAC proteins in the presence of microtubule-depolymerizing drugs (Ditchfield et al., 2003; Hauf et al., 2003), which in turn is an absolute requirement for SAC activation (e.g. Meraldi et al., 2004). Overall, these observations suggest a direct involvement of Aurora B in SAC control, reinforcing the link between error correction and SAC control. Evidence that Aurora B is required to maintain the SAC from unattached kinetochores is available in fission yeast and *Xenopus* (Kallio et al., 2002; Petersen and Hagan, 2003). In other organisms, it has been difficult to demonstrate a SAC override when inhibiting Aurora B (as discussed in Kelly and Funabiki, 2009; Pinsky and Biggins, 2005). However, this may be a consequence of residual kinase activity after an incomplete depletion of Aurora B.

Because the ability of Aurora B to correct improper attachments might be based on increased distance from its kinetochore substrates, it is logical to ask whether its function in the SAC is regulated in the same manner. In complete agreement with this idea, it was shown recently that intra-kinetochore stretching is crucial for determining the state of checkpoint signalling as well as the state of kinetochore phosphorylation (Maresca and Salmon, 2009; Uchida et al., 2009).

Reversine as a tool to study the relationship between the SAC and the error correction machinery

Reversine, a 2,6-disubsituted purine (Figure 8), has been originally identified for its ability to facilitate the de-differentiation of C2C12 myoblast into multipotent cells capable of re-differentiating into different cell types (Chen et al., 2007; Chen et al., 2004). Recently, this property of Reversine was attributed to its ability to inhibit the AURORA B kinase (Amabile et al., 2009; D'alise et al., 2008). This spurred my interest in testing the mitotic effects of Reversine, and I set out to test whether Reversine had additional mitotic targets besides AURORA B. As discussed below, in the course of this analysis I realized that Reversine is a very potent and relatively selective ATP-competitive inhibitor of human MPS1. The mitotic effects of Reversine are consistent with the idea that MPS1 is its principal target in mitosis, as shown below. Our results demonstrate that MPS1 is indeed a checkpoint component required for the recruitment of other checkpoint proteins, including the subunits of the RZZ complex and MAD1:MAD2, to unattached kinetochores. I also showed that MPS1 is implicated in bi-orientation and in error correction. My results are consistent with a model in which MPS1 operates downstream from AURORA B, and suggest that the error correction and the spindle checkpoint may respond to a single upstream sensor designed to detect lack of attachment and lack of tension.

Results

Reversine is a potent Mps1 inhibitor *in vitro*

The 2,6-disubstituted purine Reversine (Figure 8) has been shown to be an AURORA kinases inhibitor (Amabile et al., 2009; D'Alise et al., 2008).

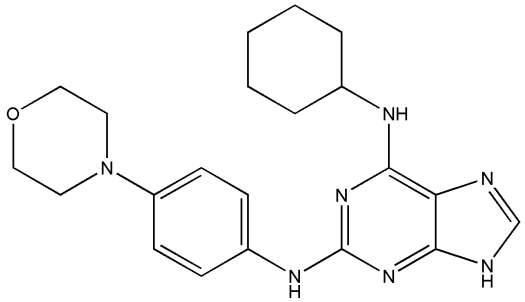

Figure 8 Chemical structure of Reversine

To further characterize AURORA kinases inhibition, I measured the potency of Reversine on AURORA kinases in an *in vitro* kinase assay. To do that, growing concentrations of Reversine were tested against recombinantly expressed human AURORA A/TPX2 complex and AURORA B/INCENP complex in an *in vitro* kinase assay using histone H3 as substrate. IC50 values were calculated from the dose-response curves (Figure 9 shows AURORA B curve; AURORA A curve is reported in Figure 10).

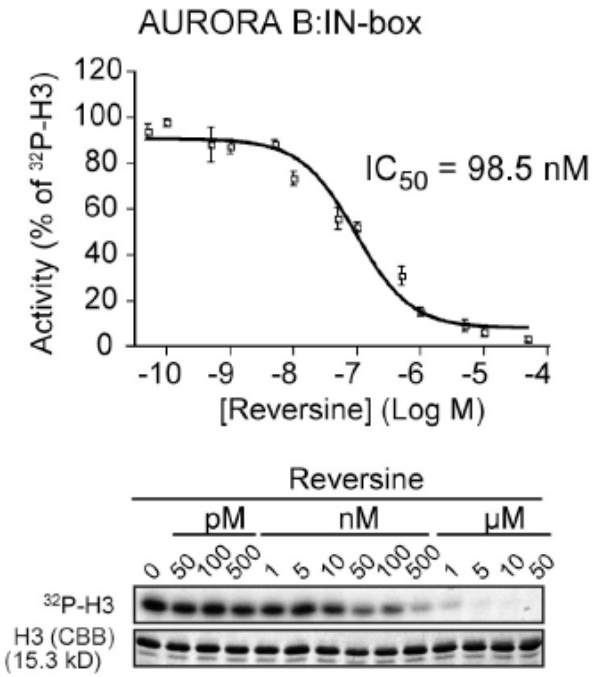

Figure 9 Reversine inhibits AURORA B in vitro

A kinase assay on human AURORA B^{1-344}-$INCENP^{835-903}$ complex with the indicated concentrations of Reversine. The substrate is Histone H3. CBB: Coomassie Blue Brilliant

In the tested conditions, AURORA A and AURORA B were inhibited with an IC50 of 876 nM and 98.5 nM, respectively. I then compared these values with those of well know and widely used AURORA inhibitors, namely ZM447439 (Ditchfield et al., 2003), Hesperadin (Hauf et al., 2003) and VX-680 (Harrington et al., 2004) (Figure 10).

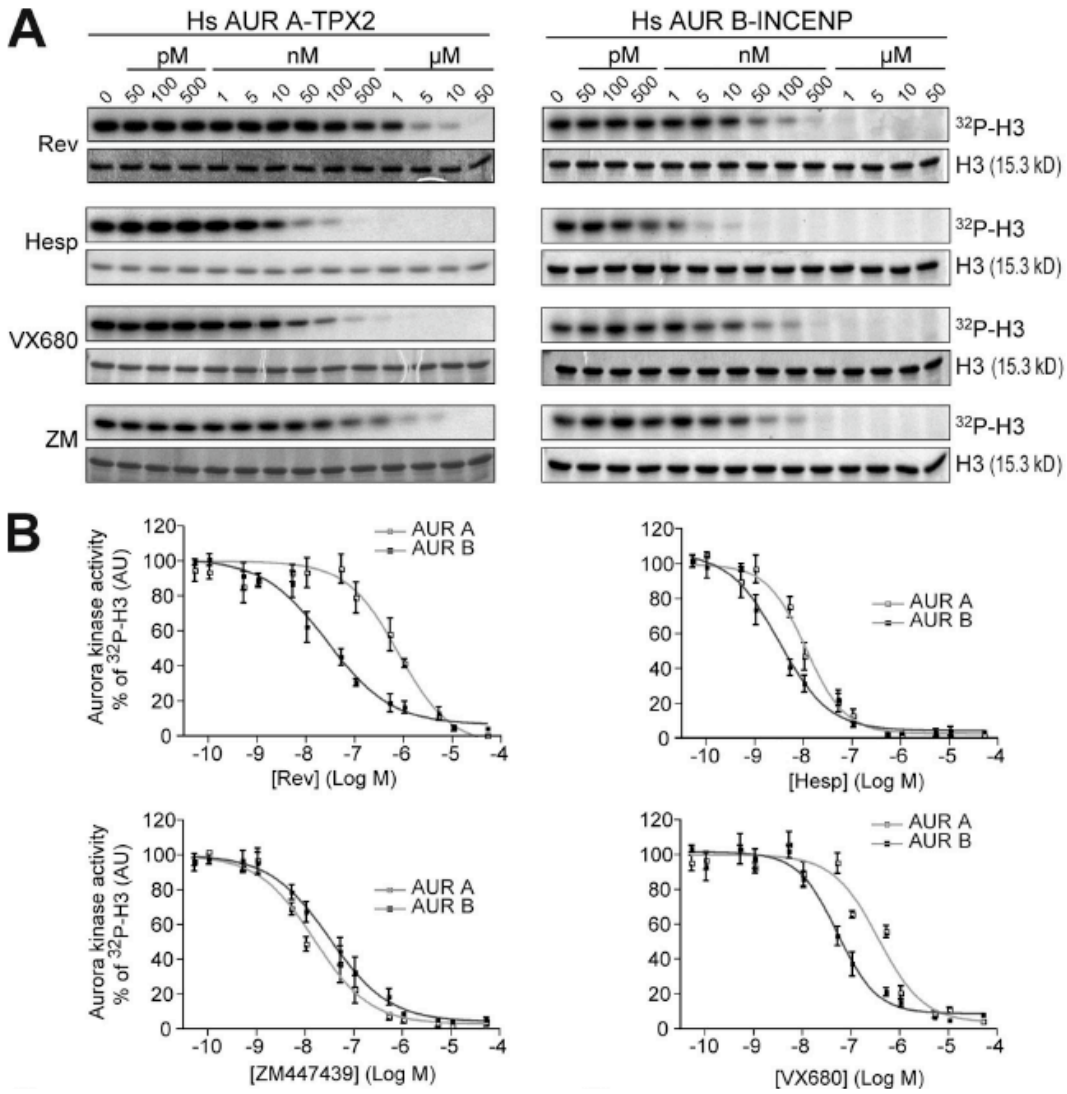

Figure 10 In vitro kinase assays of different AURORA inhibitors compared to Reversine

(A) A kinase assay on human AURORA A (AUR A)–TPX2 (Bayliss et al., 2003) and human AURORA $B^{1–344}$–$INCENP^{835–903}$ complexes with the indicated inhibitors. For each inhibitor, the incorporation of γ-[^{32}P]ATP is shown in the top panel, and the levels of substrate are loaded in the bottom panel. (B) Data from the experiments in A were plotted as a function of inhibitor concentration. IC50 values extrapolated from these curves are collected in Table I.

Under the same experimental conditions used to calculate the IC50 for Reversine, I found that Hesperadin, VX-680 and ZM447439 inhibit AURORA B with IC50 values ~30-fold, 3-fold and 2 fold below the IC50 of Reversine (Table I).

Inhibitor	AUR A–TPX2	AUR $B^{45–355}$–INCENP$^{835–903}$	AUR $B^{1–355}$–INCENP$^{835–903}$	MPS1 kinase domain	fl-MPS1
	nM	*nM*	*nM*	*nM*	*nM*
Rev	876	27	98.5	6	2.8
Hesp	11	3	ND	>1,000	>1,000
VX680	15	31	ND	>1,000	ND
ZM447439	360	51	46[a]	>1,000	ND

Table 1 IC50 values for the combination of different inhibitors and kinases

I then decided to further extend the *in vitro* inhibition studies to other mitotic kinases in order to determine whether Reversine inhibits only AURORA B among the mitotic kinases. To measure the ability of Reversine to inhibit other mitotic kinases, I tested a library of human mitotic kinases, including BUB1, CDK1-CYCLIN B, HASPIN, MPS1, NEK2A, PLK1, PRP4 and TAO1. Among the tested kinases, I noticed that 1 μM Reversine inhibited the kinase activity of MPS1 without affecting other kinase activities (Figure 11).

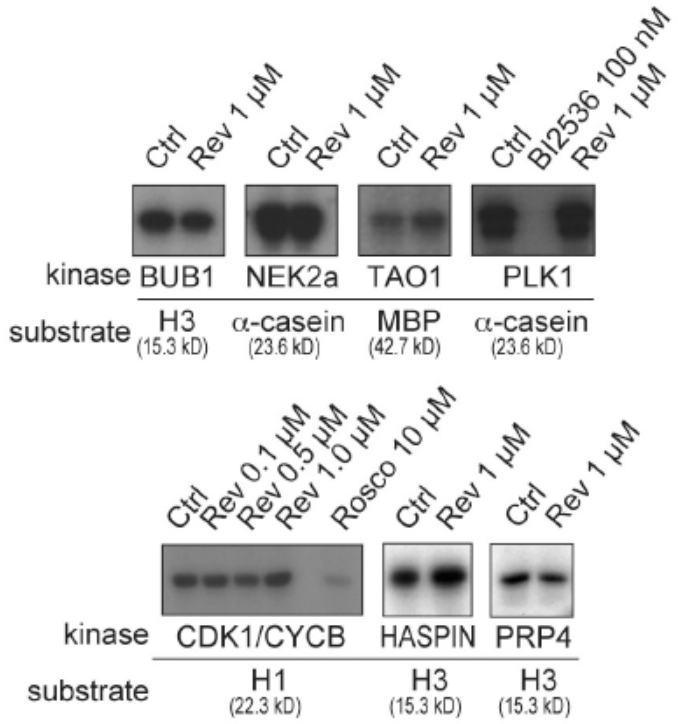

Figure 11 In vitro kinase assay of Reversine against different mitotic kinases

The indicated recombinant, purified mitotic kinases were tested with the indicated substrates for their sensitivity to 1 µM Reversine. None of the kinases were significantly inhibited. Specific inhibitors against PLK1 (BI2536) and CDK1 (Roscovitin) were used as positive controls.

Therefore, I set out to measure the IC50 value of Reversine against the kinase domain or the full-length versions of MPS1 *in vitro*. MPS`1 was inhibited *in vitro* by Reversine with an IC50 of 6 nM and 2.8 nM for its kinase domain and full-length, respectively (Figure 12). These data indicate that Reversine inhibits the full-length version of MPS1 with an IC50 ~35-fold below the IC50 value found for AURORA B inhibition.

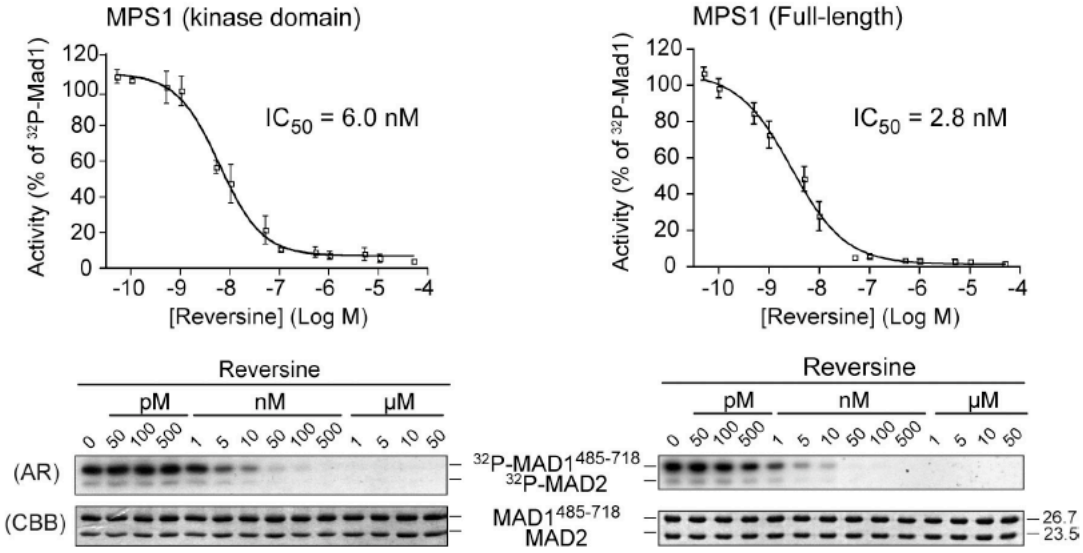

Figure 12 Reversine inhibits Mps1 in vitro

A Reversine titration experiment on the kinase domain of MPS1 (left panel) or full-length MPS1 (right panel). The substrate is the MAD1:MAD2 complex. AR = autoradiography; CBB = Coomassie Brilliant Blue staining.

Submicromolar concentrations of Reversine do not inhibit Aurora B in living cells

The *in vitro* inhibition analyses suggested that Reversine is a potent MPS1 inhibitor; nonetheless, the concurrent inhibition of AURORA B could impinge the possibility to exploit this small molecule as a selective MPS1 inhibitor in living cells. However, the ~35-fold selectivity *in vitro* towards MPS1 over AURORA B prompted us to try to determine a working concentration of Reversine that would be able to inhibit in living cells MPS1 leaving AURORA B kinase activity unaffected. To test this, I designed a series of experiments aimed to monitor the proper AURORA kinase activities in Reversine-treated cells.

First, I analyzed by WB the effect of Reversine on the phosphorylation of Ser10-Histone H3, a *bona fide* AURORA B substrate. To do that, I accumulated HeLa cells in mitosis by treatment with the spindle poison Nocodazole. Mitotic HeLa cells, obtained by shake-off, were then treated with growing concentrations of Reversine for 90' in the presence of the proteasome inhibitor MG132 to inhibit the events downstream of APC/C activation.

Treatment with Reversine leads to the disappearance of P-Ser10-H3 at concentrations above 1 μM (Figure 13).

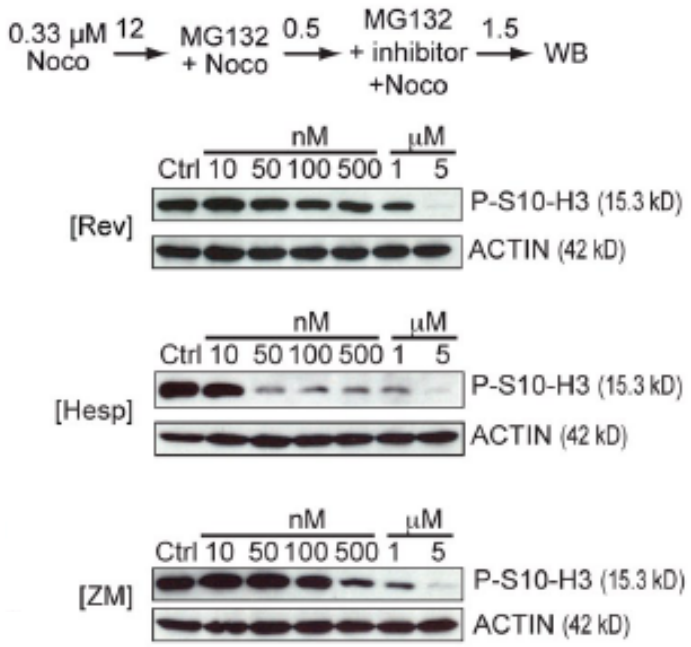

Figure 13 Sub-micromolar Reversine does not inhibit Aurora B in living cells

A comparison of the effects of Reversine, Hesperadin and ZM447439 on the levels of P-S10-H3 in total cell lysates of mitotic HeLa cells.

As positive controls of AURORA B inhibition I used the AURORA inhibitors ZM447439 (Ditchfield et al., 2003) and Hesperadin (Hauf et al., 2003) that lead to a marked decrease of this phospho-marker at concentrations of ~0.5 μM and 0.05 μM, respectively. Importantly, the pattern of P-Ser10-H3 inhibition observed in ZM447439- and Hesperadin-treated cells nicely correlates with the value of IC50s *in vitro*. Hesperadin is a ~17-fold more potent inhibitor of AURORA B than ZM447439 (IC50 values of 3 nM and 51 nM, respectively – (Table I).

Next, I monitored the ability of Reversine-treated cells to properly undergo cytokinesis. Small molecule-mediated inhibition of AURORA kinases leads to cytokinesis defects (Ditchfield et al., 2003; Hauf et al., 2003). Thus, I filmed synchronous HeLa cells treated with different concentrations of Reversine and measured the percentage of cells able

to properly undergo cytokinesis. Treatment of cells with concentrations of Reversine up to 1 μM does not grossly impair cytokinesis (Figure 14).

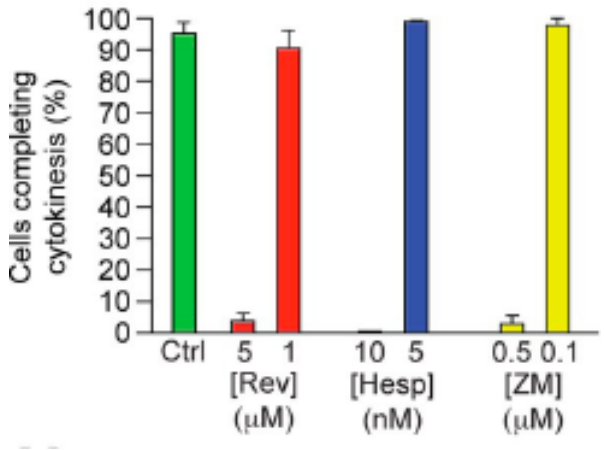

Figure 14 Sub-micromolar Reversine does not inhibit cytokinesis

The effects of Reversine, Hesperadin and ZM447439 on cytokinesis as evaluated in a time-lapse experiment.

Reversine-treated cells entered mitosis normally and correctly divide; cytokinesis defects were observed only at concentrations of Reversine of 5 μM. On the other hand, selective inhibition of AURORA kinase using the small molecules ZM447439 (Ditchfield et al., 2003) and Hesperadin (Hauf et al., 2003) impaired the ability of cells to properly divide. Interestingly, Hesperadin-treated cells showed cytokinesis defects already at concentration of 0.01 μM, a concentration that does not significantly impair P-Ser10-H3 (compare to Figure 13), suggesting that cytokinesis is a stricter parameter to judge AURORA B inhibition.

Finally, I monitored the ability of Reversine-treated cells to form a normal bipolar spindle. It has been reported that interference with AURORA A kinase activity leads to spindle monopolarization (Glover et al., 1995). AURORA A activity has been implicated in spindle assembly and centrosome separation and suppression of this protein by RNAi can lead to defects in spindle bipolarity (Girdler et al., 2006). If Reversine inhibits AURORA A, one could expect monopolar spindles in cultures treated with Reversine. Thus, I analyzed the spindle morphology in Reversine-treated cells. To test this, synchronous HeLa cells were

treated for 90' with 1 μM Reversine in the presence of the proteasome inhibitor MG132 to prevent mitotic exit. Representative images of metaphase spindles are shown in Figure 15.

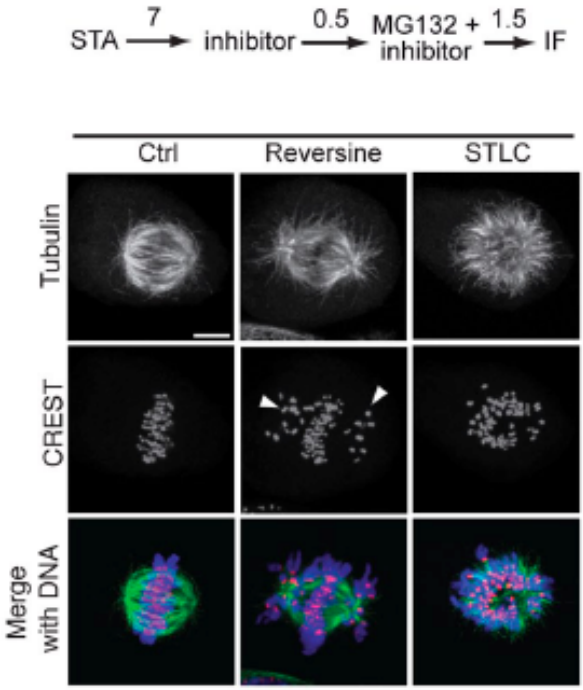

Figure 15 Reversine does not prevent spindle bipolarization but several chromosomes fail to congress

7 hours after a single thymidine arrest (STA), S-trityl-L-cysteine (STLC, an Eg5 inhibitor causing spindle monopolarization) or Reversine were added, and after an additional 0.5 hours MG132 (10 μM) was added to prevent mitotic exit. After 1.5 hours cells were then processed for immunofluorescence. Bar = 5 μm.

Importantly, at 1 μM Reversine monopolar spindles were infrequent (13.8% of cells showed monopolar structures - Figure 16) strongly suggesting that at this concentration of drug AURORA A is not inhibited. As positive control for spindle monopolarity, cells were treated with the Eg5 inhibitor STLC (DeBonis et al., 2004). Strikingly, 75.8 % of STLC-treated cells showed spindle monopolarity (Figure 15 and 16).

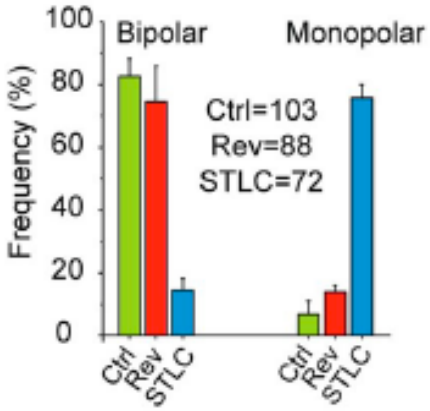

Figure 16 Reversine does not prevent spindle bipolarization but several chromosomes fail to congress

Quantification of the experiment in Figure 15 on the indicated number of cells.

I was further extending this analysis using different concentrations of Reversine and monitoring the phosphorylation of Ser10-Histone H3 by IF. Synchronous HeLa cells were treated with different concentrations of inhibitor (Figure 17) for 90' in presence of the proteasome inhibitor MG132 and stained for tubulin (green), centromeres (magenta), P-S10-H3 (red) and DNA (blue). As described above, Reversine treatment did not significantly impair spindle bipolarity; however, the most striking effect in cells treated with Reversine is the high frequency of chromosome misalignment already present at concentrations as low as 0.25 μM (Figure 17). However, the phosphorylation of Ser10-Histone H3 was affected only at concentrations above 5 μM.

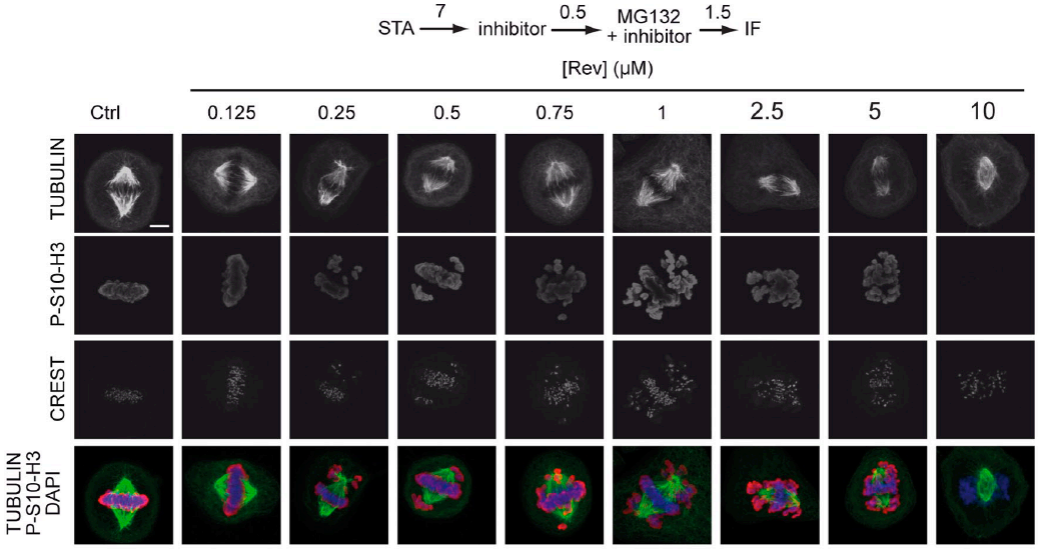

Figure 17 Reversine treatment does not impair significantly spindle bipolarity

After release from a STA, cells entered mitosis in the presence of Reversine, and were fixed and subjected to immunofluorescence to monitor the levels of P-S10-H3.

I then compared the phenotype associated with Reversine treatment, in terms of proper spindle formation and phosphorylation of Ser10-Histone H3, with that observed in cells treated with AURORA inhibitors following the same experimental scheme outlined above (Figure 18).

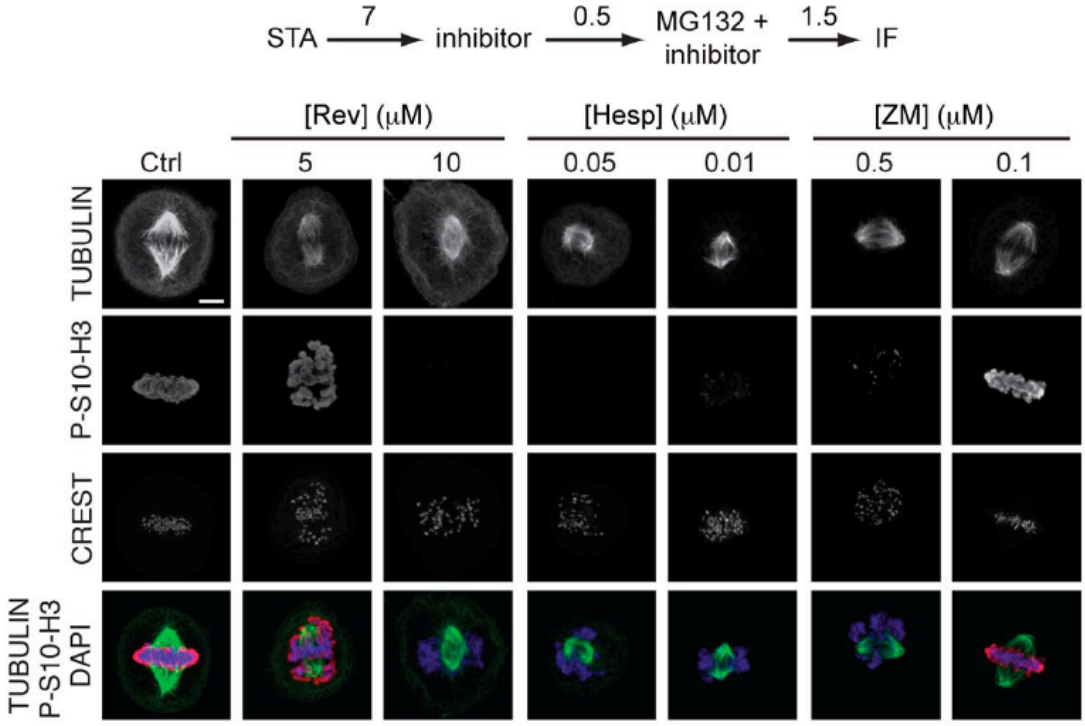

Figure 18 Comparison of the effects of Reversine, Hesperadin and ZM447439 on phosphorylation of Ser10-H3

After release from a STA, cells entered mitosis in the presence of Reversine, Hesperadin and ZM447439, and were fixed and subjected to immunofluorescence to monitor the levels of P-S10-H3.

Interestingly, cultures treated with concentrations of Reversine as high as 5 μM show a distribution of bipolar spindle similar to that observed at 1 μM (80% of bipolarity in 1 μM Reversine vs. 77 % in 5 μM treatment – Figure 17 and 18, see also Figure 20). Cells treated with Reversine have several misaligned chromosomes even if the metaphase plate is clearly visible and K-fibers are present as judged by cold-treatment before fixation(Figure19).

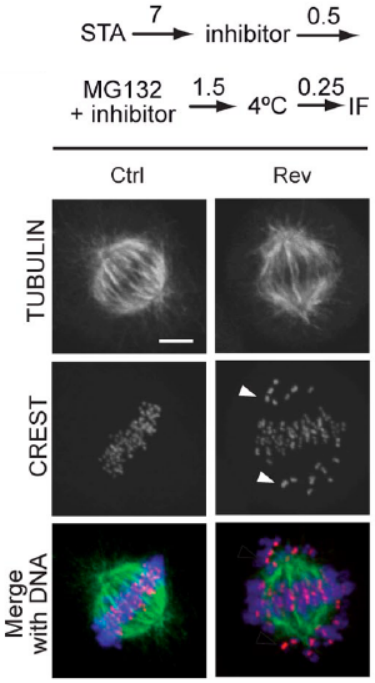

Figure 19 Reversine treatment does not interfer with K-fiber formation

Metaphase HeLa cells were kept at 4°C for 15 min before fixation for immunofluorescence. Arrowheads point to kinetochores of chromosomes that have failed to align at the metaphase plate.

On the other hand, the degree of spindle bipolarity was different in cells treated with the AURORA inhibitor Hesperadin. In cultures treated with 0.1 μM Hesperadin, ~ 60% of cells show spindle bipolarity and a metaphase plate was not clearly visible. Interestingly, in these cells I never observed the same defects of chromosomes misalignment as in cells treated with 1 μM Reversine, in which the plate was clearly evident and some chromosomes failed to correctly attach to the spindle (Figure 17 and 18). Cells treated with 2 μM ZM447439 displayed ~70% of spindle bipolarity and these cells have severe defects in chromosomes alignment, showing their DNA arranged along the spindle length. Finally, VX680 impairs severely spindle bipolarity; I observed a high amount of monopolar spindle in VX680-treated cells (~69% - Figure 20), suggesting that VX680 is not selective against AURORA B.

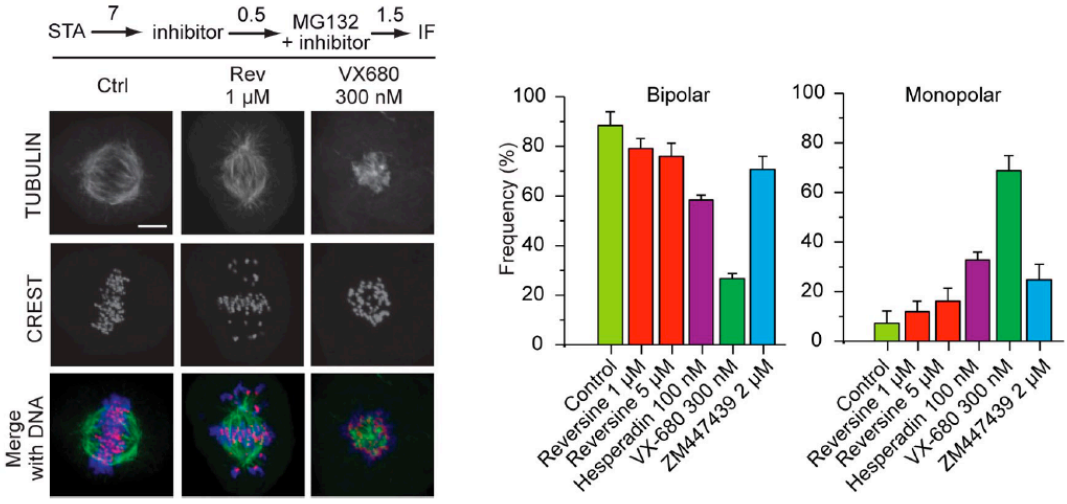

Figure 20 Characterization of spindle morphology in Reversine, Hesperadin, ZM447439 and VX680 treated cells

After release from a STA, cells entered mitosis in the presence of Reversine, Hesperadin, ZM447439 and VX680 and were fixed and subjected to immunofluorescence. *Left panel* VX680 targets Aurora A, causing spindles to remain mostly monopolar. *Right panel* A quantification of spindle morphology. Error bars are mean ± SEM.

Significantly, the chromosome misalignment phenotype observed in cells treated with the AURORA inhibitors Hesperadin or ZM447439 strikingly associates with a severe reduction of phosphorylation of Ser10-Histone H3 suggesting that the errors in chromosome congression are due to AURORA inhibition. In contrast, Reversine treatment interferes with proper chromosome alignment without affecting the proper phosphorylation of Ser10-Histone H3, at least at concentrations as high as 1-5 µM.

The simplest explanation for these data is that the concentrations of Reversine in the range of 0.1-1 µM do not affect AURORA kinase activity in living cells. However, an alternative possibility would come from the fact that AURORA A might have a compensatory effect on the phosphorylation of Ser10-Histone H3. To rule out the possibility that AURORA A could work as a vicarious kinase for AURORA B, I performed an RNAi-mediated repression of AURORA A and I monitored the levels of phosphorylation of Ser10-Histone H3 upon Reversine treatment (Figure 21). A similar experiment testing the effects on P-S7-CENP-A is reported in Figure 21D.

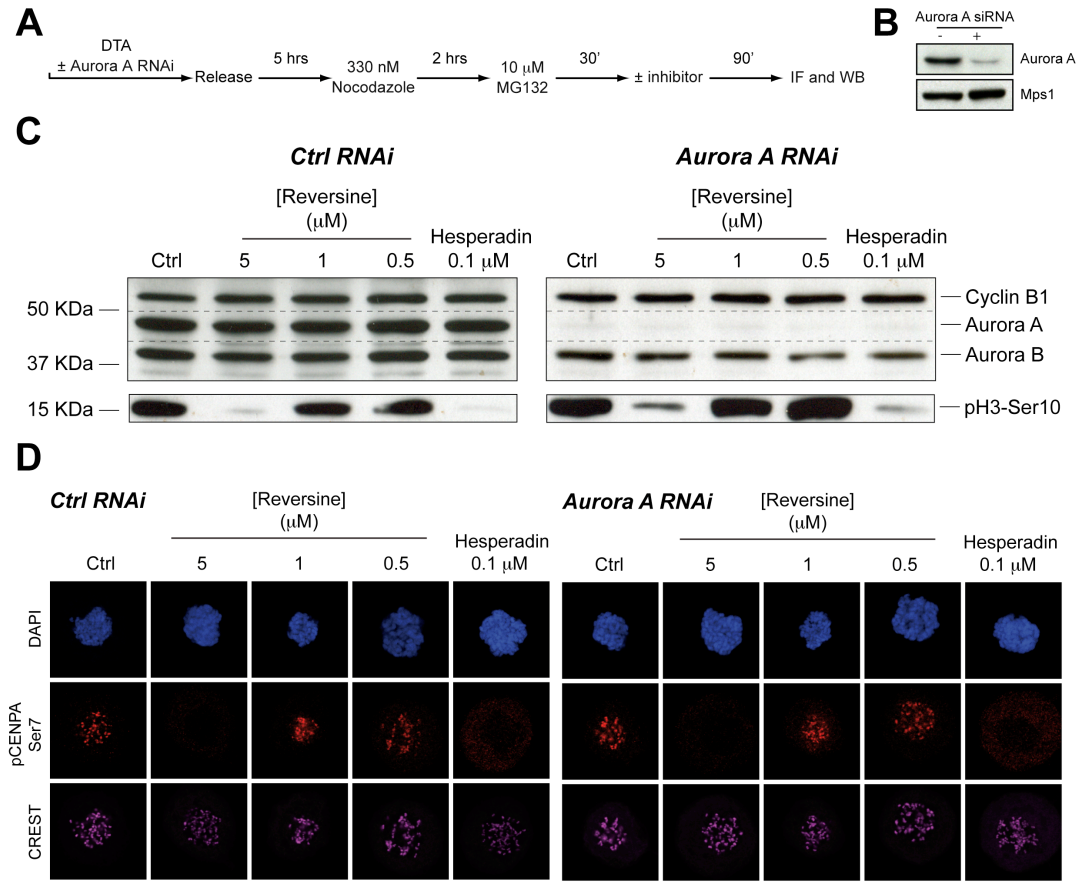

Figure 21 Sub-micromolar Reversine does not inhibit Aurora B in living cells

AURORA A does not contribute to the generation of P-S10-H3. Under conditions of RNAi of AURORA A(A and B), the disappearance of P-S10-H3 in the presence of Reversine (C) followed the same pattern as in the control experiments. The effects on P-S7-CENP-A is reported in D.

Importantly, Reversine treatment of AURORA A-repressed cells yielded the same levels of inhibition of P-Ser10-H3, suggesting that AURORA A does not balance AURORA B kinase activity in Reversine-treated cells.

Altogether, these observations strongly support the idea that sub-micromolar concentrations of Reversine can be used in cell-based assay in order to inhibit selectively MPS1 without affecting other mitotic kinases. I then decided to use Reversine in living cells at the concentration of 0.5 μM to probe the role of MPS1 kinase in mitosis.

Reversine inhibits Mps1 in living cells

The aforementioned data suggest that Reversine is a potent *in vitro* inhibitor of MPS1 and it does not inhibit AURORA kinases at sub-micromolar concentrations. Thus, I decided to measure the effect of Reversine on MPS1 kinase in cells. To do that, I monitored the electrophoretic mobility of MPS1 protein by WB in a PHOS-TAG gel (Kinoshita et al., 2006) that is commonly used to exacerbate the different migration of hyper- vs. hypo-phosphorylated forms of proteins by SDS-PAGE (Figure 22).

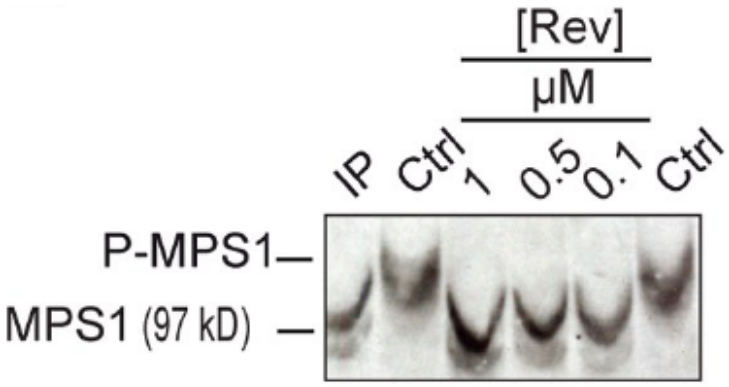

Figure 22 Reversine inhibits MPS1 in living cells

Dose-dependent inhibition of MPS1 phosphorylation in the presence of Reversine. Proteic extracts were separated in a PHOS-TAG gel (Kinoshita et al., 2006).

Proteins isolated from mitotic cells (Nocodazole-treated) showed a slower migrating band as compared to extracts obtained from inter-phase cells (Figure 22). Importantly, Reversine treatment leads to the disappearance of the slower migrating band (namely, hyper-phosphorylated, mitotic form of MPS1) in the range of 0.1-1 μM of drug and MPS1 band was running at a height virtually similar to that observed in samples isolated from inter-phase cells. These data strongly suggest that Reversine inhibits MPS1 in living cells at concentrations as low as 0.1 μM. Significantly, I observed a strong inhibition of MPS1 at concentrations of Reversine that do not affect AURORA kinase activities; inhibition of AURORA was observed in living cells at concentrations above 1 μM - as pointed above - whereas MPS1 starts to be

inhibited already at 0.1 μM of Reversine. These observations strongly support the idea that Reversine can be used as a valuable tool to investigate MPS1 function in living cells.

To further confirm the idea that the phenotype observed in cells treated with sub-micromolar concentrations of Reversine can be attributed to MPS1 inhibition, I performed a side-by-side comparison between the effects of Reversine treatment and those observed in cells in which MPS1 levels have been repressed by RNAi. MPS1 protein was virtually undetectable by WB under conditions of MPS1 RNAi (Figure 23).

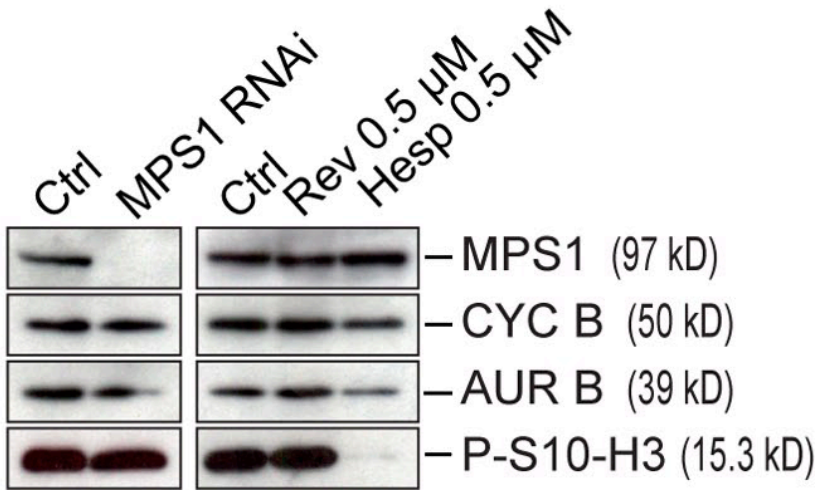

Figure 23 Interference with Mps1 kinase activity does not grossly affect phosphorylation of Ser10-H3

Western blotting demonstrates that P-S10-H3 levels are untouched upon MPS1 RNAi or inhibition with reversine. The hesperadin control illustrates the effects from inhibiting AURORA B

Of note, MPS1-depleted cells showed normal levels of P-Ser10-H3; even if this result is at odds with a paper by Kops and coworkers (Jelluma et al., 2008), it is completely in agreement with the phenotype observed in Reversine-treated cells, and with the results of two other studies by Prof Taylor lab (Hewitt et al., 2010) and Prof Jallepalli lab (Maciejowski et al., 2010) in which repression of MPS1 kinase activity has been achieved with a novel MPS1 inhibitor - AZ3146, chemically unrelated to Reversine - and by inhibiting an analogue-sensitized MPS1 allele, respectively. I then decided to compare the chromosome mis-alignment phenotype of

cells in which MPS1 kinase activity has been repressed either by Reversine treatment or MPS1 RNAi, or both of them. To do that, I performed a double round of MPS1 RNAi (where indicated – see Figure 24) followed by a Double Thymidine Arrest. Synchronous population of cells was then released into fresh medium and treated with 0.5 μM Reversine (where indicated) before entry into mitosis. Cells were then treated with the proteasome inhibitor MG132 to prevent mitotic exit, fixed after 90' and processed for IF (colors in micrographs are green for tubulin, red for P-Ser10-H3, blue for DAPI). This experimental scheme allowed us to closely resemble MPS1 depletion obtained by RNAi with Reversine treatment. In both cases the cells are entering mitosis without MPS1 kinase activity, allowing a fair comparison of the two phenotypes. Significantly, although control cells showed a clear metaphase plate with a strong P-Ser10-H3 signal, Reversine treatment leads to a severe chromosome misalignment phenotype without any obvious effect on proper P-Ser10-H3, as pointed above. MPS1 depletion by RNAi inhibits correct chromosome alignment in a fashion that is similar to that observed in Reversine-treated cells. Strikingly, in cells in which I lowered MPS1 levels by RNAi we failed to observe any effect on P-Ser10-H3. More importantly, treatment of MPS1-depleted cells with Reversine does not exacerbate the chromosome misalignment phenotype and does not significantly affect the normal phosphorylation of Ser10-H3 observed in the single treatment alone, strongly supporting the idea that sub-micromolar concentrations of Reversine targets specifically MPS1 in mitosis.

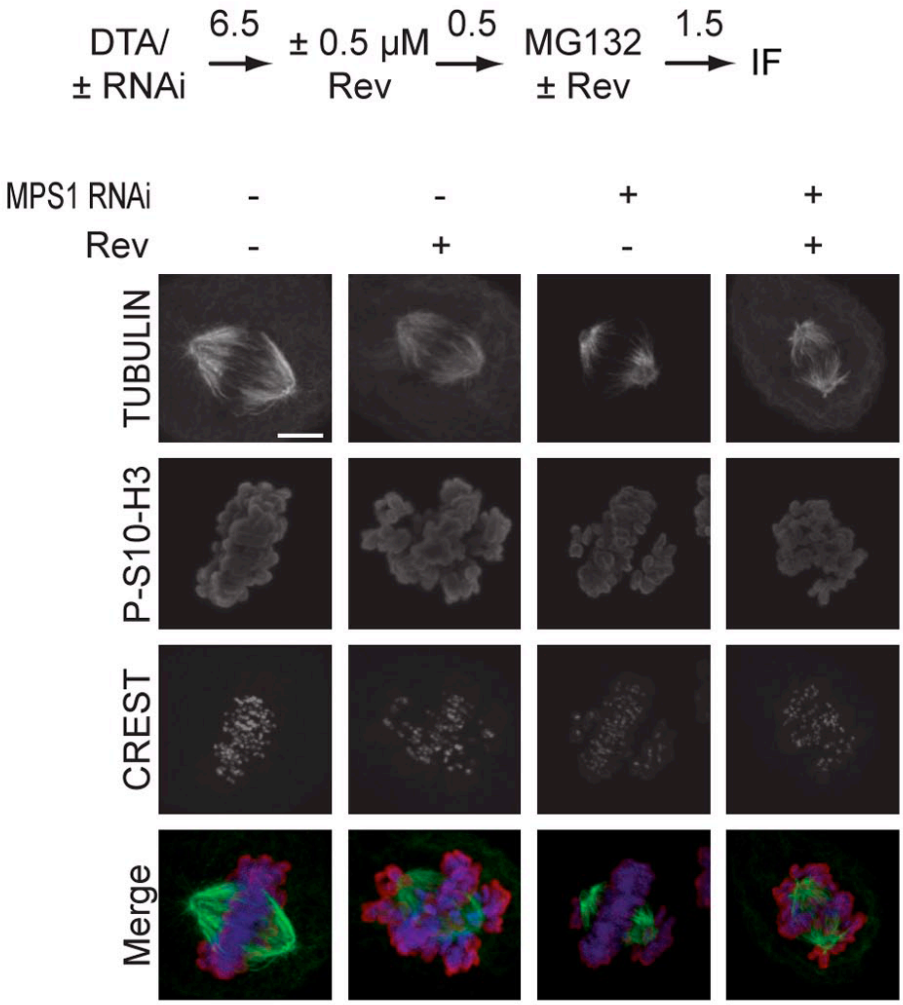

Figure 24 Reversine inhibits MPS1 in living cells

Chromosome alignment phenotypes of mitotic HeLa cells that were either depleted of MPS1 by RNAi, or treated with 0.5 µM Reversine, or both. DTA = double thymidine arrest. The levels of P-S10-H3 appeared unaltered in all three experiments. Scale bar =5 µm.

To confirm MPS1 as a target of Reversine in living cells and to further probe the role of this kinase in the SAC, I decided to monitor the proper recruitment of a series of outer kinetochore and SAC proteins to unattached kinetochores either in MPS1 depleted cells or in Reversine-treated cells. To test this, I followed an experimental workflow similar to the one used to monitor the chromosome mis-aligment phenotype (see above) with a slight modification. Briefly, synchronous HeLa cells - either MPS1-depleted or not - were exposed to Nocadozole before mitotic entry in a time-window that proceed the treatment with Reversine (where indicated). Cells were then treated with MG132 and fixed as pointed above

and in the reminder of Figure 25. In my hands, MPS1 repression – either by RNAi or Reversine treatment – leaves largely unaffected the proper localization of the centromere protein CENP-C (Figure 25 and quantified in Figure 28). On the other hand, I found a severe reduction of Mad1 localization (Figure 25) - in agreement with previous reports (Jelluma et al., 2008; Kwiatkowski et al.; Sliedrecht et al.) - as well as of the RZZ subunits ROD, ZWILCH, and ZW10 (Basto et al., 2000; Basto et al., 2004; Chan et al., 2000) and the RZZ-associated protein SPINDLY (Chan et al., 2009; Griffis et al., 2007) (Figure 25 and 26 and quantified in Figure 28).

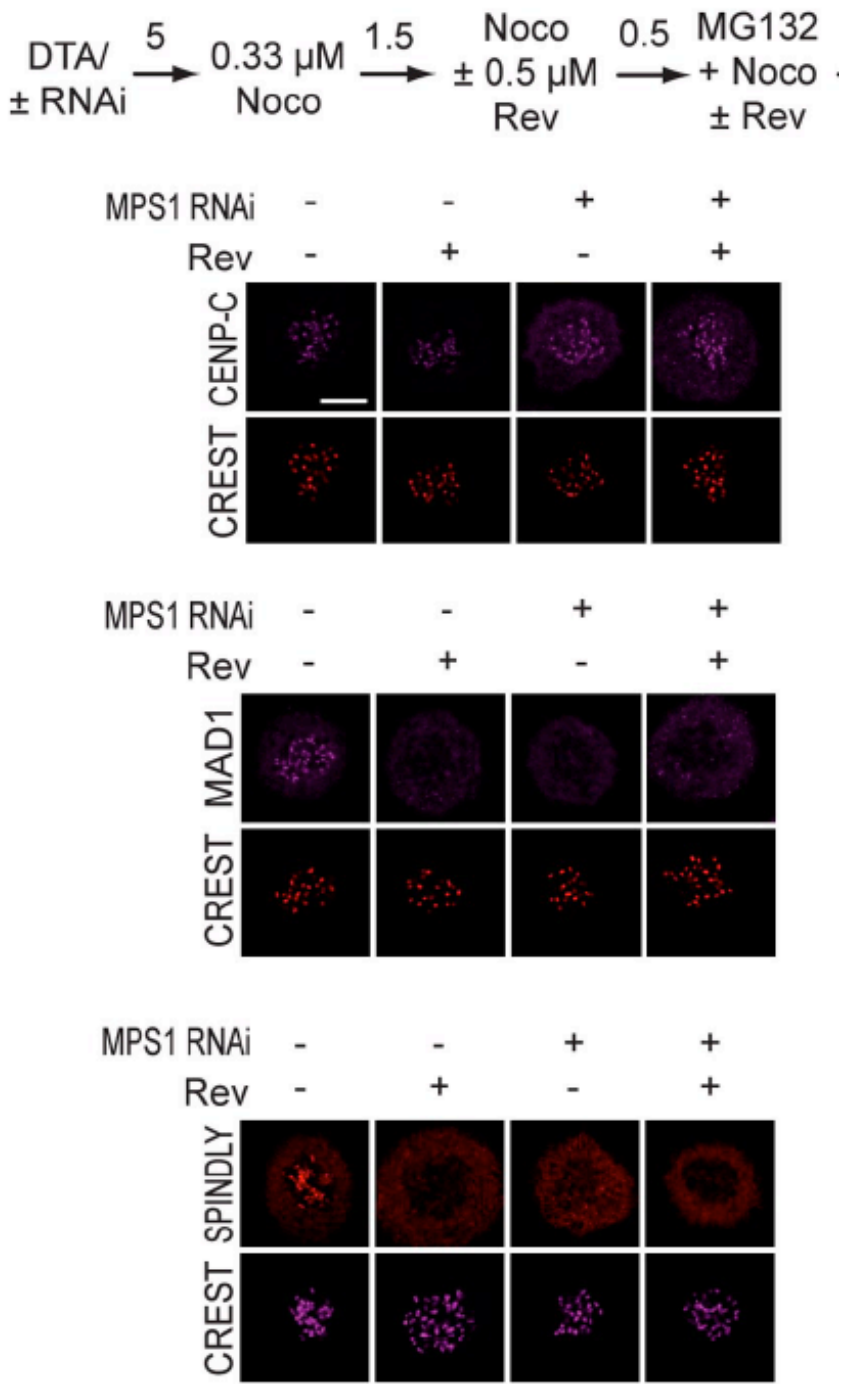

Figure 25 Mps1 kinase activity is required for MAD1 and SPINDLY localization

Representative localization experiments on different kinetochore proteins including CREST, CENP-C, MAD1, and SPINDLY

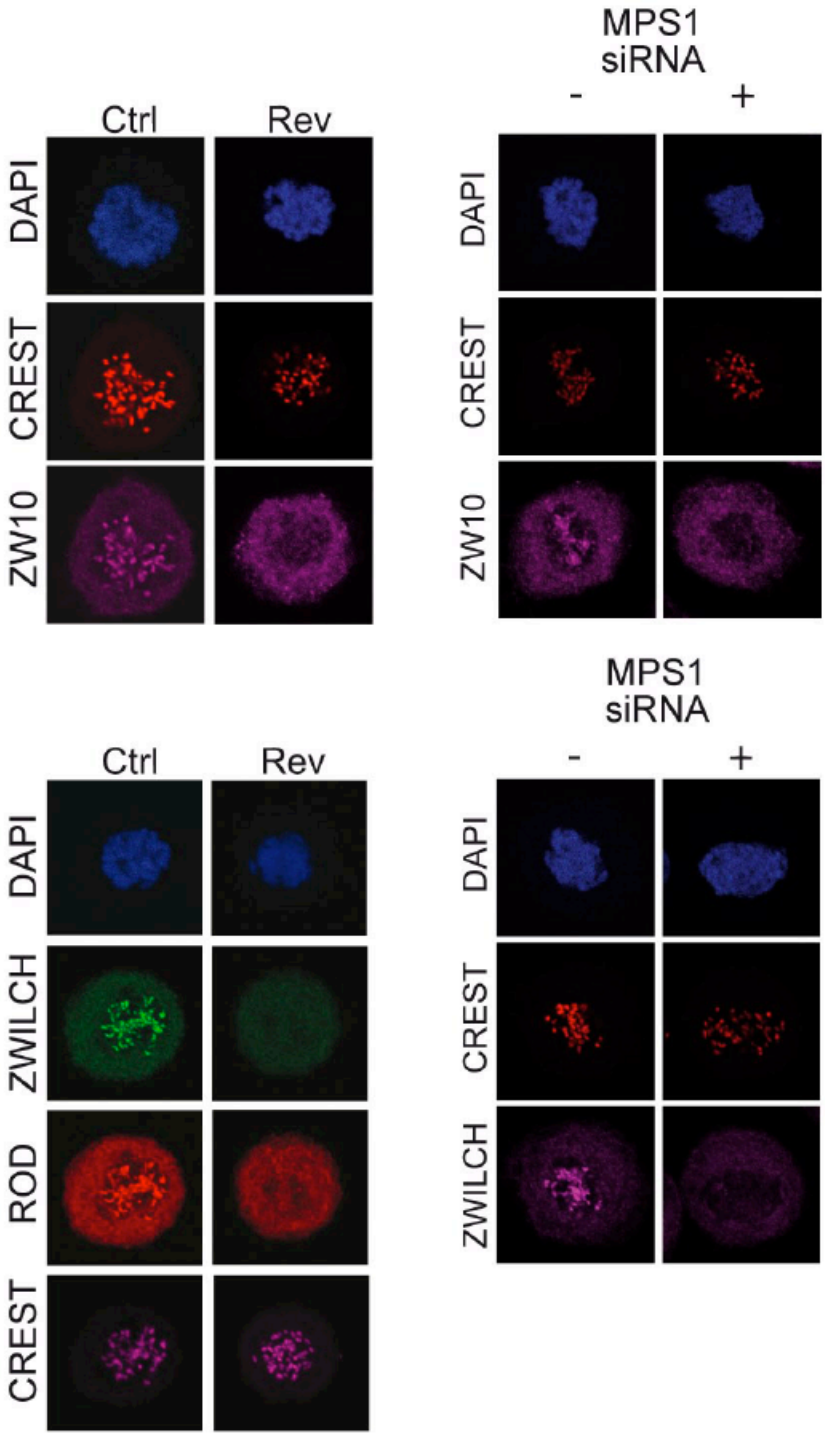

Figure 26 Mps1 kinase activity is required for RZZ localization

The effects of 0.5 μM reversine (Rev) or MPS1 RNAi on the localization of kinetochore proteins was tested at 0.33 μM nocodazole (Noco). The RZZ subunits ZW10, ZWILCH, and ROD were unable to localize to kinetochores

Under the same experimental conditions, MPS1 kinase activity does not seem to be required for the recruitment of the KMN network proteins as judged by normal staining of NDC80, KNL-1, MIS12 and ZWINT components (Figure 27 and quantified in Figure 28).

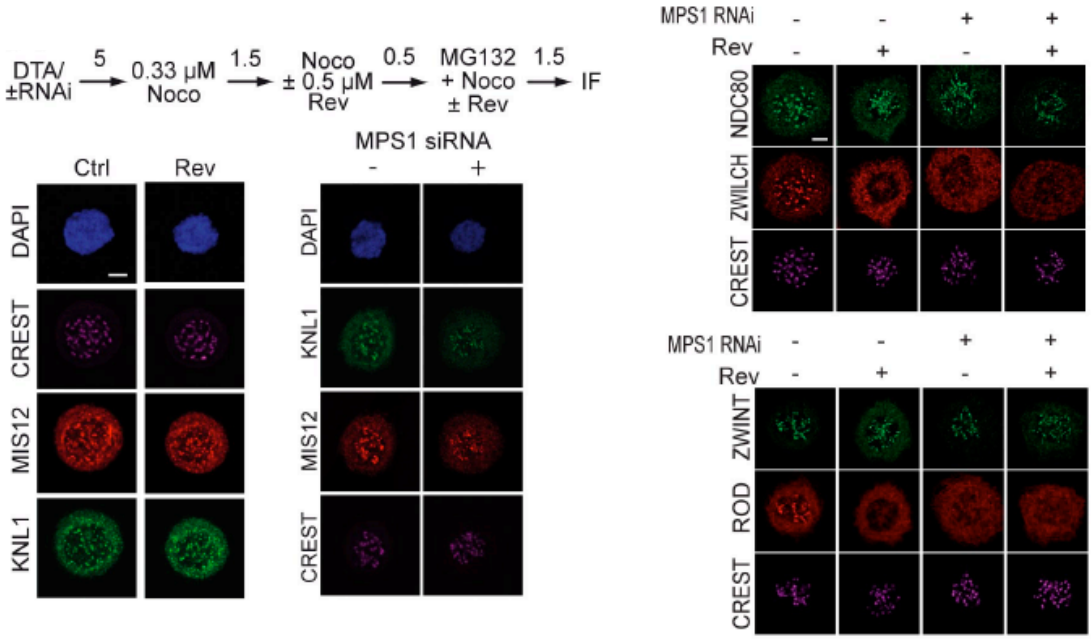

Figure 27 Mps1 kinase activity is not required for KMN localization

The effects of 0.5 µM reversine (Rev) or MPS1 RNAi on the localization of kinetochore proteins was tested at 0.33 µM nocodazole (Noco). The KMN subunits tested, including MIS12, KNL1, NDC80 and ZWINT were not displaced from kinetochores in either condition.

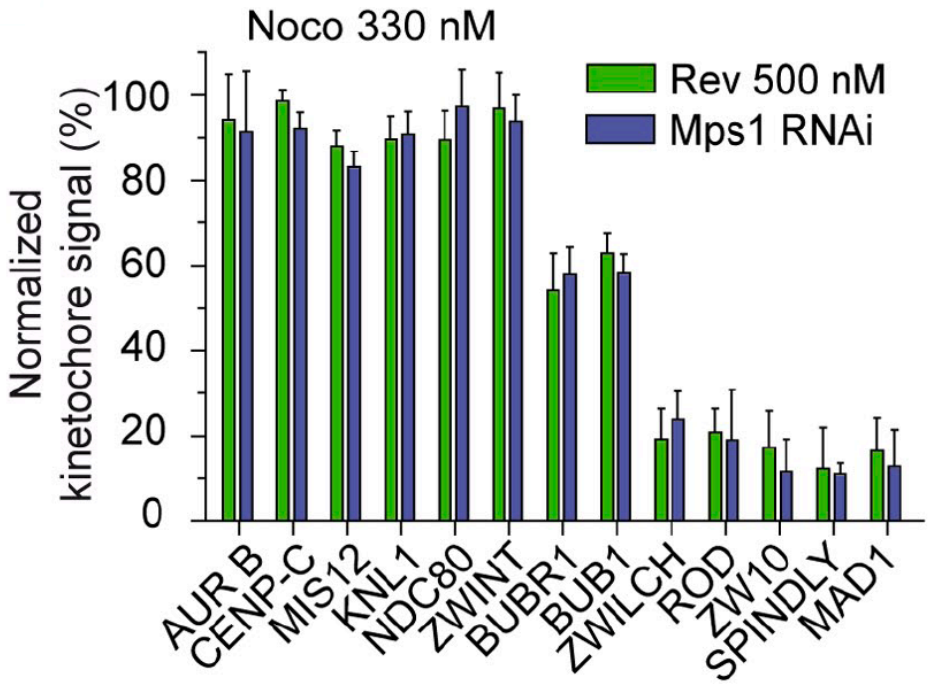

Figure 28 Quantification of kinetochore protein signal in Reversine-treated or Mps1-depleted HeLa cells

The RZZ subunits ROD, ZWILCH, and ZW10, as well as the RZZ-associated protein SPINDLY and MAD1 are all largely evicted from kinetochores when the spindle checkpoint is triggered with 330 nM nocodazole (Noco), with no significant difference between MPS1 RNAi or Reversine treatment. The effects on localization are expressed as ratios of the fluorescence value of the indicated protein to the value of CREST (both background subtracted) normalized to the equivalent ratio in control cells. Error bars are mean ± SEM.

The aforementioned data strongly suggest that MPS1 is required for the proper recruitment of the RZZ-Spindly-Mad1:Mad2 axis at unattached kinetochores. This is in agreement with a recent report by Prof. Jallepalli lab (Maciejowski et al.) in which they found virtually identical data in terms of dependencies of protein recruitment by MPS1. Furthermore, MPS1 depletion achieved by RNAi closely phenocopies Reversine treatment strongly suggesting that Reversine targets MPS1 in living cells.

Reversine causes the override of the spindle checkpoint activated by different microtubule poisons

In light of MPS1 controlling SAC proteins localization at unattached kinetochores thus affecting proper SAC signaling, I asked the question whether Reversine could affect the proper mitotic timing during an unperturbed mitosis. To test this, I filmed HeLa cells expressing a GFP-tagged version of histone H2B (hereafter HeLa H2B-GFP) treated with 1 μM Reversine and I measured the time from nuclear envelope breakdown (NEBD) to DNA decondensation (Figure 29).

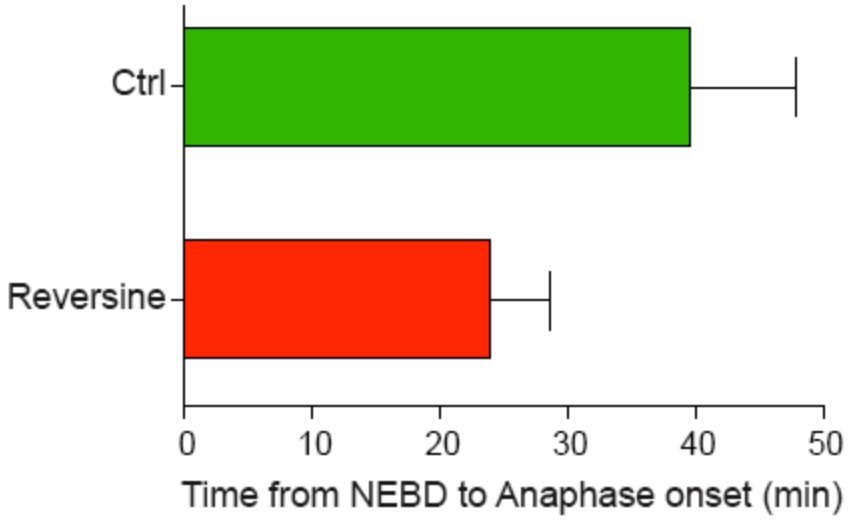

Figure 29 Reversine interferes with normal mitotic timing during an unperturbed mitosis

Reversine causes normally cycling HeLa cells to exit mitosis prematurely, which is a consequence of spindle checkpoint inactivation. The plot is a quantification of a time-lapse video microscopy experiment.

As expected, control cells entered mitosis condensing their DNA properly and anaphase onset took place on average 39 minutes after NEBD. On the other hand, Reversine treatment severely affected mitotic timing and the quality of chromosome segregation. Indeed, Reversine-treated cells entered mitosis normally, condensed their DNA with a clear metaphase plate but failed to properly align all the chromosomes starting anaphase with a severe

chromosome mis-alignment phenotype and on average 25 minutes after NEBD. Representative snapshots of live cell imaging are showed in Figure 30.

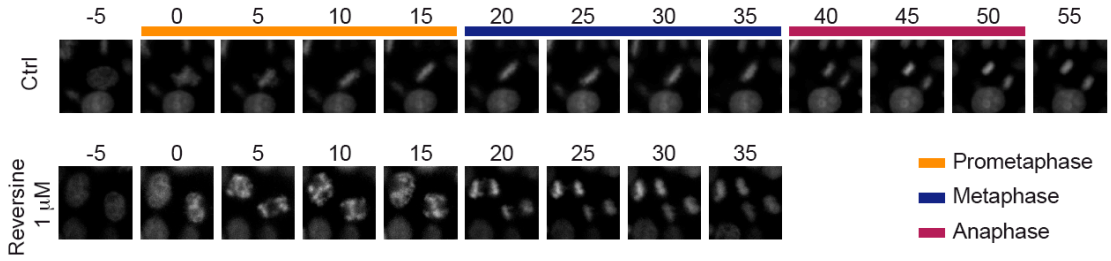

Figure 30 Representative images of live cell imaging of HeLa H2B-GFP treated with DMSO (Ctrl) or Reversine and followed during an unperturbed mitosis

Numbers above micrographs indicate time in minutes. In this case, time 0 refers to the nuclear envelope breakdown.

Next, I analyzed the ability of Reversine to override the SAC activated by several spindle poisons. To quantify the effects of Reversine-mediated MPS1-inhibition on the SAC, synchronous HeLa H2B-GFP were treated with three different microtubules drugs together with 1 μM Reversine and the cells were followed over time by live cell imaging. Reversine-treated cells quickly bypass mitotic checkpoint activation induced by the microtubules stabilizing agent taxol, which reduced intra-centromeric tension, and S-Trityl-L-cysteine, an Eg5 kinesin inhibitor that induces the formation of monopolar spindles (Figure 31 and quantification in Table II).

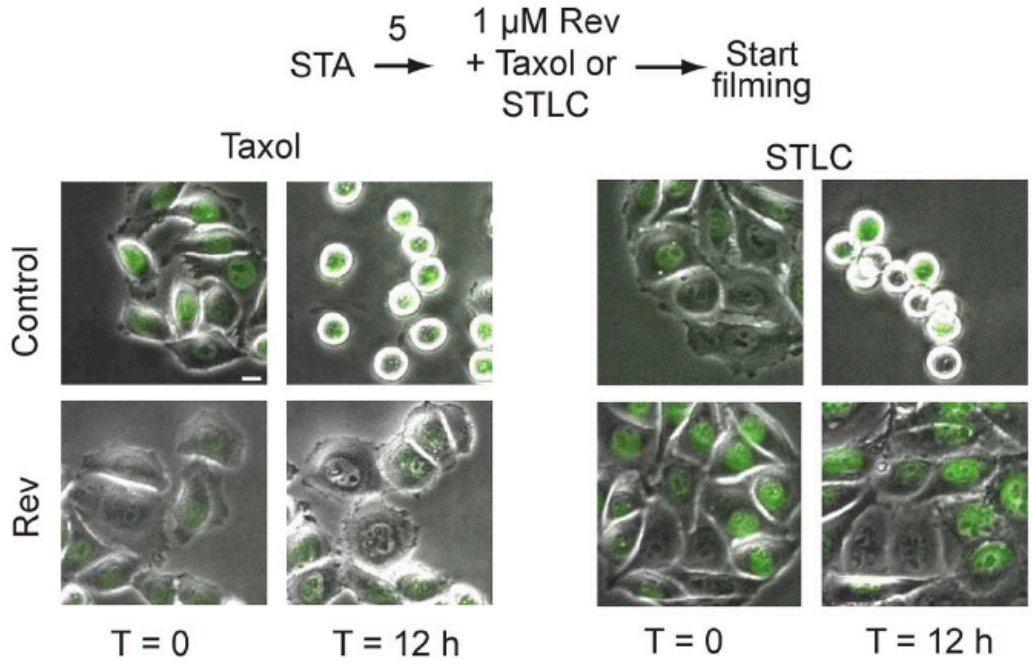

Figure 31 Reversine is a spindle checkpoint inhibitor

The ability of HeLa cells to arrest in mitosis in the presence of 500 nM Taxol or 10 µM STLC was tested in a timelapse experiment in the presence of reversine. 12 h after the beginning of the video, control cells treated with Taxol or STLC were still in mitosis, whereas the presence of reversine caused a spindle assembly checkpoint override and mitotic exit

These findings are consistent with the notion that MPS1 is required to maintain the spindle checkpoint under conditions of reduced tension. Furthermore, Reversine-treated cells override the SAC also in the presence of the Plk1 inhibitor BI2536 (Figure 32).

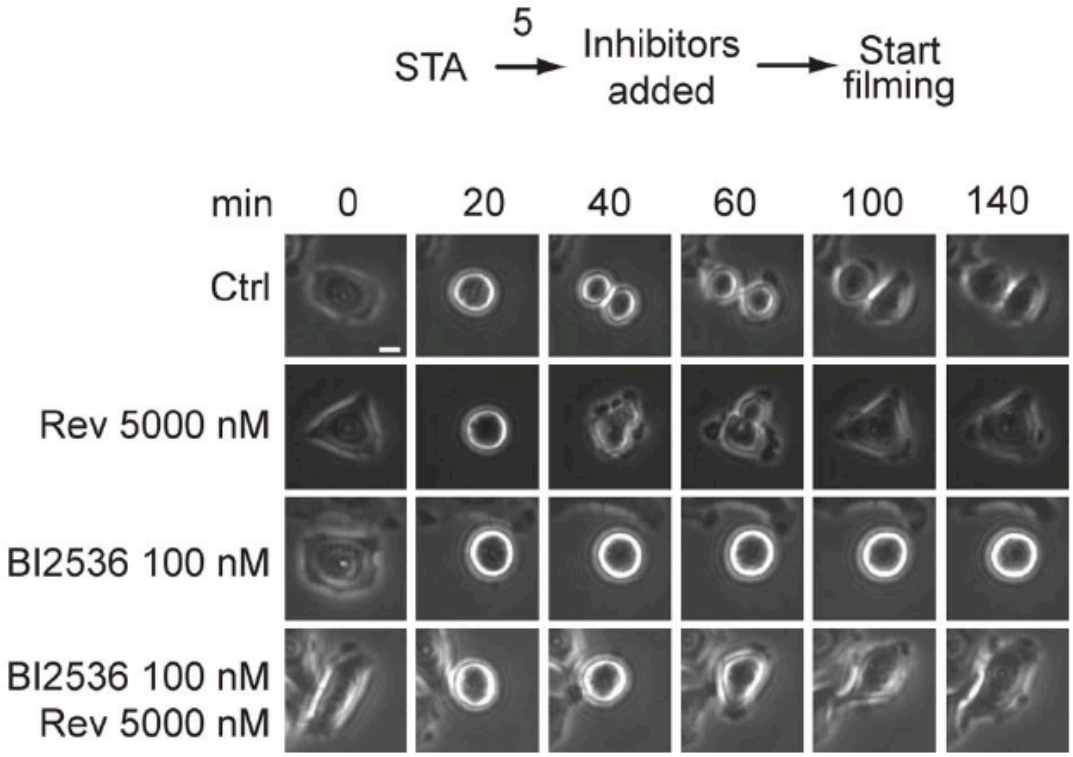

Figure 32 Reversine treatment causes a checkpoint override in the presence of BI2536

The ability of HeLa cells to arrest in mitosis in the presence of the Polo kinase inhibitor BI2536, which causes a mitotic arrest (Lénárt et al., 2007), was tested in a timelapse experiment in the presence of Reversine. In this case, time 0 refers to the last video frame before mitotic rounding up.

Moreover, MPS1 inhibition mediated by Reversine treatment led to checkpoint override in the presence of the microtubules depolymerizing agent Nocodazole. I was using Nocodazole at concentrations of 0.33 and 3.3 μM, which lead to partial and complete microtubules depolymerization, respectively (Figure 33).

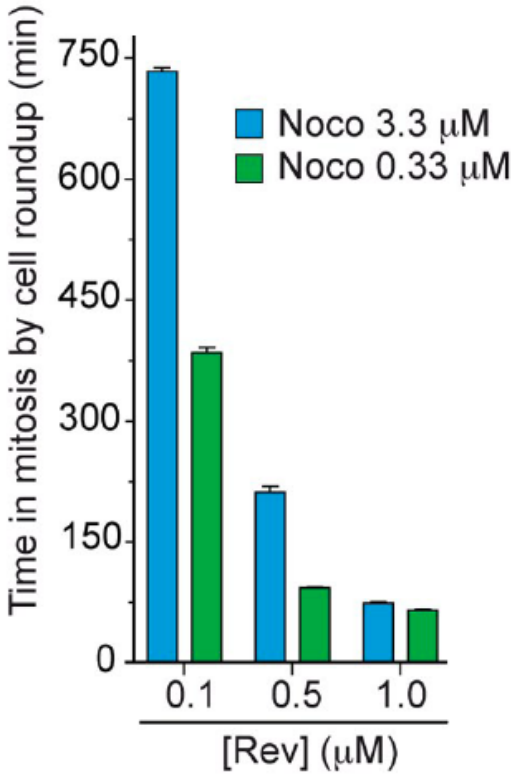

Figure 33 Reversine treatment causes a checkpoint override in the presence of Nocodazole

The experiment quantifies the behavior of cells in time-lapse video microscopy experiments in which HeLa cells were treated with two concentrations of nocodazole (Noco). Additional values (including controls) are collected in Table II.

The degree of checkpoint override in nocodazole was dose-dependent and was complete at 1 μM Reversine (Table II), a concentration sufficient for the vast majority of cells to bypass a nocodazole-induced arrest in less than 90'.

Treatment	Duration of mitosis
	min
330 nM nocodazole	947 ± 105
330 nM nocodazole + 1 μM reversine	66 ± 14
330 nM nocodazole + 500 nM reversine	96 ± 9
330 nM nocodazole + 100 nM reversine	384 ± 111
330 nM nocodazole + 1 μM hesperadin	117 ± 17
330 nM nocodazole + 500 nM hesperadin	164 ± 39
330 nM nocodazole + 100 nM hesperadin	244 ± 62
3.3 μM nocodazole	1,107 ± 116
3.3 μM nocodazole + 1 μM reversine	75 ± 13
3.3 μM nocodazole + 500 nM reversine	205 ± 63
3.3 μM nocodazole + 100 nM reversine	724 ± 154
3.3 μM nocodazole + 1 μM hesperadin	178 ± 35
3.3 μM nocodazole + 500 nM hesperadin	304 ± 29
3.3 μM nocodazole + 100 nM hesperadin	785 ± 149
500 nM Taxol	1,144 ± 119
500 nM Taxol + 1 μM reversine	60 ± 7
500 nM Taxol + 500 nM reversine	77 ± 22
500 nM Taxol + 100 nM reversine	273 ± 49
500 nM Taxol + 1 μM hesperadin	103 ± 17
500 nM Taxol + 500 nM hesperadin	179 ± 40
500 nM Taxol + 100 nM hesperadin	166 ± 38

Data from time-lapse videos reporting timing of HeLa cell rounding up (duration of mitosis).

Table 2 Duration of mitosis in cells treated in the indicated conditions

To rule out the possibility that the observed checkpoint override in nocodazole was cell line-dependent, I decided to extend the analysis to different cell lines. I then used U20S osteosarcoma cells, as a model of transformed p53 competent cell line, and RPE1-hTERT retinal pigment epithelia cells as normal cell lines. Consistent with the data described above, 1 μM Reversine was able to induce a mitotic exit in these cell lines (Figure 34). Interestingly, Reversine overrode the SAC more rapidly in U20S and RPE1-hTERT cell lines compared to HeLa cells (~40' vs 65', respectively). The timing of mitotic exit, however, was not influenced by the concentration of nocodazole even at concentrations as high as 3.3 μM that completely abolishes MT assembly (Yang et al., 2009).

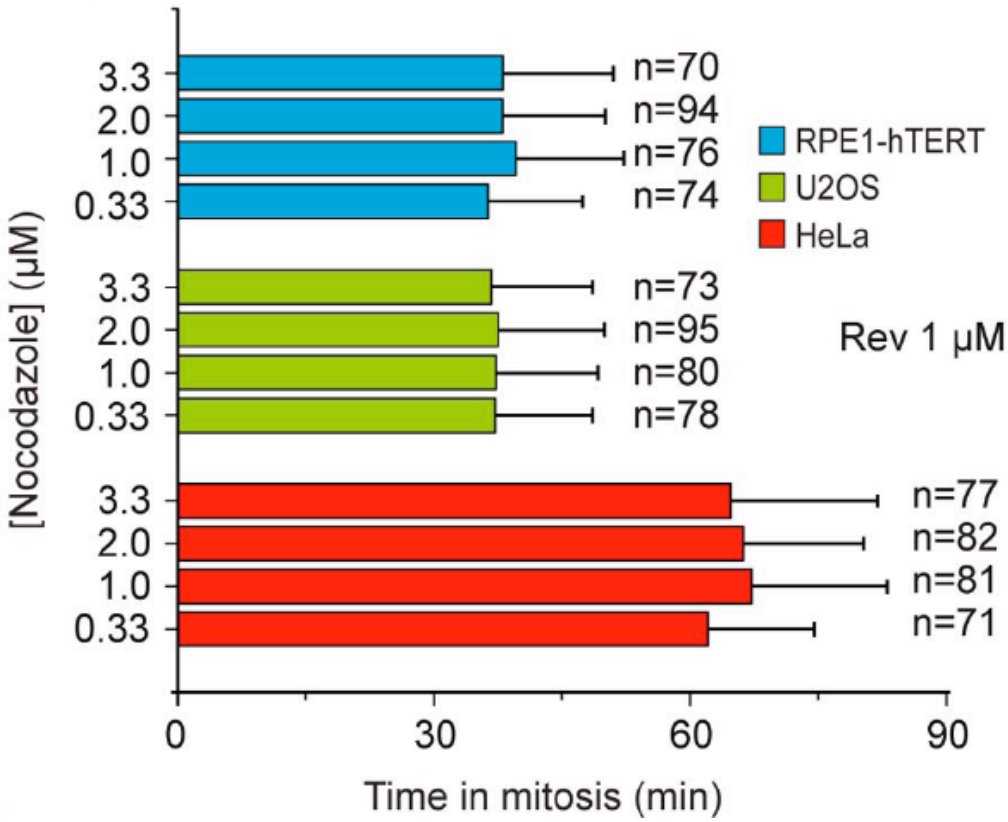

Figure 34 The ability of reversine to drive HeLa cells out of mitosis extends to U2OS and RPE1-hTERT

The plot quantifies the behavior of indicated cell lines in time-lapse video microscopy experiments in which cells were treated with several concentrations of nocodazole (Noco).

Thus, taking these data together, it appears that MPS1 is strictly required for the SAC and that Reversine is a powerful tool to inhibit the SAC.

MPS1 acts downstream of AURORA B

My results suggest that Reversine is an MPS1 inhibitor *in vitro* and *in vivo*. They also demonstrate that Reversine does not cause a prominent reduction in the levels of P-S10-H3 in living cells at concentrations (e.g. 0.5 μM) that cause substantial problems in chromosome bi-orientation. Similarly, Reversine does not significantly inhibit cytokinesis at 0.5 μM (see Figure 14). Overall these results strongly suggest that MPS1 does not exercise a strong direct control over AURORA B activity. In agreement with this idea, the kinetochore levels of P-CENP-A

were not influenced at concentrations of Reversine up to 5 μM or above (Figure 35A), and were also not inhibited upon MPS1 RNAi (Figure 35A-B). Incidentally, it is worth noting that these experiments were carried out in Nocodazole, i.e. in the presence of unattached kinetochores. The presence of an intense P-CENP-A signal in Nocodazole shows, in agreement with a recent report (Liu et al., 2009a), that AURORA B is active on unattached kinetochores.

I also assessed whether Reversine or MPS1 RNAi influenced the localization of AURORA B. In either case, I failed to observe defects in the localization of AURORA B (Figure 35C). Furthermore, the presence of Reversine did not influence the state of activation of AURORA B, as monitored by activation loop auto-phosphorylation (P-T232), at least until concentrations at which Reversine appears to hit AURORA B directly (Figure 35D).

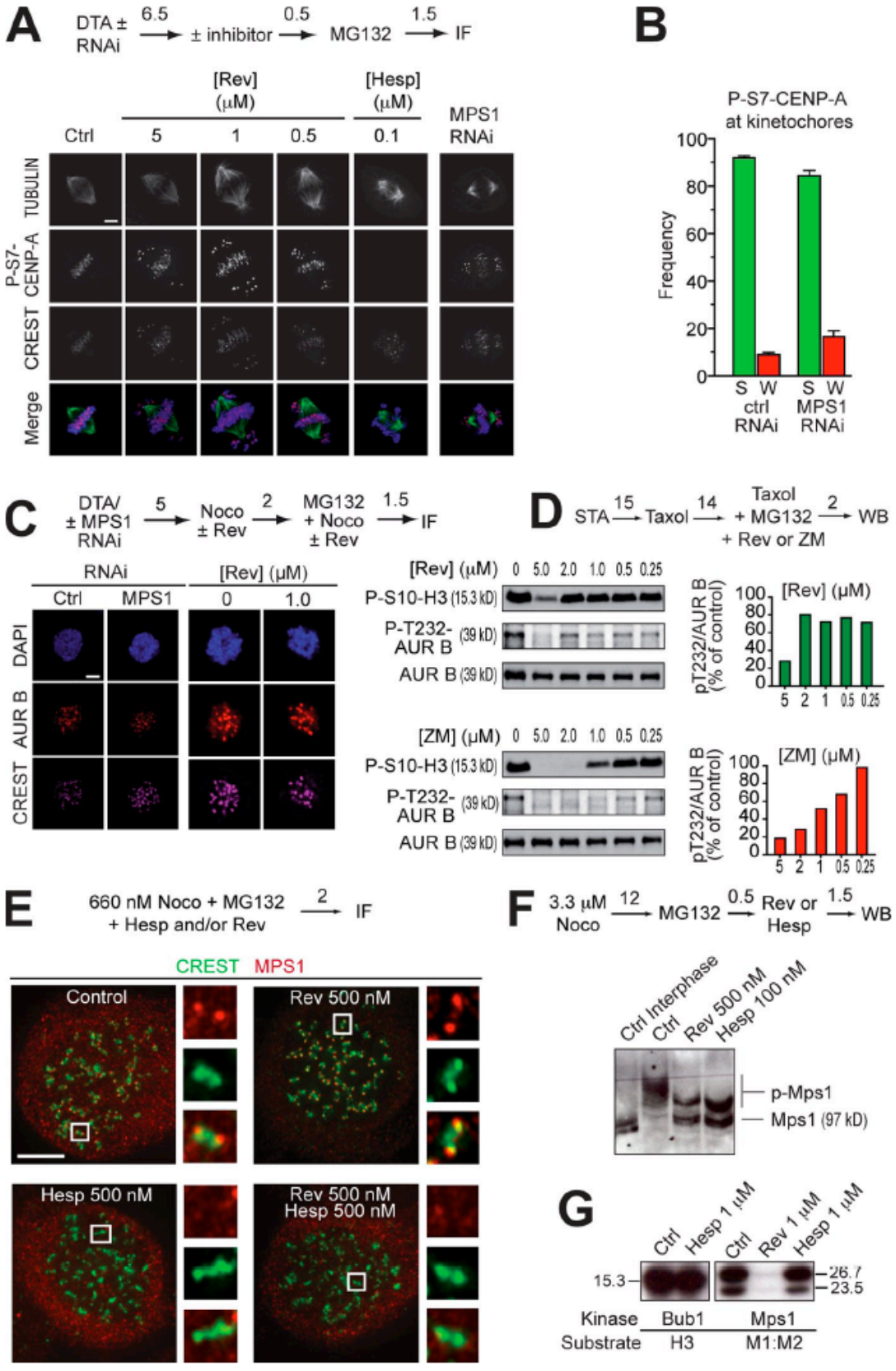

Figure 35 MPS1 acts downstream from Aurora B

(**A**) P-S7-CENP-A in mitotic HeLa cells is unaltered even at 5 μM Reversine. The antigen is present on centromere/kinetochores of chromosomes near the poles, as well as of chromosomes at the equator. The

antigen is invisible in the presence of 100 nM Hesperadin. No compensation from Aurora A was observed (Figure 21). Bar =5 μm. (**B**) A quantification of the results in (**A**). (**C**) Kinetochore localization of AURORA B in HeLa cells is unaffected after MPS1 RNAi or addition of Reversine. (**D**) (*Top*) Phosphorylation of the activation loop of AURORA B (P-T232) is not affected by Reversine until above 2 μM. The pattern of loss of activation loop phosphorylation follows the pattern of loss of P-S10-H3 phosphorylation. (*Bottom*) The same experiment with ZM447439 as a positive control. (**E**) Kinetochore localization of MPS1 in Nocodazole (660 nM) is enhanced by 0.5 μM Reversine. If AURORA B is inhibited with 0.5 μM Hesperadin, Reversine-induced localization of MPS1 is abrogated. Images were taken on a Deltavision microscope. Scale bar = 5 μM. (**F**) Both MPS1 and AURORA B inhibitors reduce the phosphorylation of mitotic MPS1, as visualized through the PHOS-tag method (Kinoshita et al., 2006). (**G**) Hesperadin does not inhibit BUB1 or MPS1.

I monitored MPS1 localization in the presence of Reversine and/or Hesperadin. In unperturbed mitoses (data not shown) or in Nocodazole (Figure 35E), I observed a significant cytosolic signal and relatively weak MPS1 kinetochore staining. However, strong kinetochore staining was observed when MPS1 activity was inhibited with 0.5 μM Reversine. This result is inconsistent with a recent report that auto-phosphorylation of MPS1 is required for kinetochore localization (Xu et al., 2009). Inhibition of AURORA B with 0.5 μM Hesperadin prevented kinetochore localization of MPS1 in Nocodazole, as well as the kinetochore enrichment of MPS1 caused by Reversine (Figure 35E). Similar results were obtained with 100 nM Hesperadin and 3.3 μM Nocodazole (Figure 36). These results demonstrate that AURORA B is required for kinetochore localization of MPS1.

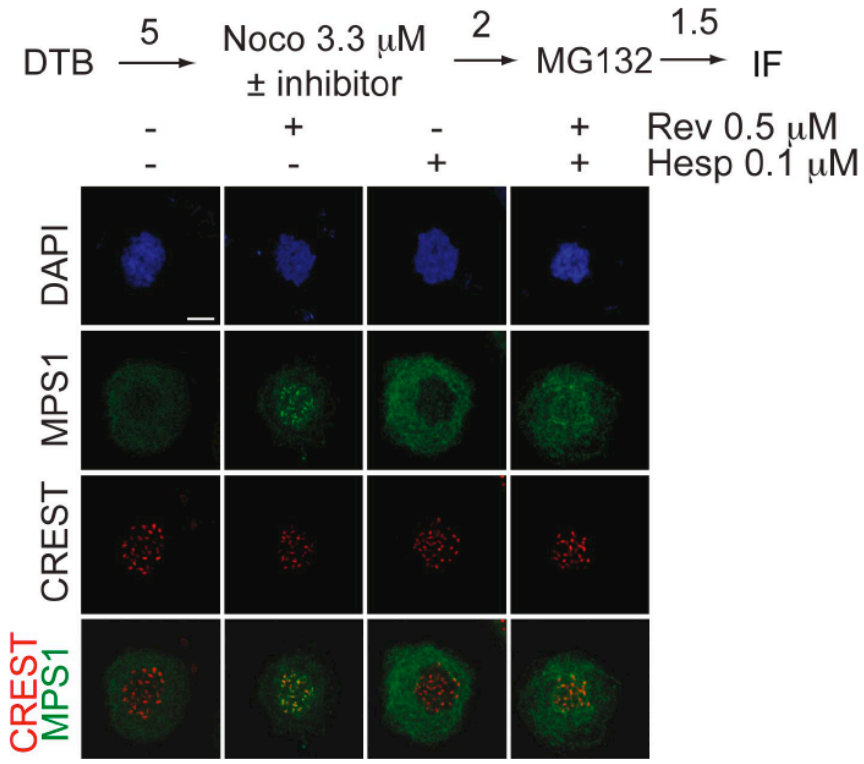

Figure 36 AURORA B inhibition prevents accumulation of kinetochore MPS1

Kinetochore localization of MPS1 is enhanced at 0.5 µM reversine (Rev). If AURORA B is inhibited with 100 nM hesperadin (Hesp), reversine-induced localization of MPS1 is abrogated. This experiment is equivalent to that shown in Fig. 35E. In this version of the experiment, nocodazole (Noco) was used at 3.3 µM instead of 0.66 µM, and hesperadin was used at 0.1 µM. Cells were fixed in 1% formaldehyde and imaged in a confocal microscope. Numbers above arrows indicate time in hours. DTB, double thymidine block; IF, immunofluorescence. Bar, 5 µm.

Both Reversine and Hesperadin reduced the mitotic phosphorylation of MPS1 (Figure 35F). This was not due to a direct effect of Hesperadin on MPS1, because I failed to observe significant MPS1 (and BUB1) inhibition by 1 µM Hesperadin *in vitro* (Figure 35G). Collectively, the experiments in Figure 35 strongly support the idea that MPS1 acts downstream of AURORA B, rather than upstream, as recently proposed (Jelluma et al., 2008).

Role of MPS1 in error correction

The work so far demonstrates that MPS1 is important for bi-orientation, in agreement with previous observations (Jelluma et al., 2008; Jones et al., 2005; Maure et al., 2007; Tighe et al., 2008). I wished to exploit the availability of a small-molecule inhibitor of MPS1 to test whether this kinase is implicated in error correction. For this, I applied an assay previously developed to test the implication of AURORA B in error correction (Lampson et al., 2004). HeLa cells were first treated with the Eg5 inhibitor STLC to induce a monopolar spindle and a large number of kinetochore-microtubule attachment errors (Figure 37). Cells were then allowed to recover by washing out the Eg5 inhibitor in the presence of MG132. Control cells formed a bipolar spindle. If the recovery phase was carried out in the presence of Reversine to inhibit MPS1, or ZM447439 to inhibit AURORA B, bipolar spindles also formed, but several mis-aligned chromosomes were evident (as quantified in Figure 37B). Thus, both MPS1 and AURORA B activity are required to recover from the attachment errors induced by mono-polarization. Of note, while the P-CENP-A signal disappeared in ZM447439, no inhibition of P-CENP-A was evident in the presence of Reversine, indicating that the target of Reversine in error correction is unlikely to be, or to act upstream of, AURORA B in this pathway. At 1 μM, ZM447439 did not inhibit MPS1 in vitro (Table I).

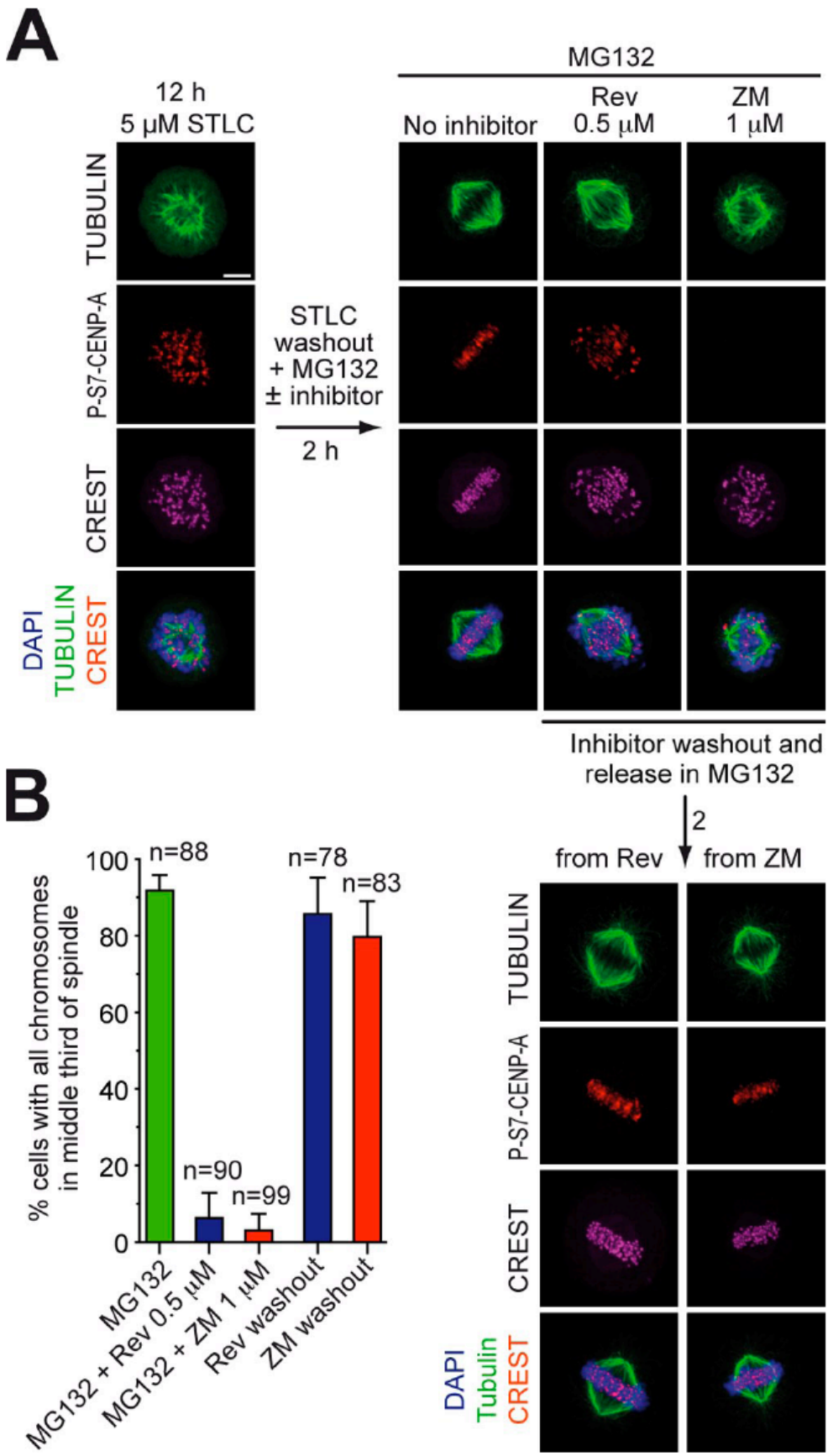

Figure 37 MPS1 is involved in error correction

(**A**) Cycling HeLa cells were treated with STLC for 12 hours. Most cells arrested in mitosis with a monopolar spindle. After STLC washout in MG132, control cells bipolarized and formed a normal metaphase. If STLC washout is carried out in the presence of Reversine or ZM447439, the spindle bipolarizes normally but a large fraction of improper attachments are visible. P-S7-CENP-A, a *bona fide* AURORA B substrate, appears unaltered in Reversine-treated cells but disappears in ZM447439. After removal of the inhibitors, a metaphase plate forms. P-S7-CENP-A reappears after washout of ZM447439. In vitro, 2 μM ZM447439 does not inhibit MPS1 (not shown). Bar =5 μm. (**B**) Quantification of results with number of cells monitored in the experiment.

After washout of ZM447439 or Reversine, normal metaphases with properly aligned chromosomes formed, indicating that the targets of these inhibitors are required for EC. Overall, these results implicate MPS1, like AURORA B, in the correction of improper kinetochore-microtubule attachments. A similar assay was recently conducted (Jelluma et al., 2008) with an inhibitor, SP600125, previously claimed to target MPS1 (Schmidt et al., 2005). However, I have found that SP600125 inhibits AURORA B in vitro with 13-fold selectivity over MPS1 (Figure 38), in agreement with a previous report (Bain et al., 2007). Thus, I suspect that the primary target of SP600125 in error correction is AURORA B, rather than MPS1.

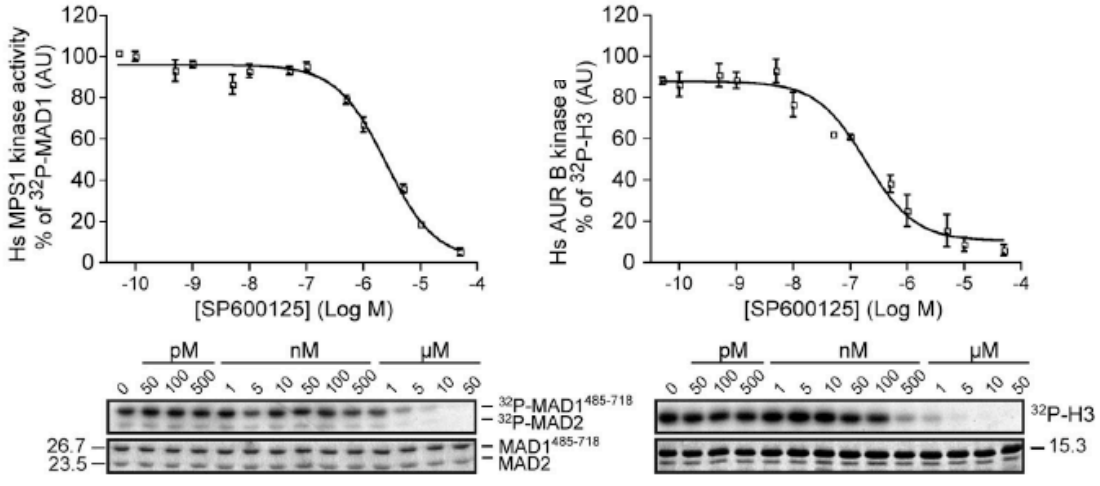

Figure 38 SP600125 inhibits AURORA B in vitro with 13-fold selectivity over MPS1

Left panel A kinase assay on human full-length MPS1 in the presence of growing concentrations of the SP600125 inhibitor. *Right panel* An equivalent assay with AURORA $B^{1–344}$–$INCENP^{835–903}$. As already reported by Bain et al. (2007), Aurora B is a target of SP600125.

MPS1 is required for localization of checkpoint proteins when microtubules are completely depolymerized

Kinetochore-bound microtubules contribute to removing the checkpoint proteins from kinetochores (Musacchio and Salmon, 2007). A consequence of the artificial stabilization of kinetochore-microtubule attachment when the error correction pathway is inhibited is that the levels of checkpoint proteins at kinetochores are strongly reduced (Yang et al., 2009). To demonstrate beyond reasonable doubt that the inhibition of MPS1 causes a genuine checkpoint override, rather than a mere satisfaction of the spindle checkpoint in the absence of error correction, as has been previously proposed for AURORA B inhibitors (Yang et al., 2009), I monitored the recruitment of the checkpoint proteins, an established hallmark of checkpoint activity, to kinetochores at 3.3 μM Nocodazole, a concentration that caused complete depolymerization of the microtubules (Figure 39A) (see also Brito et al., 2008). Even at 3.3 μM Nocodazole, both the RZZ and MAD1 were unable to localize to kinetochores (Figure 39). Thus, the disappearance of checkpoint proteins from kinetochores when MPS1 is inhibited is not due to satisfaction of the spindle checkpoint by residual kinetochore-microtubules in the absence of an error correction mechanism. Rather, this behaviour reflects a genuine requirement of MPS1 in kinetochore recruitment of a subset of checkpoint components.

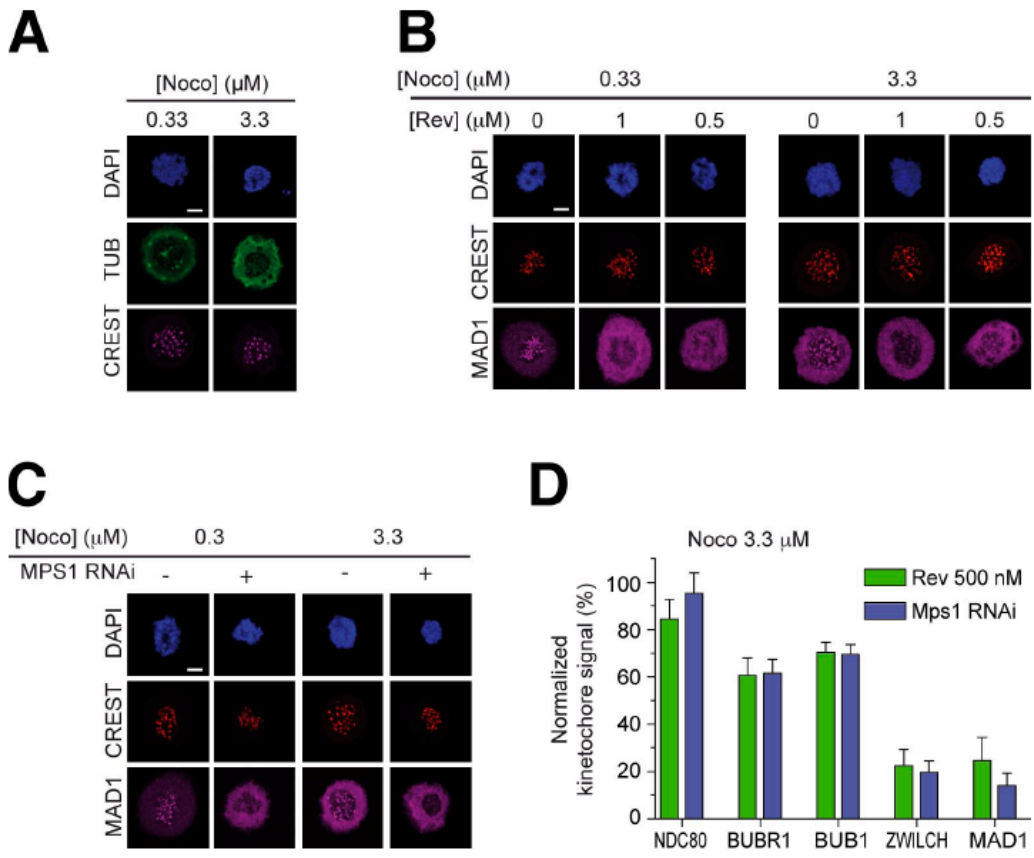

Figure 39 MPS1 is required for kinetochore recruitment of the RZZ and MAD1 even in high nocodazole

(A) Immunofluorescence analysis of the distribution of TUBULIN (TUB) in the presence of 0.33 and 3.3 μM nocodazole (Noco). Residual foci of polymerized TUBULIN are visible in 0.33 μM nocodazole but not in 3.3 μM nocodazole. HeLa cells were incubated in the presence of nocodazole for 15 min before fixation for immunofluorescence. (B) 5 h after release from a double thymidine arrest, reversine (Rev; at the indicated concentrations) and nocodazole (0.33 or 3.3 μM) were added. MAD1 failed to localize to kinetochores at either nocodazole concentration. (C) The same experimental scheme as in B was used under conditions of RNAi-based depletion of MPS1. (D) The histogram summarizes results on localization experiments equivalent to those in B and C on MAD1 and the additional indicated kinetochore proteins. Localization data were quantified as in Fig. 39 C. Error bars are mean ± SEM. Bars, 5 μm.

Discussion

In this study, I have demonstrated a role for the small molecule Reversine in mitotic inhibition of MPS1. After the discovery of cincreasin as an MPS1 inhibitor in budding yeast (Dorer et al., 2005), Reversine now provides a tool for interfering with the spindle checkpoint in human cells. The previously described role of Reversine in the de-differentiation of lineage committed mouse-derived C2C12 myoblasts (Chen et al., 2004) was initially tentatively ascribed to MEK1 and NMMII (Chen et al., 2007). More recently, inhibition of AURORA B was identified as a possible cause in this process (Amabile et al., 2009; D'Alise et al., 2008). Reversine inhibits AURORA B in mitosis, but at concentrations that are incompatible with the observed adverse effects of sub-micromolar Reversine on bi-orientation, error correction and the spindle checkpoint. On the other hand, the reported accumulation of polyploid cells at micromolar concentrations of Reversine (presumably due to a failure in cytokinesis) is consistent with AURORA B and/or NMMII inhibition (D'alise et al., 2008; Hsieh et al., 2007). The systematic comparison of the effects from using Reversine at sub-micromolar concentrations with the effects from ablating MPS1 by RNAi imply that MPS1 is the main mitotic target of Reversine. Inhibition of additional targets in other cell cycle phases and in post-mitotic cells may be responsible for the de-differentiation function of Reversine (Chen et al., 2004).

My analysis indicates that the catalytic activity of MPS1 is implicated both in error correction and in the spindle checkpoint. It is formally possible that MPS1 is selectively activated to phosphorylate targets relevant to error correction or to the spindle checkpoint under different conditions (e.g. lack of attachment, or lack of tension in the presence of attachment). However, it is simpler to hypothesize that the error correction and spindle checkpoint pathways intersect at MPS1 when its kinase activity becomes activated at kinetochores, so that substrates in both pathways become concomitantly phosphorylated.

Among the mechanisms through which MPS1 may contribute to bi-orientation and error correction is the ability of MPS1 to regulate the motor activity of CENP-E, a plus-end directed motor that crucially contributes to chromosome congression (Espeut et al., 2008).

Furthermore, the ablation of kinetochore recruitment of the RZZ complex in the absence of MPS1 activity likely prevents kinetochore recruitment of Dynein, which also contributes to kinetochore-microtubule attachment (reviewed in Musacchio and Salmon, 2007). In yeast, Mps1 regulation of bi-orientation may proceed through phosphorylation of the subunits of the Dam1 and Ndc80 complexes (Kemmler et al., 2009; Shimogawa et al., 2006). On the other hand, MPS1 may control the spindle checkpoint by contributing, among additional functions, to kinetochore recruitment of the RZZ complex and MAD1.

It is important to characterize the hierarchical relationships at the apex of the sensory apparatus that distinguishes correct from incorrect attachments and that ignites the error correction and checkpoint responses. Two recent studies demonstrated that intra-kinetochore stretch upon microtubule binding, as opposed to inter-kinetochore stretch, is the crucial parameter in the checkpoint response (Maresca and Salmon, 2009; Uchida et al., 2009). Upon microtubule binding, the distance between certain fluorescence markers within the kinetochore, projected onto the inter-kinetochore axis, increases up to 35-40 nm (Maresca and Salmon, 2009; Uchida et al., 2009; Wan et al., 2009). These changes may reflect a distortion in the structure of kinetochores caused by the application of a physical force (tension) upon microtubule binding. Alternatively, they may reflect a conformational change in the kinetochore triggered by microtubule binding. The first hypothesis is reinforced by the observation that microtubule binding is *per se* insufficient to cause full intra-kinetochore stretching, and that dynamic microtubules are required for full stretching (Maresca and Salmon, 2009; Maresca and Salmon, 2010).

The AURORA B kinase has emerged as a key regulator of the error correction pathway. It has been proposed that AURORA B may monitor variations in the distance from its substrates as microtubules attach to kinetochores (Andrews et al., 2004; Tanaka et al., 2002). Strong experimental evidence in favour of this idea has been recently gathered (Liu et al., 2009a; Liu et al., 2010; Vader et al., 2007). Tension exerted by bound microtubules may contribute to the

gradual displacement of substrates from AURORA B, resulting in turn in substrate dephosphorylation.

How does Aurora B distinguish correct from incorrect attachments? How is its activity differentially regulated at correct and incorrect attachments? Bi-oriented sister chromatids are under tension, i.e. they experience a force that tends to part the sisters, stretching centromeric chromatin as well as the kinetochore (Maresca and Salmon, 2009; Skibbens et al., 1993; Uchida et al., 2009; Waters et al., 1996). Incompletely (monotelic or even unbound) or incorrectly (syntelic) attached sisters, on the other hand, are not under tension (e.g. Ditchfield et al., 2003; Liu et al., 2009b). Because 1) the distance between centromeres and kinetochores increases when the sisters are under tension, and 2) the CPC is located at the centromere, it was proposed that the Ipl1/Aurora B kinase might be measuring the distance of its substrates under different stretching conditions (Figure 40) (Tanaka et al., 2002). Recently, this hypothesis was corroborated by elegant experiments in which an Aurora B substrate docked at a sufficiently large distance from the centromere-kinetochore interface became dephosphorylated as microtubule attachment ensued (Liu et al., 2009a). Closer substrates, on the other hand, were constitutively phosphorylated with or without microtubule attachment, showing that Aurora B delivers constitutive levels of phosphorylation during the attachment phase, and that the regulation depends on the accessibility of the substrates (Figure 40) (Liu et al., 2009a).

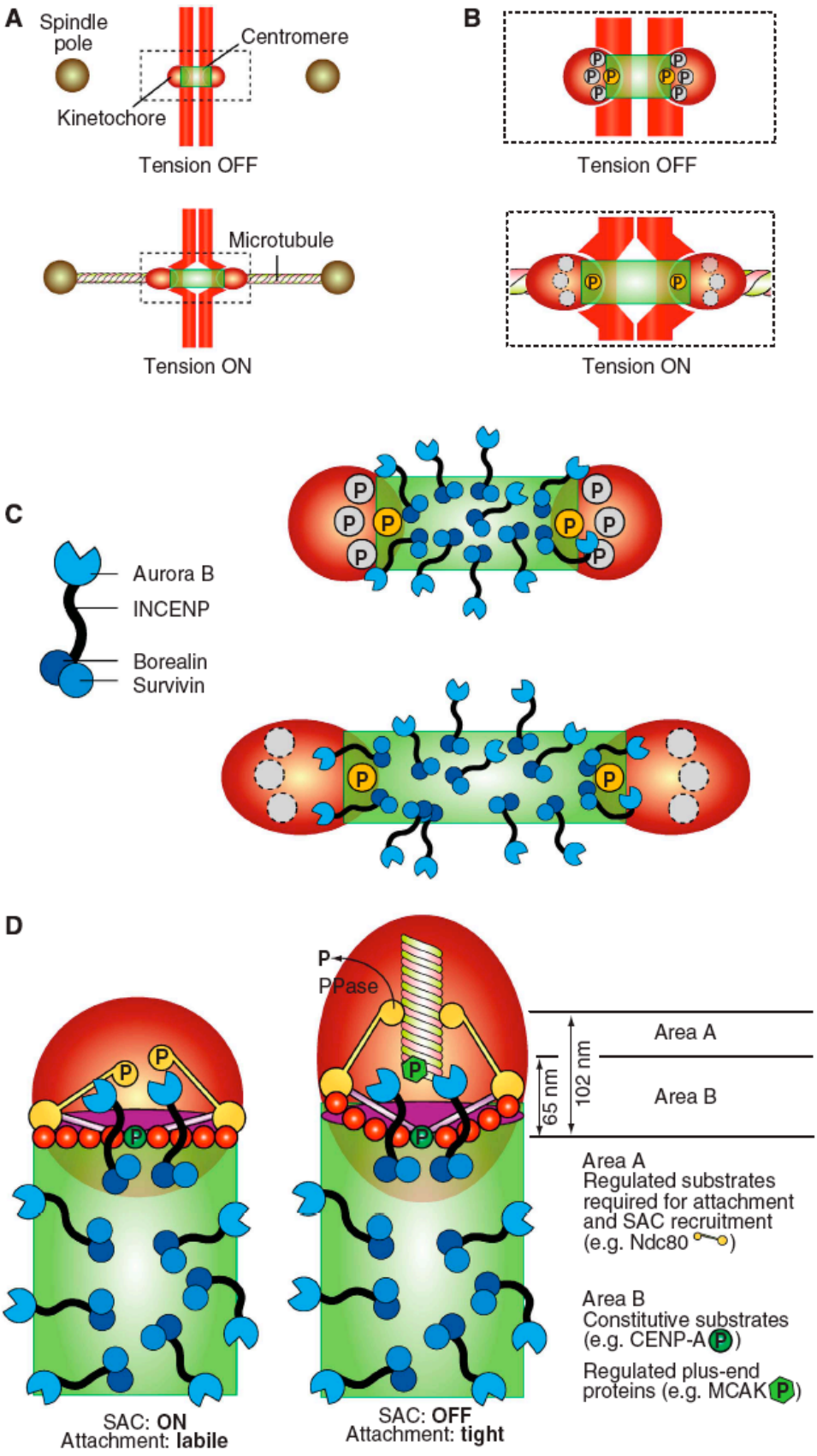

Figure 40 Error correction and the spindle checkpoint

(A) Schematic description of the geometry of the centromere–kinetochore interface in the absence and presence of tension. **(B)** The boxed area in **(A)** enlarged. Phosphorylation of certain substrates at the centromere–kinetochore interface is constitutive (the yellow circle marked by 'P'), that is the substrate is phosphorylated with or without tension. Other substrates are only phosphorylated in the absence of tension, because their separation from the centromere exceeds a threshold value when tension is present. **(C)** Left: schematic description of the CPC complex. Right: the CPC occupies the centromere, and only a subset of complexes is located near the centromere–kinetochore interface. **(D)** A comprehensive model of checkpoint control and error correction. In the absence of tension, either substrate like Ndc80 become phosphorylated by Aurora B or by other kinases whose activation requires Aurora B. This creates a condition for SAC activation through the recruitment of SAC proteins (Ditchfield et al, 2003; Hauf et al, 2003). On the other hand, the phosphorylation of Ndc80 decreases the binding affinity for microtubules (Cheeseman et al, 2006; DeLuca et al, 2006; Ciferri et al, 2008). This creates a state of labile attachment that will become corrected unless a force is applied. The removal of Ndc80 and possibly other substrates from the reach of Aurora B stabilizes the attachment through the action of a phosphatase.

A perplexing aspect of this model is that Aurora B is tethered, through the INCENP linker, to a Borealin:Survivin complex embedded in the centromere (Figure 40D) (Ruchaud et al., 2007; Vader et al., 2006). Because the inter-kinetochore centromere region extends for 1 μM or more, it is difficult to envision how CPC complexes with much smaller linear dimensions and tethered within this domain could reach substrates in the kinetochore. The existence of a gradient of Aurora B activity might be advocated to resolve this conceptual difficulty and soluble pools of Aurora B have been visualized. However, the distance dependency of substrate phosphorylation by Aurora B is exercised over nanometer-scale distances, over which the enforcement of a steep gradient is very unlikely.

A possible solution to this conundrum is that only a subset of Aurora B molecules, and in particular those belonging to CPC complexes located near the centromere-kinetochore interface, are able to reach substrates in the kinetochore. If these molecules were tethered and were only able to reach as far as a certain distance from the point of tethering, kinetochore stretching upon microtubule attachment might indeed result in the separation of Aurora B

from its substrates (Figure 40D). Indeed, two recent seminal papers demonstrated that kinetochores become stretched during kinetochore-microtubule attachment. For instance, the distance between the C-terminus of Aurora B and CENP-A decreases from approximately 102 nm to approximately 65 nm when chromosomes are or are not under tension, respectively (Maresca and Salmon, 2009; Uchida et al., 2009).

The fact that Aurora B is active in the presence of unattached kinetochores poses a conceptual difficulty. It suggests that a model in which Aurora B activity is required to destabilize tensionless kinetochore-microtubule attachments is probably simplistic. As unattached kinetochores are also tensionless, the destabilization model predicts that they would be targeted by Aurora B and would be permanently prevented from attaching. Rather, Aurora B may function by preventing premature stabilization of the attachments, i.e. by creating an initial condition of labile attachment that would allow correction (for instance, by the intrinsic instability of microtubules) unless microtubules pulled in the right direction and enforced tension, subtracting kinetochore substrates from the Aurora B kinase and making them become stabilized (Figure 40C). Experiments with a deletion mutant of INCENP are consistent with this idea (Vader et al., 2007).

I provide evidence that AURORA B acts upstream of MPS1, and that the perturbation of MPS1 activity does not grossly alter the phosphorylation of AURORA B substrates or the localization of AURORA B. Conversely, inhibition of AURORA B causes a mislocalization of MPS1, and a reduction of its phosphorylation. Because MPS1 turns over rapidly at kinetochores (Howell et al., 2004), its activation at kinetochores, which probably involves dimerization and auto-phosphorylation (Jelluma et al., 2008; Kang et al., 2007; Mattison et al., 2007), may precede its release in the cytosol in an active form.

These conclusions may appear inconsistent with the recent proposal that MPS1 controls AURORA B through phosphorylation of BOREALIN, a subunit of the chromosome passenger complex (Jelluma et al., 2008). Because a phospho-mimicking mutant of BOREALIN simulating MPS1 phosphorylation rescues the effects on bi-orientation from

loosing MPS1 (Jelluma et al., 2008), MPS1 and BOREALIN may participate in an AURORA B-independent pathway implicated in bi-orientation. More studies will be required to assess this idea, but the possibility that AURORA B acts upstream of MPS1 is consistent with the pattern of recruitment of different spindle checkpoint proteins in different systems (Emanuele et al., 2008; Famulski and Chan, 2007; Vigneron et al., 2004).

If MPS1, which is implicated in error correction and in the checkpoint, acts downstream from AURORA B and is activated by it, then AURORA B is also expected to control both error correction and the spindle checkpoint. While the involvement of AURORA B in error correction is widely accepted, its participation in the spindle checkpoint is more controversial. In at least two model systems, *Schyzosaccharaomyces pombe* and *Xenopus laevis*, Aurora B is required for the checkpoint response to unattached kinetochores (Kallio et al., 2002; Petersen and Hagan, 2003; Vanoosthuyse and Hardwick, 2009). Direct involvement of AURORA B in checkpoint signalling has also been observed upon expression of an INCENP mutant deleted of the coiled-coil domain of INCENP (Vader et al., 2007). This mutant does not affect the ability of AURORA B to phosphorylate some of its centromeric substrates, suggesting that it is impairing a specific function of the chromosome passenger complex in spindle checkpoint control (Vader et al., 2007).

In many additional settings, including experiments with yeast temperature-sensitive mutants (Biggins and Murray, 2001) or small molecule inhibitors (Ditchfield et al., 2003; Hauf et al., 2003), the inhibition of AURORA B has been shown to reduce the strength of the checkpoint arrest to unattached kinetochores, but not to lead to complete override. It is possible that these effects result from residual AURORA B activity as a consequence of incomplete depletion or inactivation. Small residual AURORA B activity may be sufficient to maintain the arrest under the strong checkpoint activating conditions created by spindle-depolymerising agents. On the other hand, the requirements on MPS1 may be more stringent, explaining why it is relatively easier to observe a checkpoint override when targeting MPS1.

A confusing aspect of the relationship between error correction and the spindle checkpoint is that the inhibition of error correction can influence the pattern of kinetochore localization of the spindle checkpoint proteins, and therefore the strength of the checkpoint response at low concentrations of spindle depolymerising drugs such as Nocodazole (Brito et al., 2008; Yang et al., 2009). Evidence of this can be extrapolated from Figure 33: the same concentration of Reversine (i.e. the same expected degree of target kinase inhibition) has significantly different effects on the duration of mitotic arrest at low or high Nocodazole doses. Thus, residual microtubules may contribute to checkpoint satisfaction if kinetochores cannot let go of them because error correction is impaired (Yang et al., 2009). A pathway that removes the checkpoint proteins from microtubule-bound kinetochores (reviewed in Musacchio and Salmon, 2007) is likely responsible for this phenomenon. Future studies will have to refer to the rigorous test proposed by Yang and co-coworkers for evaluating the participation of MPS1 and AURORA B in the checkpoint response (Yang et al., 2009). The test consists in evaluating the effects from ablating a putative checkpoint component when spindle depolymerising drugs are present at concentrations (3.2 μM Nocodazole in HeLa cells) that remove any residual tubulin polymer (Figure 39A). By applying this test to AURORA B, Yang and colleagues (Yang et al., 2009) demonstrated that at 100 nM Hesperadin the presence or absence of residual microtubules results in dramatic differences in the localization of the checkpoint protein MAD2 to kinetochores. At high Nocodazole concentrations (3.2 μM), MAD2 is retained on kinetochores despite the presence of Hesperadin. Conversely, at low Nocodazole concentrations and at the same concentration of Hesperadin, MAD2 is absent from kinetochores (Yang et al., 2009).

This result predicts that previous studies implicating AURORA B in MAD2 recruitment might have been at least in part biased by the low Nocodazole concentrations used (e.g. Ditchfield et al., 2003; Hauf et al., 2003). On the other hand, at higher Hesperadin concentrations (0.5 μM) MAD1 (which is required for MAD2 recruitment) and the RZZ complex are lost from kinetochores even at high concentrations of Nocodazole (data not

shown). Thus, AURORA B may be ultimately required for the recruitment of these checkpoint proteins, but higher levels of inhibition may be required for its involvement to become explicit. These higher concentrations of Hesperadin do not inhibit BUB1 and MPS1, but it remains formally possible that Hesperadin inhibits additional kinases in the MAD1 and RZZ recruitment pathway. Thus, a formal assessment of the role of AURORA B in the checkpoint response will require more penetrant and selective inhibition of AURORA B.

Materials and Methods

Cell culture and synchronization

HeLa cells and U2OS cells were grown in Dulbecco's modified Eagle medium (DMEM, Euroclone) supplemented with 10% fetal bovine serum (Hyclone) and 2 mM L-glutamine. hTERT-RPE cells were grown in Minimal Essential Medium: HAM's F12K Medium 1:1 supplemnted with 10 % fetal bovine serum (Hyclone), 15 mM HEPES, 0.5 mM Sodium Pyruvate. Nocodazole (0.33 and 3.3 μM), Taxol (0.5 μM), STLC (5 μM), and thymidine (2 mM) were obtained from Sigma-Aldrich. MG132 (Calbiochem) was used at 10 μM throughout.

RNAi

Previously described siRNA duplexes were used to repress AURORA A and AURORA B (Ditchfield et al., 2003), BUB1 (Johnson et al., 2004) and BUBR1 (Lampson and Kapoor, 2005). siRNA duplexes were purchased from Dharmacon Research and transfected using Lipofectamine 2000 reagent (Invitrogen) according to the manufacturer's instructions.

Immunofluorescence microscopy and antibodies for immunofluorescence

In all cases except Figure 7E, immunofluorescence microscopy was carried out on cells fixed using PFA 4% in PBS, permeabilized using Triton X-100 0.1 % in PBS, then treated with BSA 4% in PBS as blocking agent and incubated with the proper antibodies diluted in BSA 4% in PBS. The following antibodies (Ab) were used for immunofluorescence: Anti-Centromeric Ab (working dilution 1:50, Antibodies Inc.); Mouse anti-HEC1 (human NDC80) (working dilution 1:1000, Genetex Clone 9G3.23); Mouse anti-α-TUBULIN (working dilution 1:2000, Sigma-Aldrich Clone B512); Rabbit anti-SPINDLY (working dilution 1:250, Bethyl

Laboratories); Rabbit anti-AURORA B (working dilution 1:1000, Abcam); Rabbit anti-P-H3 Ser10 (working dilution 1:500, Abcam); Rabbit anti-pCENPA Ser7 (working dilution 1:300, Abcam). The anti-MAD1 Ab has been described previously. Antibodies against MPS1, BUB1, BUBR1 and CENP-C have been described (Taylor et al., 2001; Tighe et al., 2008; Trazzi et al., 2009). Antibodies against ZW10, ZWILCH and ROD were kind gifts from Filiz Çivril and Tim Yen.

Cy3- and Cy5-labeled and Alexa-488-labeled secondary Abs for immunofluorescence were from Jackson Immunoresearch and Invitrogen, respectively. DNA was stained with 4',6-diamidino-2-phenylindole (DAPI). The coverslips were mounted using Mowiol mounting media. Cells were imaged using a Leica TCS SP2 confocal microscope equipped with a 63× NA 1.4 objective lens using the LCS 3D software (Leica).

Antibodies for IB

The following antibodies were used for immunobloting: Mouse anti-AURORA A (working dilution 1:1000, Sigma); Rabbit anti-AURORA B (working dilution 1:1000, Abcam); Rabbit anti-BUB1 (working dilution 1:2000, Abcam); Mouse anti-BUBR1 (working dilution 1:1000, Transduction Laboratories, BD); Mouse anti-MPS1 (working dilution 1:2000, Upstate); Rabbit anti-pH3 Ser10 (working dilution 1:1000, Abcam).

Video Microscopy

Live cell imaging was performed using a IX70 inverted microscope (Nikon) equipped with an incubation chamber (Solent Scientific) maintained at 37°C in an atmosphere of 5% CO_2. Movies were acquired using a 20× magnification objective controlled by ScanR software (Olympus).

In vitro Kinase Assays

In vitro kinase assays were performed and analyzed as previously described (DeMoe et al., 2009) with slight modifications. Briefly, IC_{50} values were determined using 5 nM human AURORA B^{45-344}:$INCENP^{835-903}$ or AURORA B^{1-344}:$INCENP^{835-903}$, or 1 nM full length human MPS1 (Invitrogen) according to the manufacturer's instructions. Haspin purification protocol and kinase assay conditions have been described (Villa et al., 2009). PRP4 kinase was expressed as a fusion to a hexahistine tag in Hi5 insect cells infected with recombinant baculoviruses. The complex was isolated on Ni-NTA beads, eluted using 200 mM Imidazole and further dialyzed against PBS. PRP4 kinase reaction buffer contained 50 mM Tris-HCl pH 7.6, 150 mM NaCl, 10 mM MgCl2, 1 mM EDTA and histone H3 was used as substrate. Purification and kinase assay of TAO1 have been described (DeMoe et al., 2009). The kinase domain of Mps1 (residues 515-857) was expressed from pNIC28-Bsa4 (a kind gift of S. Knapp; http://www.sgc.ox.ac.uk/structures/MM/TTKA_3h9f_MM.html).

References

Alexander, S.P., and C.L. Rieder. 1991. Chromosome motion during attachment to the vertebrate spindle: initial saltatory-like behavior of chromosomes and quantitative analysis of force production by nascent kinetochore fibers. *J Cell Biol.* 113:805-15.

Allshire, R.C., and G.H. Karpen. 2008. Epigenetic regulation of centromeric chromatin: old dogs, new tricks? *Nat Rev Genet.* 9:923-37.

Amabile, G., A.M. D'Alise, M. Iovino, P. Jones, S. Santaguida, A. Musacchio, S. Taylor, and R. Cortese. 2009. The Aurora B kinase activity is required for the maintenance of the differentiated state of murine myoblasts. *Cell Death Differ.* 16:321-30.

Ando, S., H. Yang, N. Nozaki, T. Okazaki, and K. Yoda. 2002. CENP-A, -B, and -C chromatin complex that contains the I-type alpha-satellite array constitutes the prekinetochore in HeLa cells. *Mol Cell Biol.* 22:2229-41.

Andrews, P.D., Y. Ovechkina, N. Morrice, M. Wagenbach, K. Duncan, L. Wordeman, and J.R. Swedlow. 2004. Aurora B regulates MCAK at the mitotic centromere. *Dev Cell.* 6:253-68.

Asbury, C.L., D.R. Gestaut, A.F. Powers, A.D. Franck, and T.N. Davis. 2006. The Dam1 kinetochore complex harnesses microtubule dynamics to produce force and movement. *Proc Natl Acad Sci U S A.* 103:9873-8.

Bain, J., L. Plater, M. Elliott, N. Shpiro, C.J. Hastie, H. McLauchlan, I. Klevernic, J.S. Arthur, D.R. Alessi, and P. Cohen. 2007. The selectivity of protein kinase inhibitors: a further update. *Biochem J.* 408:297-315.

Bakhoum, S.F., S.L. Thompson, A.L. Manning, and D.A. Compton. 2009. Genome stability is ensured by temporal control of kinetochore-microtubule dynamics. *Nat Cell Biol.* 11:27-35.

Basto, R., R. Gomes, and R.E. Karess. 2000. Rough deal and Zw10 are required for the metaphase checkpoint in Drosophila. *Nat Cell Biol.* 2:939-43.

Basto, R., F. Scaerou, S. Mische, E. Wojcik, C. Lefebvre, R. Gomes, T. Hays, and R. Karess. 2004. In vivo dynamics of the rough deal checkpoint protein during Drosophila mitosis. *Curr Biol.* 14:56-61.

Biggins, S., and A.W. Murray. 2001. The budding yeast protein kinase Ipl1/Aurora allows the absence of tension to activate the spindle checkpoint. *Genes Dev.* 15:3118-29.

Black, B.E., and E.A. Bassett. 2008. The histone variant CENP-A and centromere specification. *Curr Opin Cell Biol.* 20:91-100.

Bloom, K., S. Sharma, and N.V. Dokholyan. 2006. The path of DNA in the kinetochore. *Curr Biol.* 16:R276-8.

Blower, M.D., B.A. Sullivan, and G.H. Karpen. 2002. Conserved organization of centromeric chromatin in flies and humans. *Dev Cell.* 2:319-30.

Brito, D.A., Z. Yang, and C.L. Rieder. 2008. Microtubules do not promote mitotic slippage when the spindle assembly checkpoint cannot be satisfied. *J Cell Biol.* 182:623-9.

Burke, D.J., and P.T. Stukenberg. 2008. Linking kinetochore-microtubule binding to the spindle checkpoint. *Dev Cell.* 14:474-9.

Chan, G.K., S.A. Jablonski, D.A. Starr, M.L. Goldberg, and T.J. Yen. 2000. Human Zw10 and ROD are mitotic checkpoint proteins that bind to kinetochores. *Nat Cell Biol.* 2:944-7.

Chan, Y.W., L.L. Fava, A. Uldschmid, M.H. Schmitz, D.W. Gerlich, E.A. Nigg, and A. Santamaria. 2009. Mitotic control of kinetochore-associated dynein and spindle orientation by human Spindly. *J Cell Biol.* 185:859-74.

Cheeseman, I.M., C. Brew, M. Wolyniak, A. Desai, S. Anderson, N. Muster, J.R. Yates, T.C. Huffaker, D.G. Drubin, and G. Barnes. 2001. Implication of a novel multiprotein Dam1p complex in outer kinetochore function. *J Cell Biol.* 155:1137-45.

Cheeseman, I.M., J.S. Chappie, E.M. Wilson-Kubalek, and A. Desai. 2006. The conserved KMN network constitutes the core microtubule-binding site of the kinetochore. *Cell.* 127:983-97.

Cheeseman, I.M., and A. Desai. 2008. Molecular architecture of the kinetochore-microtubule interface. *Nat Rev Mol Cell Biol.* 9:33-46.

Cheeseman, I.M., S. Niessen, S. Anderson, F. Hyndman, J.R. Yates, 3rd, K. Oegema, and A. Desai. 2004. A conserved protein network controls assembly of the outer kinetochore and its ability to sustain tension. *Genes Dev.* 18:2255-68.

Chen, S., S. Takanashi, Q. Zhang, W. Xiong, S. Zhu, E.C. Peters, S. Ding, and P.G. Schultz. 2007. Reversine increases the plasticity of lineage-committed mammalian cells. *Proc Natl Acad Sci U S A.* 104:10482-7.

Chen, S., Q. Zhang, X. Wu, P.G. Schultz, and S. Ding. 2004. Dedifferentiation of lineage-committed cells by a small molecule. *J Am Chem Soc.* 126:410-1.

Ciferri, C., J. De Luca, S. Monzani, K.J. Ferrari, D. Ristic, C. Wyman, H. Stark, J. Kilmartin, E.D. Salmon, and A. Musacchio. 2005. Architecture of the human ndc80-hec1 complex, a critical constituent of the outer kinetochore. *J Biol Chem.* 280:29088-95.

Ciferri, C., S. Pasqualato, E. Screpanti, G. Varetti, S. Santaguida, G. Dos Reis, A. Maiolica, J. Polka, J.G. De Luca, P. De Wulf, M. Salek, J. Rappsilber, C.A. Moores, E.D. Salmon, and A. Musacchio. 2008. Implications for kinetochore-microtubule attachment from the structure of an engineered Ndc80 complex. *Cell.* 133:427-39.

Cimini, D., B. Moree, J.C. Canman, and E.D. Salmon. 2003. Merotelic kinetochore orientation occurs frequently during early mitosis in mammalian tissue cells and error correction is achieved by two different mechanisms. *J Cell Sci.* 116:4213-25.

Cimini, D., X. Wan, C.B. Hirel, and E.D. Salmon. 2006. Aurora kinase promotes turnover of kinetochore microtubules to reduce chromosome segregation errors. *Curr Biol.* 16:1711-8.

Civril, F., and A. Musacchio. 2008. Spindly attachments. *Genes Dev.* 22:2302-7.

Cleveland, D.W., Y. Mao, and K.F. Sullivan. 2003. Centromeres and kinetochores: from epigenetics to mitotic checkpoint signaling. *Cell.* 112:407-21.

Coue, M., V.A. Lombillo, and J.R. McIntosh. 1991. Microtubule depolymerization promotes particle and chromosome movement in vitro. *J Cell Biol.* 112:1165-75.

D'alise, A., G. Amabile, M. Iovino, F. Di Giorgio, M. Bartiromo, F. Sessa, F. Villa, A. Musacchio, and R. Cortese. 2008. Reversine, a novel Aurora kinases inhibitor, inhibits colony formation of human acute myeloid leukemia cells. *Mol Cancer Ther.* 7:1140-1149.

D'Alise, A.M., G. Amabile, M. Iovino, F.P. Di Giorgio, M. Bartiromo, F. Sessa, F. Villa, A. Musacchio, and R. Cortese. 2008. Reversine, a novel Aurora kinases inhibitor, inhibits colony formation of human acute myeloid leukemia cells. *Mol Cancer Ther.* 7:1140-9.

Davis, T.N., and L. Wordeman. 2007. Rings, bracelets, sleeves, and chevrons: new structures of kinetochore proteins. *Trends Cell Biol.* 17:377-82.

De Wulf, P., A.D. McAinsh, and P.K. Sorger. 2003. Hierarchical assembly of the budding yeast kinetochore from multiple subcomplexes. *Genes Dev.* 17:2902-21.

DeBonis, S., D.A. Skoufias, L. Lebeau, R. Lopez, G. Robin, R.L. Margolis, R.H. Wade, and F. Kozielski. 2004. In vitro screening for inhibitors of the human mitotic kinesin Eg5 with antimitotic and antitumor activities. *Mol Cancer Ther.* 3:1079-90.

DeLuca, J.G., Y. Dong, P. Hergert, J. Strauss, J.M. Hickey, E.D. Salmon, and B.F. McEwen. 2005. Hec1 and nuf2 are core components of the kinetochore outer plate essential for organizing microtubule attachment sites. *Mol Biol Cell.* 16:519-31.

DeLuca, J.G., W.E. Gall, C. Ciferri, D. Cimini, A. Musacchio, and E.D. Salmon. 2006. Kinetochore microtubule dynamics and attachment stability are regulated by Hec1. *Cell.* 127:969-82.

DeMoe, J.H., S. Santaguida, J.R. Daum, A. Musacchio, and G.J. Gorbsky. 2009. A high throughput, whole cell screen for small molecule inhibitors of the mitotic spindle checkpoint identifies OM137, a novel Aurora kinase inhibitor. *Cancer Res.* 69:1509-16.

Desai, A., S. Rybina, T. Muller-Reichert, A. Shevchenko, A. Hyman, and K. Oegema. 2003. KNL-1 directs assembly of the microtubule-binding interface of the kinetochore in C. elegans. *Genes Dev.* 17:2421-35.

Ditchfield, C., V.L. Johnson, A. Tighe, R. Ellston, C. Haworth, T. Johnson, A. Mortlock, N. Keen, and S.S. Taylor. 2003. Aurora B couples chromosome alignment with anaphase by targeting BubR1, Mad2, and Cenp-E to kinetochores. *J Cell Biol.* 161:267-80.

Dong, Y., K.J. Vanden Beldt, X. Meng, A. Khodjakov, and B.F. McEwen. 2007. The outer plate in vertebrate kinetochores is a flexible network with multiple microtubule interactions. *Nat Cell Biol.* 9:516-22.

Dorer, R.K., S. Zhong, J.A. Tallarico, W.H. Wong, T.J. Mitchison, and A.W. Murray. 2005. A small-molecule inhibitor of Mps1 blocks the spindle-checkpoint response to a lack of tension on mitotic chromosomes. *Curr Biol.* 15:1070-6.

Emanuele, M.J., W. Lan, M. Jwa, S.A. Miller, C.S. Chan, and P.T. Stukenberg. 2008. Aurora B kinase and protein phosphatase 1 have opposing roles in modulating kinetochore assembly. *J Cell Biol.* 181:241-54.

Emanuele, M.J., M.L. McCleland, D.L. Satinover, and P.T. Stukenberg. 2005. Measuring the stoichiometry and physical interactions between components elucidates the architecture of the vertebrate kinetochore. *Mol Biol Cell.* 16:4882-92.

Espeut, J., A. Gaussen, P. Bieling, V. Morin, S. Prieto, D. Fesquet, T. Surrey, and A. Abrieu. 2008. Phosphorylation relieves autoinhibition of the kinetochore motor Cenp-E. *Mol Cell.* 29:637-43.

Euteneuer, U., and J.R. McIntosh. 1981. Structural polarity of kinetochore microtubules in PtK1 cells. *J Cell Biol.* 89:338-45.

Famulski, J.K., and G.K. Chan. 2007. Aurora B Kinase-Dependent Recruitment of hZW10 and hROD to Tensionless Kinetochores. *Curr Biol.* 17:2143-9.

Foltz, D.R., L.E. Jansen, B.E. Black, A.O. Bailey, J.R. Yates, 3rd, and D.W. Cleveland. 2006. The human CENP-A centromeric nucleosome-associated complex. *Nat Cell Biol.* 8:458-69.

Franck, A.D., A.F. Powers, D.R. Gestaut, T. Gonen, T.N. Davis, and C.L. Asbury. 2007. Tension applied through the Dam1 complex promotes microtubule elongation providing a direct mechanism for length control in mitosis. *Nat Cell Biol.* 9:832-7.

Fukagawa, T., Y. Mikami, A. Nishihashi, V. Regnier, T. Haraguchi, Y. Hiraoka, N. Sugata, K. Todokoro, W. Brown, and T. Ikemura. 2001. CENP-H, a constitutive centromere component, is required for centromere targeting of CENP-C in vertebrate cells. *EMBO J.* 20:4603-17.

Gachet, Y., C. Reyes, T. Courtheoux, S. Goldstone, G. Gay, C. Serrurier, and S. Tournier. 2008. Sister kinetochore recapture in fission yeast occurs by two distinct mechanisms, both requiring Dam1 and Klp2. *Mol Biol Cell.* 19:1646-62.

Gaitanos, T.N., A. Santamaria, A.A. Jeyaprakash, B. Wang, E. Conti, and E.A. Nigg. 2009. Stable kinetochore-microtubule interactions depend on the Ska complex and its new component Ska3/C13Orf3. *EMBO J.* 28:1442-52.

Gassmann, R., A. Essex, J.S. Hu, P.S. Maddox, F. Motegi, A. Sugimoto, S.M. O'Rourke, B. Bowerman, I. McLeod, J.R. Yates, 3rd, K. Oegema, I.M. Cheeseman, and A. Desai. 2008. A new mechanism controlling kinetochore-microtubule interactions revealed by comparison of two dynein-targeting components: SPDL-1 and the Rod/Zwilch/Zw10 complex. *Genes Dev.* 22:2385-99.

Gestaut, D.R., B. Graczyk, J. Cooper, P.O. Widlund, A. Zelter, L. Wordeman, C.L. Asbury, and T.N. Davis. 2008. Phosphoregulation and depolymerization-driven movement of the Dam1 complex do not require ring formation. *Nat Cell Biol.* 10:407-14.

Girdler, F., K.E. Gascoigne, P.A. Eyers, S. Hartmuth, C. Crafter, K.M. Foote, N.J. Keen, and S.S. Taylor. 2006. Validating Aurora B as an anti-cancer drug target. *J Cell Sci.* 119:3664-75.

Glover, D.M., M.H. Leibowitz, D.A. McLean, and H. Parry. 1995. Mutations in aurora prevent centrosome separation leading to the formation of monopolar spindles. *Cell.* 81:95-105.

Griffis, E.R., N. Stuurman, and R.D. Vale. 2007. Spindly, a novel protein essential for silencing the spindle assembly checkpoint, recruits dynein to the kinetochore. *J Cell Biol.* 177:1005-15.

Grishchuk, E.L., and J.R. McIntosh. 2006. Microtubule depolymerization can drive poleward chromosome motion in fission yeast. *EMBO J.* 25:4888-96.

Grishchuk, E.L., M.I. Molodtsov, F.I. Ataullakhanov, and J.R. McIntosh. 2005. Force production by disassembling microtubules. *Nature.* 438:384-8.

Grishchuk, E.L., I.S. Spiridonov, V.A. Volkov, A. Efremov, S. Westermann, D. Drubin, G. Barnes, F.I. Ataullakhanov, and J.R. McIntosh. 2008. Different assemblies of the DAM1 complex follow shortening microtubules by distinct mechanisms. *Proc Natl Acad Sci U S A.* 105:6918-23.

Guimaraes, G., Y. Dong, B. Mcewen, and J. Deluca. 2008. Kinetochore-Microtubule Attachment Relies on the Disordered N-Terminal Tail Domain of Hec1. *Current Biology*:16.

Hanisch, A., H.H. Sillje, and E.A. Nigg. 2006. Timely anaphase onset requires a novel spindle and kinetochore complex comprising Ska1 and Ska2. *EMBO J.* 25:5504-15.

Harrington, E.A., D. Bebbington, J. Moore, R.K. Rasmussen, A.O. Ajose-Adeogun, T. Nakayama, J.A. Graham, C. Demur, T. Hercend, A. Diu-Hercend, M. Su, J.M. Golec, and K.M. Miller. 2004. VX-680, a potent and selective small-molecule inhibitor of the Aurora kinases, suppresses tumor growth in vivo. *Nat Med.* 10:262-7.

Hartwell, L.H., and T.A. Weinert. 1989. Checkpoints: controls that ensure the order of cell cycle events. *Science*. 246:629-34.

Hauf, S., R.W. Cole, S. LaTerra, C. Zimmer, G. Schnapp, R. Walter, A. Heckel, J. van Meel, C.L. Rieder, and J.M. Peters. 2003. The small molecule Hesperadin reveals a role for Aurora B in correcting kinetochore-microtubule attachment and in maintaining the spindle assembly checkpoint. *J Cell Biol*. 161:281-94.

Hayashi, T., Y. Fujita, O. Iwasaki, Y. Adachi, K. Takahashi, and M. Yanagida. 2004. Mis16 and Mis18 are required for CENP-A loading and histone deacetylation at centromeres. *Cell*. 118:715-29.

Hewitt, L., A. Tighe, S. Santaguida, A.M. White, C.D. Jones, A. Musacchio, S. Green, and S.S. Taylor. Sustained Mps1 activity is required in mitosis to recruit O-Mad2 to the Mad1-C-Mad2 core complex. *J Cell Biol*. 190:25-34.

Hill, T.L. 1985. Theoretical problems related to the attachment of microtubules to kinetochores. *Proc Natl Acad Sci U S A*. 82:4404-8.

Hori, T., M. Amano, A. Suzuki, C.B. Backer, J.P. Welburn, Y. Dong, B.F. McEwen, W.H. Shang, E. Suzuki, K. Okawa, I.M. Cheeseman, and T. Fukagawa. 2008. CCAN makes multiple contacts with centromeric DNA to provide distinct pathways to the outer kinetochore. *Cell*. 135:1039-52.

Howell, B.J., B. Moree, E.M. Farrar, S. Stewart, G. Fang, and E.D. Salmon. 2004. Spindle checkpoint protein dynamics at kinetochores in living cells. *Curr Biol*. 14:953-64.

Hsieh, T.C., F. Traganos, Z. Darzynkiewicz, and J.M. Wu. 2007. The 2,6-disubstituted purine reversine induces growth arrest and polyploidy in human cancer cells. *Int J Oncol*. 31:1293-300.

Huang, H., J. Feng, J. Famulski, J.B. Rattner, S.T. Liu, G.D. Kao, R. Muschel, G.K. Chan, and T.J. Yen. 2007. Tripin/hSgo2 recruits MCAK to the inner centromere to correct defective kinetochore attachments. *J Cell Biol*. 177:413-24.

Hyman, A.A., K. Middleton, M. Centola, T.J. Mitchison, and J. Carbon. 1992. Microtubule-motor activity of a yeast centromere-binding protein complex. *Nature*. 359:533-6.

Jelluma, N., A.B. Brenkman, N.J. van den Broek, C.W. Cruijsen, M.H. van Osch, S.M. Lens, R.H. Medema, and G.J. Kops. 2008. Mps1 phosphorylates Borealin to control Aurora B activity and chromosome alignment. *Cell*. 132:233-46.

Joglekar, A.P., K. Bloom, and E.D. Salmon. 2009. In vivo protein architecture of the eukaryotic kinetochore with nanometer scale accuracy. *Curr Biol*. 19:694-9.

Joglekar, A.P., D. Bouck, K. Finley, X. Liu, Y. Wan, J. Berman, X. He, E.D. Salmon, and K.S. Bloom. 2008. Molecular architecture of the kinetochore-microtubule attachment site is conserved between point and regional centromeres. *J Cell Biol*. 181:587-94.

Joglekar, A.P., D.C. Bouck, J.N. Molk, K.S. Bloom, and E.D. Salmon. 2006. Molecular architecture of a kinetochore-microtubule attachment site. *Nat Cell Biol.* 8:581-5.

Johnson, V.L., M.I. Scott, S.V. Holt, D. Hussein, and S.S. Taylor. 2004. Bub1 is required for kinetochore localization of BubR1, Cenp-E, Cenp-F and Mad2, and chromosome congression. *J Cell Sci.* 117:1577-89.

Jones, M.H., B.J. Huneycutt, C.G. Pearson, C. Zhang, G. Morgan, K. Shokat, K. Bloom, and M. Winey. 2005. Chemical genetics reveals a role for Mps1 kinase in kinetochore attachment during mitosis. *Curr Biol.* 15:160-5.

Kallio, M.J., M.L. McCleland, P.T. Stukenberg, and G.J. Gorbsky. 2002. Inhibition of aurora B kinase blocks chromosome segregation, overrides the spindle checkpoint, and perturbs microtubule dynamics in mitosis. *Curr Biol.* 12:900-5.

Kang, J., Y. Chen, Y. Zhao, and H. Yu. 2007. Autophosphorylation-dependent activation of human Mps1 is required for the spindle checkpoint. *Proc Natl Acad Sci U S A.* 104:20232-7.

Kang, J., and H. Yu. 2009. Kinase signaling in the spindle checkpoint. *J Biol Chem.* 284:15359-63.

Kapoor, T.M., M.A. Lampson, P. Hergert, L. Cameron, D. Cimini, E.D. Salmon, B.F. McEwen, and A. Khodjakov. 2006. Chromosomes can congress to the metaphase plate before biorientation. *Science.* 311:388-91.

Kelly, A., and H. Funabiki. 2009. Correcting aberrant kinetochore microtubule attachments: an Aurora B-centric view. *Curr Opin Cell Biol.*8.

Kemmler, S., M. Stach, M. Knapp, J. Ortiz, J. Pfannstiel, T. Ruppert, and J. Lechner. 2009. Mimicking Ndc80 phosphorylation triggers spindle assembly checkpoint signalling. *Embo J.* 28:1099-110.

Kerres, A., C. Vietmeier-Decker, J. Ortiz, I. Karig, C. Beuter, J. Hegemann, J. Lechner, and U. Fleig. 2004. The fission yeast kinetochore component Spc7 associates with the EB1 family member Mal3 and is required for kinetochore-spindle association. *Mol Biol Cell.* 15:5255-67.

Khodjakov, A., L. Copenagle, M.B. Gordon, D.A. Compton, and T.M. Kapoor. 2003. Minus-end capture of preformed kinetochore fibers contributes to spindle morphogenesis. *J Cell Biol.* 160:671-83.

Kingsbury, J., and D. Koshland. 1991. Centromere-dependent binding of yeast minichromosomes to microtubules in vitro. *Cell.* 66:483-95.

Kinoshita, E., E. Kinoshita-Kikuta, K. Takiyama, and T. Koike. 2006. Phosphate-binding tag, a new tool to visualize phosphorylated proteins. *Mol Cell Proteomics.* 5:749-57.

Kirschner, M., and T. Mitchison. 1986. Beyond self-assembly: from microtubules to morphogenesis. *Cell.* 45:329-42.

Kiyomitsu, T., C. Obuse, and M. Yanagida. 2007. Human Blinkin/AF15q14 is required for chromosome alignment and the mitotic checkpoint through direct interaction with Bub1 and BubR1. *Dev Cell.* 13:663-76.

Kline, S.L., I.M. Cheeseman, T. Hori, T. Fukagawa, and A. Desai. 2006. The human Mis12 complex is required for kinetochore assembly and proper chromosome segregation. *J Cell Biol.* 173:9-17.

Knowlton, A.L., W. Lan, and P.T. Stukenberg. 2006. Aurora B is enriched at merotelic attachment sites, where it regulates MCAK. *Curr Biol.* 16:1705-10.

Knowlton, A.L., V.V. Vorozhko, W. Lan, G.J. Gorbsky, and P.T. Stukenberg. 2009. ICIS and Aurora B coregulate the microtubule depolymerase Kif2a. *Curr Biol.* 19:758-63.

Koshland, D.E., T.J. Mitchison, and M.W. Kirschner. 1988. Polewards chromosome movement driven by microtubule depolymerization in vitro. *Nature.* 331:499-504.

Kwiatkowski, N., N. Jelluma, P. Filippakopoulos, M. Soundararajan, M.S. Manak, M. Kwon, H.G. Choi, T. Sim, Q.L. Deveraux, S. Rottmann, D. Pellman, J.V. Shah, G.J. Kops, S. Knapp, and N.S. Gray. Small-molecule kinase inhibitors provide insight into Mps1 cell cycle function. *Nat Chem Biol.* 6:359-68.

Lampson, M.A., and T.M. Kapoor. 2005. The human mitotic checkpoint protein BubR1 regulates chromosome–spindle attachments. *Nat Cell Biol.* 7:93-98.

Lampson, M.A., K. Renduchitala, A. Khodjakov, and T.M. Kapoor. 2004. Correcting improper chromosome-spindle attachments during cell division. *Nat Cell Biol.* 6:232-7.

Lan, W., X. Zhang, S.L. Kline-Smith, S.E. Rosasco, G.A. Barrett-Wilt, J. Shabanowitz, D.F. Hunt, C.E. Walczak, and P.T. Stukenberg. 2004. Aurora B phosphorylates centromeric MCAK and regulates its localization and microtubule depolymerization activity. *Curr Biol.* 14:273-86.

Li, X., and R.B. Nicklas. 1995. Mitotic forces control a cell-cycle checkpoint. *Nature.* 373:630-2.

Liu, D., G. Vader, M. Vromans, M. Lampson, and S. Lens. 2009a. Sensing Chromosome Bi-Orientation by Spatial Separation of Aurora B Kinase from Kinetochore Substrates. *Science.* 323:1350-1353.

Liu, D., G. Vader, M.J. Vromans, M.A. Lampson, and S.M. Lens. 2009b. Sensing chromosome bi-orientation by spatial separation of aurora B kinase from kinetochore substrates. *Science.* 323:1350-3.

Liu, D., M. Vleugel, C.B. Backer, T. Hori, T. Fukagawa, I.M. Cheeseman, and M.A. Lampson. 2010. Regulated targeting of protein phosphatase 1 to the outer kinetochore by KNL1 opposes Aurora B kinase. *J Cell Biol.* 188:809-20.

Liu, S.T., J.C. Hittle, S.A. Jablonski, M.S. Campbell, K. Yoda, and T.J. Yen. 2003. Human CENP-I specifies localization of CENP-F, MAD1 and MAD2 to kinetochores and is essential for mitosis. *Nat Cell Biol.* 5:341-5.

Liu, S.T., J.B. Rattner, S.A. Jablonski, and T.J. Yen. 2006. Mapping the assembly pathways that specify formation of the trilaminar kinetochore plates in human cells. *J Cell Biol.* 175:41-53.

Liu, X., I. McLeod, S. Anderson, J.R. Yates, 3rd, and X. He. 2005. Molecular analysis of kinetochore architecture in fission yeast. *EMBO J.* 24:2919-30.

Lombillo, V.A., R.J. Stewart, and J.R. McIntosh. 1995. Minus-end-directed motion of kinesin-coated microspheres driven by microtubule depolymerization. *Nature.* 373:161-4.

Maciejowski, J., K.A. George, M.E. Terret, C. Zhang, K.M. Shokat, and P.V. Jallepalli. Mps1 directs the assembly of Cdc20 inhibitory complexes during interphase and mitosis to control M phase timing and spindle checkpoint signaling. *J Cell Biol.* 190:89-100.

Maiato, H., J. DeLuca, E.D. Salmon, and W.C. Earnshaw. 2004. The dynamic kinetochore-microtubule interface. *J Cell Sci.* 117:5461-77.

Maiolica, A., D. Cittaro, D. Borsotti, L. Sennels, C. Ciferri, C. Tarricone, A. Musacchio, and J. Rappsilber. 2007. Structural analysis of multiprotein complexes by cross-linking, mass spectrometry, and database searching. *Mol Cell Proteomics.* 6:2200-11.

Mandelkow, E.M., E. Mandelkow, and R.A. Milligan. 1991. Microtubule dynamics and microtubule caps: a time-resolved cryo-electron microscopy study. *J Cell Biol.* 114:977-91.

Maresca, T.J., and E.D. Salmon. 2009. Intrakinetochore stretch is associated with changes in kinetochore phosphorylation and spindle assembly checkpoint activity. *J Cell Biol.* 184:373-81.

Maresca, T.J., and E.D. Salmon. 2010. Welcome to a new kind of tension: translating kinetochore mechanics into a wait-anaphase signal. *J Cell Sci.* 123:825-35.

Margolis, R.L., and L. Wilson. 1981. Microtubule treadmills--possible molecular machinery. *Nature.* 293:705-11.

Marshall, O.J., A.T. Marshall, and K.H. Choo. 2008. Three-dimensional localization of CENP-A suggests a complex higher order structure of centromeric chromatin. *J Cell Biol.* 183:1193-202.

Mattison, C.P., W.M. Old, E. Steiner, B.J. Huneycutt, K.A. Resing, N.G. Ahn, and M. Winey. 2007. Mps1 activation loop autophosphorylation enhances kinase activity. *J Biol Chem.* 282:30553-61.

Maure, J.F., E. Kitamura, and T.U. Tanaka. 2007. Mps1 Kinase Promotes Sister-Kinetochore Bi-orientation by a Tension-Dependent Mechanism. *Curr Biol.* 17:2175-82.

McAinsh, A.D., J.D. Tytell, and P.K. Sorger. 2003. Structure, function, and regulation of budding yeast kinetochores. *Annu Rev Cell Dev Biol.* 19:519-39.

McCleland, M.L., R.D. Gardner, M.J. Kallio, J.R. Daum, G.J. Gorbsky, D.J. Burke, and P.T. Stukenberg. 2003. The highly conserved Ndc80 complex is required for kinetochore assembly, chromosome congression, and spindle checkpoint activity. *Genes Dev.* 17:101-14.

McClelland, S.E., S. Borusu, A.C. Amaro, J.R. Winter, M. Belwal, A.D. McAinsh, and P. Meraldi. 2007. The CENP-A NAC/CAD kinetochore complex controls chromosome congression and spindle bipolarity. *EMBO J.* 26:5033-47.

McIntosh, J.R. 1991. Structural and mechanical control of mitotic progression. *Cold Spring Harb Symp Quant Biol.* 56:613-9.

McIntosh, J.R. 2005. Rings around kinetochore microtubules in yeast. *Nat Struct Mol Biol.* 12:210-2.

McIntosh, J.R., E.L. Grishchuk, M.K. Morphew, A.K. Efremov, K. Zhudenkov, V.A. Volkov, I.M. Cheeseman, A. Desai, D.N. Mastronarde, and F.I. Ataullakhanov. 2008. Fibrils connect microtubule tips with kinetochores: a mechanism to couple tubulin dynamics to chromosome motion. *Cell.* 135:322-33.

Meraldi, P., V.M. Draviam, and P.K. Sorger. 2004. Timing and checkpoints in the regulation of mitotic progression. *Dev Cell.* 7:45-60.

Mikami, Y., T. Hori, H. Kimura, and T. Fukagawa. 2005. The functional region of CENP-H interacts with the Nuf2 complex that localizes to centromere during mitosis. *Mol Cell Biol.* 25:1958-70.

Miller, S., M. Johnson, and P. Stukenberg. 2008. Kinetochore Attachments Require an Interaction between Unstructured Tails on Microtubules and Ndc80Hec1. *Current Biology*:13.

Minoshima, Y., T. Hori, M. Okada, H. Kimura, T. Haraguchi, Y. Hiraoka, Y.C. Bao, T. Kawashima, T. Kitamura, and T. Fukagawa. 2005. The constitutive centromere component CENP-50 is required for recovery from spindle damage. *Mol Cell Biol.* 25:10315-28.

Miranda, J.J., P. De Wulf, P.K. Sorger, and S.C. Harrison. 2005. The yeast DASH complex forms closed rings on microtubules. *Nat Struct Mol Biol.* 12:138-43.

Mitchison, T., L. Evans, E. Schulze, and M. Kirschner. 1986. Sites of microtubule assembly and disassembly in the mitotic spindle. *Cell.* 45:515-27.

Mitchison, T.J., and E.D. Salmon. 1992. Poleward kinetochore fiber movement occurs during both metaphase and anaphase-A in newt lung cell mitosis. *J Cell Biol.* 119:569-82.

Musacchio, A., and E.D. Salmon. 2007. The spindle-assembly checkpoint in space and time. *Nat Rev Mol Cell Biol.* 8:379-393.

Nekrasov, V.S., M.A. Smith, S. Peak-Chew, and J.V. Kilmartin. 2003. Interactions between centromere complexes in Saccharomyces cerevisiae. *Mol Biol Cell.* 14:4931-46.

Nicklas, R.B., and C.A. Koch. 1969. Chromosome micromanipulation. 3. Spindle fiber tension and the reorientation of mal-oriented chromosomes. *J Cell Biol.* 43:40-50.

Nishihashi, A., T. Haraguchi, Y. Hiraoka, T. Ikemura, V. Regnier, H. Dodson, W.C. Earnshaw, and T. Fukagawa. 2002. CENP-I is essential for centromere function in vertebrate cells. *Dev Cell.* 2:463-76.

O'Connell, C.B., J. Loncarek, P. Hergert, A. Kourtidis, D.S. Conklin, and A. Khodjakov. 2008. The spindle assembly checkpoint is satisfied in the absence of interkinetochore tension during mitosis with unreplicated genomes. *J Cell Biol.* 183:29-36.

O'Toole, E.T., M. Winey, and J.R. McIntosh. 1999. High-voltage electron tomography of spindle pole bodies and early mitotic spindles in the yeast Saccharomyces cerevisiae. *Mol Biol Cell.* 10:2017-31.

Obuse, C., O. Iwasaki, T. Kiyomitsu, G. Goshima, Y. Toyoda, and M. Yanagida. 2004. A conserved Mis12 centromere complex is linked to heterochromatic HP1 and outer kinetochore protein Zwint-1. *Nat Cell Biol.* 6:1135-41.

Ohi, R., M.L. Coughlin, W.S. Lane, and T.J. Mitchison. 2003. An inner centromere protein that stimulates the microtubule depolymerizing activity of a KinI kinesin. *Dev Cell.* 5:309-21.

Okada, M., I.M. Cheeseman, T. Hori, K. Okawa, I.X. McLeod, J.R. Yates, 3rd, A. Desai, and T. Fukagawa. 2006. The CENP-H-I complex is required for the efficient incorporation of newly synthesized CENP-A into centromeres. *Nat Cell Biol.* 8:446-57.

Peters, J.M. 2006. The anaphase promoting complex/cyclosome: a machine designed to destroy. *Nat Rev Mol Cell Biol.* 7:644-56.

Petersen, J., and I.M. Hagan. 2003. S. pombe aurora kinase/survivin is required for chromosome condensation and the spindle checkpoint attachment response. *Curr Biol.* 13:590-7.

Pinsky, B.A., and S. Biggins. 2005. The spindle checkpoint: tension versus attachment. *Trends Cell Biol.* 15:486-93.

Pinsky, B.A., C. Kung, K.M. Shokat, and S. Biggins. 2006. The Ipl1-Aurora protein kinase activates the spindle checkpoint by creating unattached kinetochores. *Nat Cell Biol.* 8:78-83.

Pinsky, B.A., S.Y. Tatsutani, K.A. Collins, and S. Biggins. 2003. An Mtw1 complex promotes kinetochore biorientation that is monitored by the Ipl1/Aurora protein kinase. *Dev Cell.* 5:735-45.

Powers, A.F., A.D. Franck, D.R. Gestaut, J. Cooper, B. Gracyzk, R.R. Wei, L. Wordeman, T.N. Davis, and C.L. Asbury. 2009. The Ndc80 kinetochore complex forms load-bearing attachments to dynamic microtubule tips via biased diffusion. *Cell.* 136:865-75.

Przewloka, M.R., W. Zhang, P. Costa, V. Archambault, P.P. D'Avino, K.S. Lilley, E.D. Laue, A.D. McAinsh, and D.M. Glover. 2007. Molecular analysis of core kinetochore composition and assembly in Drosophila melanogaster. *PLoS One.* 2:e478.

Rieder, C.L. 1981. The structure of the cold-stable kinetochore fiber in metaphase PtK1 cells. *Chromosoma.* 84:145-58.

Rieder, C.L., and R.E. Palazzo. 1992. Colcemid and the mitotic cycle. *Journal of Cell Science.* 102 (Pt 3):387-92.

Rieder, C.L., and E.D. Salmon. 1998. The vertebrate cell kinetochore and its roles during mitosis. *Trends Cell Biol.* 8:310-8.

Ruchaud, S., M. Carmena, and W.C. Earnshaw. 2007. Chromosomal passengers: conducting cell division. *Nat Rev Mol Cell Biol.* 8:798-812.

Saitoh, S., K. Ishii, Y. Kobayashi, and K. Takahashi. 2005. Spindle checkpoint signaling requires the mis6 kinetochore subcomplex, which interacts with mad2 and mitotic spindles. *Mol Biol Cell.* 16:3666-77.

Sanchez-Perez, I., S.J. Renwick, K. Crawley, I. Karig, V. Buck, J.C. Meadows, A. Franco-Sanchez, U. Fleig, T. Toda, and J.B. Millar. 2005. The DASH complex and Klp5/Klp6 kinesin coordinate bipolar chromosome attachment in fission yeast. *EMBO J.* 24:2931-43.

Sandall, S., F. Severin, I.X. McLeod, J.R. Yates, 3rd, K. Oegema, A. Hyman, and A. Desai. 2006. A Bir1-Sli15 complex connects centromeres to microtubules and is required to sense kinetochore tension. *Cell.* 127:1179-91.

Santaguida, S., and A. Musacchio. 2009. The life and miracles of kinetochores. *EMBO J.* 28:2511-31.

Schittenhelm, R.B., S. Heeger, F. Althoff, A. Walter, S. Heidmann, K. Mechtler, and C.F. Lehner. 2007. Spatial organization of a ubiquitous eukaryotic kinetochore protein network in Drosophila chromosomes. *Chromosoma.* 116:385-402.

Schmidt, M., Y. Budirahardja, R. Klompmaker, and R.H. Medema. 2005. Ablation of the spindle assembly checkpoint by a compound targeting Mps1. *EMBO Rep.* 6:866-72.

Severin, F.F., P.K. Sorger, and A.A. Hyman. 1997. Kinetochores distinguish GTP from GDP forms of the microtubule lattice. *Nature.* 388:888-91.

Shimogawa, M.M., B. Graczyk, M.K. Gardner, S.E. Francis, E.A. White, M. Ess, J.N. Molk, C. Ruse, S. Niessen, J.R. Yates, 3rd, E.G. Muller, K. Bloom, D.J. Odde, and T.N. Davis. 2006. Mps1 phosphorylation of Dam1 couples kinetochores to microtubule plus ends at metaphase. *Curr Biol.* 16:1489-501.

Skibbens, R.V., V.P. Skeen, and E.D. Salmon. 1993. Directional instability of kinetochore motility during chromosome congression and segregation in mitotic newt lung cells: a push-pull mechanism. *J Cell Biol.* 122:859-75.

Sliedrecht, T., C. Zhang, K.M. Shokat, and G.J. Kops. Chemical genetic inhibition of Mps1 in stable human cell lines reveals novel aspects of Mps1 function in mitosis. *PLoS One.* 5:e10251.

Sorger, P.K., F.F. Severin, and A.A. Hyman. 1994. Factors required for the binding of reassembled yeast kinetochores to microtubules in vitro. *J Cell Biol.* 127:995-1008.

Tanaka, K., E. Kitamura, Y. Kitamura, and T.U. Tanaka. 2007. Molecular mechanisms of microtubule-dependent kinetochore transport toward spindle poles. *J Cell Biol.* 178:269-81.

Tanaka, T.U., and A. Desai. 2008. Kinetochore-microtubule interactions: the means to the end. *Curr Opin Cell Biol.* 20:53-63.

Tanaka, T.U., N. Rachidi, C. Janke, G. Pereira, M. Gálová, E. Schiebel, M.J. Stark, and K. Nasmyth. 2002. Evidence that the Ipl1-Sli15 (Aurora kinase-INCENP) complex promotes chromosome bi-orientation by altering kinetochore-spindle pole connections. *Cell.* 108:317-29.

Taylor, S.S., D. Hussein, Y. Wang, S. Elderkin, and C.J. Morrow. 2001. Kinetochore localisation and phosphorylation of the mitotic checkpoint components Bub1 and BubR1 are differentially regulated by spindle events in human cells. *J Cell Sci.* 114:4385-95.

Theis, M., M. Slabicki, M. Junqueira, M. Paszkowski-Rogacz, J. Sontheimer, R. Kittler, A.K. Heninger, T. Glatter, K. Kruusmaa, I. Poser, A.A. Hyman, M.T. Pisabarro, M. Gstaiger, R. Aebersold, A. Shevchenko, and F. Buchholz. 2009. Comparative profiling identifies C13orf3 as a component of the Ska complex required for mammalian cell division. *EMBO J.* 28:1453-65.

Tighe, A., O. Staples, and S. Taylor. 2008. Mps1 kinase activity restrains anaphase during an unperturbed mitosis and targets Mad2 to kinetochores. *J Cell Biol.* 181:893-901.

Trazzi, S., G. Perini, R. Bernardoni, M. Zoli, J.C. Reese, A. Musacchio, and G. Della Valle. 2009. The C-terminal domain of CENP-C displays multiple and critical functions for mammalian centromere formation. *PLoS One.* 4:e5832.

Tulu, U.S., C. Fagerstrom, N.P. Ferenz, and P. Wadsworth. 2006. Molecular requirements for kinetochore-associated microtubule formation in mammalian cells. *Curr Biol.* 16:536-41.

Uchida, K.S., K. Takagaki, K. Kumada, Y. Hirayama, T. Noda, and T. Hirota. 2009. Kinetochore stretching inactivates the spindle assembly checkpoint. *J Cell Biol.* 184:383-90.

Vader, G., C.W. Cruijsen, T. van Harn, M.J. Vromans, R.H. Medema, and S.M. Lens. 2007. The chromosomal passenger complex controls spindle checkpoint function independent from its role in correcting microtubule kinetochore interactions. *Mol Biol Cell.* 18:4553-64.

Vader, G., and S.M. Lens. 2008. The Aurora kinase family in cell division and cancer. *Biochim Biophys Acta.* 1786:60-72.

Vader, G., R.H. Medema, and S.M. Lens. 2006. The chromosomal passenger complex: guiding Aurora-B through mitosis. *J Cell Biol.* 173:833-7.

Vanoosthuyse, V., and K.G. Hardwick. 2009. A novel protein phosphatase 1-dependent spindle checkpoint silencing mechanism. *Curr Biol.* 19:1176-81.

Vigneron, S., S. Prieto, C. Bernis, J.C. Labbe, A. Castro, and T. Lorca. 2004. Kinetochore Localization of Spindle Checkpoint Proteins: Who Controls Whom? *Mol Biol Cell.* 21:21.

Villa, F., P. Capasso, M. Tortorici, F. Forneris, A. de Marco, A. Mattevi, and A. Musacchio. 2009. Crystal structure of the catalytic domain of Haspin, an atypical kinase implicated in chromatin organization. *Proc Natl Acad Sci U S A.*

Vorozhko, V.V., M.J. Emanuele, M.J. Kallio, P.T. Stukenberg, and G.J. Gorbsky. 2008. Multiple mechanisms of chromosome movement in vertebrate cells mediated through the Ndc80 complex and dynein/dynactin. *Chromosoma.* 117:169-79.

Walczak, C.E., and R. Heald. 2008. Mechanisms of mitotic spindle assembly and function. *Int Rev Cytol.* 265:111-58.

Wan, X., R.P. O'Quinn, H.L. Pierce, A.P. Joglekar, W.E. Gall, J.G. DeLuca, C.W. Carroll, S.T. Liu, T.J. Yen, B.F. McEwen, P.T. Stukenberg, A. Desai, and E.D. Salmon. 2009. Protein architecture of the human kinetochore microtubule attachment site. *Cell.* 137:672-84.

Wang, H.W., S. Long, C. Ciferri, S. Westermann, D. Drubin, G. Barnes, and E. Nogales. 2008. Architecture and flexibility of the yeast Ndc80 kinetochore complex. *J Mol Biol.* 383:894-903.

Waters, J.C., R.V. Skibbens, and E.D. Salmon. 1996. Oscillating mitotic newt lung cell kinetochores are, on average, under tension and rarely push. *J Cell Sci.* 109 (Pt 12):2823-31.

Weaver, B.A., and D.W. Cleveland. 2006. Does aneuploidy cause cancer? *Curr Opin Cell Biol.* 18:658-67.

Wei, R.R., J. Al-Bassam, and S.C. Harrison. 2007. The Ndc80/HEC1 complex is a contact point for kinetochore-microtubule attachment. *Nat Struct Mol Biol.* 14:54-9.

Wei, R.R., P.K. Sorger, and S.C. Harrison. 2005. Molecular organization of the Ndc80 complex, an essential kinetochore component. *Proc Natl Acad Sci U S A.* 102:5363-7.

Welburn, J.P., E.L. Grishchuk, C.B. Backer, E.M. Wilson-Kubalek, J.R. Yates, 3rd, and I.M. Cheeseman. 2009. The human kinetochore Ska1 complex facilitates microtubule depolymerization-coupled motility. *Dev Cell.* 16:374-85.

Westermann, S., A. Avila-Sakar, H.W. Wang, H. Niederstrasser, J. Wong, D.G. Drubin, E. Nogales, and G. Barnes. 2005. Formation of a dynamic kinetochore- microtubule interface through assembly of the Dam1 ring complex. *Mol Cell.* 17:277-90.

Westermann, S., I.M. Cheeseman, S. Anderson, J.R. Yates, 3rd, D.G. Drubin, and G. Barnes. 2003. Architecture of the budding yeast kinetochore reveals a conserved molecular core. *J Cell Biol.* 163:215-22.

Westermann, S., D.G. Drubin, and G. Barnes. 2007. Structures and functions of yeast kinetochore complexes. *Annu Rev Biochem.* 76:563-91.

Westermann, S., H.W. Wang, A. Avila-Sakar, D.G. Drubin, E. Nogales, and G. Barnes. 2006. The Dam1 kinetochore ring complex moves processively on depolymerizing microtubule ends. *Nature.* 440:565-9.

Wigge, P.A., and J.V. Kilmartin. 2001. The Ndc80p complex from Saccharomyces cerevisiae contains conserved centromere components and has a function in chromosome segregation. *J Cell Biol.* 152:349-60.

Wilson-Kubalek, E.M., I.M. Cheeseman, C. Yoshioka, A. Desai, and R.A. Milligan. 2008. Orientation and structure of the Ndc80 complex on the microtubule lattice. *J Cell Biol.* 182:1055-61.

Witt, P.L., H. Ris, and G.G. Borisy. 1980. Origin of kinetochore microtubules in Chinese hamster ovary cells. *Chromosoma.* 81:483-505.

Wittmann, T., A. Hyman, and A. Desai. 2001. The spindle: a dynamic assembly of microtubules and motors. *Nat Cell Biol.* 3:E28-34.

Xu, Q., S. Zhu, W. Wang, X. Zhang, W. Old, N. Ahn, and X. Liu. 2009. Regulation of kinetochore recruitment of two essential mitotic spindle checkpoint proteins by Mps1 phosphorylation. *Mol Biol Cell.* 20:10-20.

Yamamoto, T.G., S. Watanabe, A. Essex, and R. Kitagawa. 2008. SPDL-1 functions as a kinetochore receptor for MDF-1 in Caenorhabditis elegans. *J Cell Biol.* 183:187-94.

Yang, Z., A.E. Kenny, D.A. Brito, and C.L. Rieder. 2009. Cells satisfy the mitotic checkpoint in Taxol, and do so faster in concentrations that stabilize syntelic attachments. *J Cell Biol.* 186:675-84.

Zhai, Y., P.J. Kronebusch, and G.G. Borisy. 1995. Kinetochore microtubule dynamics and the metaphase-anaphase transition. *J Cell Biol.* 131:721-34.

Zhang, X., W. Lan, S.C. Ems-McClung, P.T. Stukenberg, and C.E. Walczak. 2007. Aurora B phosphorylates multiple sites on mitotic centromere-associated kinesin to spatially and temporally regulate its function. *Mol Biol Cell.* 18:3264-76.

Zinkowski, R.P., J. Meyne, and B.R. Brinkley. 1991. The centromere-kinetochore complex: a repeat subunit model. *J Cell Biol.* 113:1091-110.